2019

Novel Application of Melt Extrusion and Additive Manufacturing on Developing Diverse Dosages

Jiaxiang Zhang
University of Mississippi

NOVEL APPLICATION OF MELT EXTRUSION AND ADDITIVE MANUFACTURING ON DEVELOPING DIVERSE DOSAGES

A
Dissertation presented in the partial fulfillment of requirements for the Doctoral of Philosophy degree in the Department of Pharmaceutics and Drug Delivery
The University of Mississippi

by

JIAXIANG ZHANG

December, 2018

ABSTRACT

New drug product development is a time consuming and costly process. One of the significant challenges is the poor aqueous solubility of many active pharmaceutical ingredients (APIs). Among those techniques, hot-melt extrusion(HME) is optimal for pharmaceutical solid dispersion development because of it free of using an organic solvent, easy scale up, and suitable for continuous processing with ensured optimal quality control.

Inter-individual variability is always an issue when treating patients of different races, genders, ages, pharmacogenetics, and pharmacokinetic characteristics. Also, developing new drugs is complicated and expensive, so optimizing the bioavailability, or therapeutic effect of existing drugs has gained much interest. Additive manufacturing (AM) is a new alternative solution for the development of controlled release dosages because it can produce personalized or unique dosage forms and more complex drug-release profiles.

In this dissertation, a comprehensive study of patient-focused drug development by combining HME and 3D printing technologies has been conducted. The feasibility of conjugating HME and 3D printing was studied first. Then a series of the polymer screening studies were conducted to determine the widely available drug loaded printable filaments for fused depositional modeling (FDM) based 3D printer, fast release, extended release, and controlled release dosage were produced via different polymer matrix and structure design. In addition, due to the highly customized structure of 3D printed tablets, the release kinetics and correlation of the drug release to the structure has been studied, which demonstrated a comprehensive understanding the in vitro drug release mechanisms and kinetics from the 3D printed dosages. After the series studies of HME and 3D printing, the optimization of the oral drug administration also been conducted via a specific 3D structure design, which can rapidly effective and maintains a long therapeutic time synchronously.

LIST OF ABBREVIATIONS

AM	Additive manufacturing
RP	Rapid prototyping
FDA	Food and Drug Administration
API	Active pharmaceutical ingredients
FDM	Fused deposition modeling
FFF	Fused filament fabrication
PVA	Polyvinyl alcohol
HME	Hot-melt extrusion
ADME	Absorption, distribution, metabolism, and excretion
PAM	Pressure-assisted microsyringes
PAB	Pressure-assisted bioprinting
3DP	3D-printed
EC	Ethyl cellulose
HPMC	Hydroxypropyl methylcellulose
PVP	Polyvinylpyrrolidone
APAP	Acetaminophen
PLA	Polylactic acid
DSC	Differential scanning calorimetry
TGA	Thermogravimetric analysis
PM	Physical mixed/physical mixture
EXT	Extrusion/extruded
SEM	Scanning electronic microscopy
USP	United States Pharmacopeia
HPLC	High Performance Liquid Chromatography
HPC	High Performance Liquid Chromatography
DDS	Drug delivery systems
QOL	Quality of life
RE	Rotary evaporation
CP	Co-precipitation
CVD	Centrifuge vacuum drying
BCS	Biopharmaceutics Classification System
HPMCAS	Hypromellose acetate succinate
PLM	Polarized light microscopy
PAT	PROCESS ANALYTICAL TOOL
XRPD	Powder X-ray diffraction
ASD	Amorphous solid dispersion
NIR	Near Infrared
FTIR	Fourier-transform infrared spectroscopy
NME	New molecular entity
DC	Direct compressed
KSD	KinetiSol® dispersing
FD	Freeze-drying
SD	Spray drying

ACKNOWLEDGMENT

Firstly, I would like to express my sincere gratitude to my advisor, Prof. Michael A. Repka, for the continuous support of my Ph.D. study and related research, for his patience, motivation, and immense knowledge. His guidance helped me in all the time of research and writing of this thesis. I could not have imagined having a better advisor and mentor for my Ph.D. study.

Besides my advisor, I would like to thank the rest of my thesis committee: Prof. Chalet Tan, Prof. Mahavir B. Chougule, and Dr. John O'Haver, for their insightful comments and encouragement, but also for the hard question which incented me to widen my research from various perspectives.

My sincere thanks also go to Dr. Soumyajit Majumdar, Dr. Narasimha Murthy, and Dr. Seongbong Jo, who provided me comprehensive courses on the pharmaceutics, and who also gave me access to the laboratory and research facilities. Without they precious support it would not be possible to conduct this research.

I thank my fellow labmates in for the stimulating discussions, for the sleepless nights we were working together before deadlines, and for all the fun we have had in the last four years.

Last but not the least, I would like to thank my family: my parents and to my wife Weiwei Yang and son Geoffrey Zhang for supporting me spiritually throughout writing this thesis and my life in general.

TABLE OF CONTENTS

LIST OF TABLES

LIST OF FIGURES

INTRODUCTION

Solid dispersions represent a promising formulation approach undertaken by many pharmaceutical scientists to improve the bioavailability of active pharmaceutical ingredients (API) with poor aqueous solubility [1][2][3]. Hot-melt extrusion (HME) is one of the preferred methods in pharmaceutical solid dispersion development. This is because the technology can generate extrudates/ granules with favorable properties. In addition, it is free from the use of organic solvents and suitable for continuous processing [4][5][6].

HME was first used in the plastics and rubber industry. However, since the 1970s, the use of HME has been promoted in pharmaceutical research [7][8]. The pharmaceutical use of HME is currently under investigation as a method for increasing the release rate of poorly water-soluble APIs. The bioavailability of such APIs are enhanced by melt-mixing them with hydrophilic, water-soluble polymers [9][10]. Apart from increasing the bioavailability of an API, HME can be used to develop modified-release drug systems with delayed drug delivery characteristics and the ability to mask the bitter taste of an API [11][12]. Moreover, HME can be easily coupled with other technologies, such as high-pressure homogenization, to prepare solid lipid nanoparticles [9] and nanocrystals [13]. It can also be used with high-pressurized carbon dioxide to enhance milling efficiency and to prepare a floating drug delivery system by creating porous extrudates [14][15]. In recent years, researchers have started exploring the conjugation of HME with three-dimensional (3D) printing to prepare pharmaceutical dosage forms [16][17][18].

3D printing is a layer-by-layer production of 3D objects with the help of digital designs [11]. It is also known as additive manufacturing (AM). AM equipment and materials were developed in the early 1980s, mainly for chemistry, optics, and robotics research [19]. The first powder-based free-form fabrication using 3D printing methods became available in 1993 at the Massachusetts Institute of Technology (MIT) [20], in which a standard inkjet head was used to print binders onto loose powders in a powder bed.

Compared with the traditional process of manufacturing dosage forms, 3D printing can create complex products, personalized products, and products made for immediate consumption [21]. Based on the advantages offered by 3D printing technology, interest in this technique within the pharmaceutical industry has grown over the last few years. This is reflected in the increasing number of scientific reports and patents describing the pharmaceutical applications of 3D printing. Recently, the U.S. Food and Drug Administration (FDA) approved the first 3D-printed (3DP) orally disintegrating tablet SPRITAM1 (levetiracetam), which was manufactured based on the ZipDose Technology (Aprecia Pharmaceuticals, Langhorne, PA, USA).

The traditional process of manufacturing pharmaceuticals involves a complex downstream procedure, which includes milling extrudates, sieving, compressing, and coating. However, 3D printing technology can streamline these processes. Compared to the traditional process of manufacturing pharmaceutical products, combining HME and 3D printing into a continuous process can offer advantages. These include increased solubility and bioavailability of drugs, as well as production of more complex-structured dosage forms and personalized drug products. In addition, combining the two technologies can simplify the downstream process and make it more effective and economical (Figure. 1). In particular, the FDA encourages drug manufacturers to

produce oral solid dosage forms that meet the increasing demands of oral drug delivery, in terms of API bioavailability and drug release characteristics, in a continuous and controlled process [22].

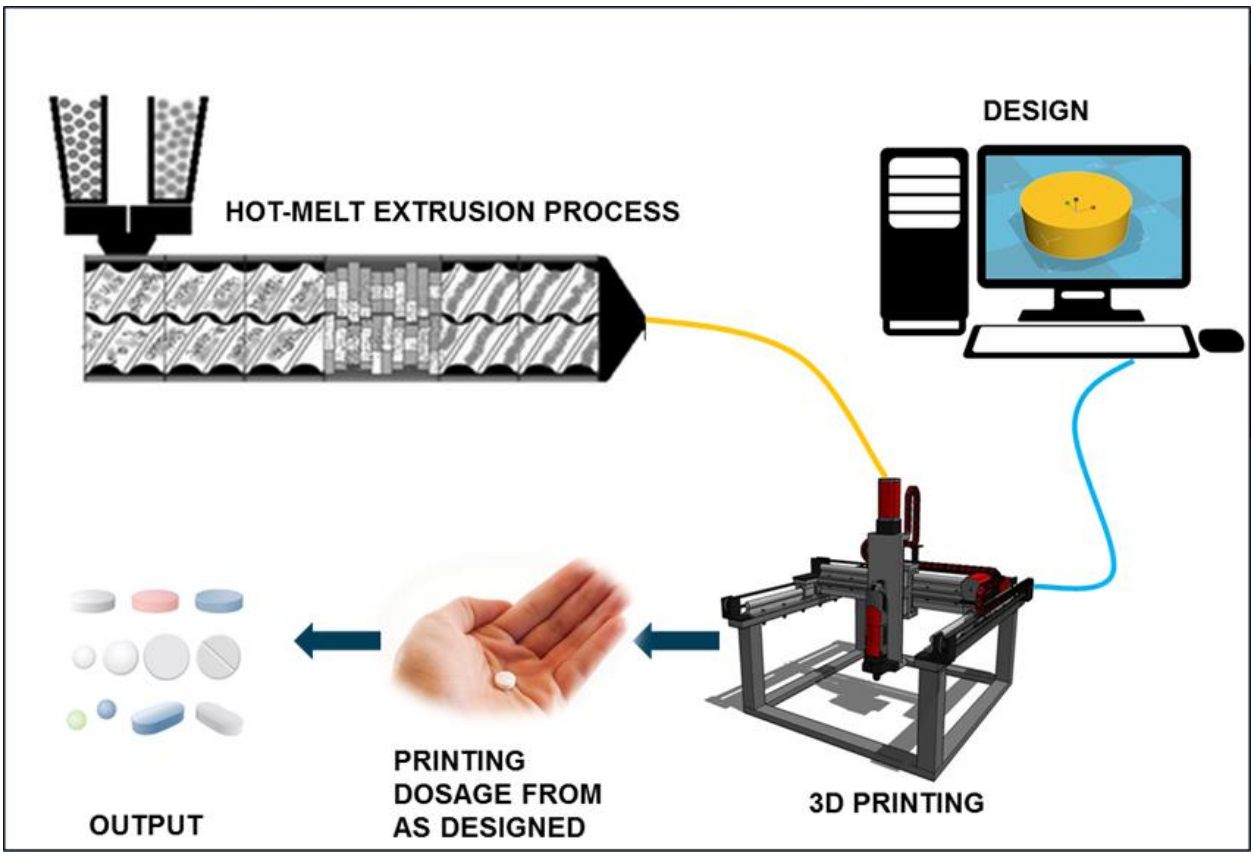

Figure 1. Schematic of the combination of HME and 3D process.

Based on the advantages of coupling the two technologies, the elementary steps involved in producing dosage forms by continuous HME-3D printing are as follows: 1) dosage form design and conversion to a printer-readable format; 2) preparation of raw materials (such as powders, particulates, granules, or pastes); 3) preparation of hot-melt extruded filaments; 4) cooling of the filaments; 5) 3D printing; and 6) removal of printed material and downstream processes such as cooling, drying, and packing. However, for continuous pharmaceutical HME and 3D printing, extruding the 3D-printable filaments is a very important elementary step, along with dissolving

the poorly water-soluble API in molten polymeric excipients and mixing them to improve the bioavailability of the API.

In this thesis, HME and 3D printing technologies were conjugated for the highly customized or personalized development. For the 1st chapter, the feasibility studies of the combining the two technologies were conducted. Moreover, the preliminary screening of the 3D printable filaments formulation were studied as well. To understand the different of the 3D printed and conventional dosages, the compression studies of size, hardness, and *in vitro* drug release between 3D printed tablets and direct compressed tablets were conducted as well. For the 2nd chapter, characterization and evaluation of a series filament formulations were studied. After we optimized the filaments for pharmaceutical 3D printing process, the correlation of the drug release profiles with the 3D structure of the tablets, as well as the drug release mechanism and kinetics from the 3D printed matrix were studied in the 3rd chapter. Finally, the optimization of oral drug administration by using optimized filament formulation and 3D printing technologies were discussed in the 4th chapter.

CHAPTER 1

COUPLING 3D PRINTING WITH HOT-MELT EXTRUSION TO PRODUCE CONTROLLED-RELEASE TABLETS

1.1. Introduction

3D printing is an emerging technology which has been introduced to the medical area few decades ago, and has been applied to pharmaceutical area in recent years. Previous studies have used powder/binder-based biodegradable polymers, such as polyethylene oxide/polycyclooctene [23], ethyl cellulose (EC), hydroxypropyl methylcellulose (HPMC) E50, polyvinylpyrrolidone K30 [24], and Eudragit1 L100 (Rathbone, 2008), to print pharmaceutical dosage forms. Recently, biodegradable polymer filaments, prepared from HPMC K100M CR [25] and polyvinyl alcohol [16][17], were manufactured by 3D printing.

The present study investigated the use of different types of pharmaceutical polymers to prepare fused filaments suitable for 3D printing of a desired pharmaceutical formulation. The main objectives of this study were as follows: 1) to couple fused deposition modeling (FDM)-based 3D printing with HME technology to print controlled-release tablets, 2) to screen different grades of pharmaceutical polymers suitable for 3D printing based on the HME-fused filaments' physical and chemical properties, and 3) to study the drug release profiles of 3DP tablets in comparison to those of directly-compressed milled extrudate and physical-mixture tablets.

1.2. Materials and methods

1.2.1. Materials

Acetaminophen (APAP) (Spectrum Chemical, New Brunswick, NJ, USA) was used as the model API. APAP is a crystalline Class I Biopharmaceutics Classification System drug (high permeability, high solubility) with a melting point of 169–170 °C. Benecel™ HPMC E5, Klucel™ HPC EF and LF, and Aqualon™ EC N14 were donated by Ashland Inc. (Covington, KY, USA). Soluplus1 was donated by BASF (Ludwigshafen, Germany). Eudragit1 L100 was donated by Evonik Industries (Essen, Germany). All other reagents were of either high-performance liquid chromatography (HPLC) or analytical grade.

1.2.2. Methods

1.2.2.1. Formulations

Table 1. Formulation of different polymers

Formulation		Drug (w/w)	Polymer (w/w)	Disintegrator (w/w)
I		0	100% PLA	-
Stage 1	**I-1**	30%	70%HPC LF	-
	I-2	30%	70%HPC EF	-
	I-3	30%	70%HPMC E5	-
	I-4	30%	70%EC N14	-
	I-5	30%	70%Soluplus	-
	I-6	30%	70% Eudragit L100	
Stage 2	**II-1**	30%	35% HPMC E5+35% EC N14	-
	II-2	30%	35% HPMC E5+35% HPC EF	-
	II-3	30%	35% HPMC E5+35% HPC LF	-
	II-4	30%	35% HPMC E5+35% Soluplus	-
	II-5	30%	35%HPMC E5+35% Eudragit L100	-
	II-6	30%	35% EC N14+35% Soluplus	-
	II-7	30%	35%HPC LF+35% EC N14	-
Stage 3	**III-1**	30%	45.5% HPMC E5+19.5% EC N14	5%
	III-2	30%	45.5% HPMC E5+19.5% HPC EF	5%
	III-3	30%	45.5% HPMC E5+19.5% HPC LF	5%
	III-4	30%	50% HPMC E5+15% Soluplus	5%
	III-5	30%	50% HPMC E5+15% Eudragit L100	5%
	III-6	30%	50% EC N14+15% Eudragit L100	5%

Polylactic acid (PLA) without drug deposition was used as the reference standard. Various formulations were prepared, in which the polymers were used at different ratios. The procedure was divided into three different stages. The first strategy was to use a single polymer at 30% w/w of the drug load (I 1–6) (Table 1). The second strategy was based on the results of the 3-point bend test and 3D printing process; thus, a binary combination of polymer blending ratios was used to improve the mechanical properties of the filaments (II 1–7). The third strategy was based on the results of the second strategy and an *in vitro* drug release study. The combinations of polymer blending ratios were further modified or a super disintegrate (Kollidon CL-F) was added to the formulations to improve both the mechanical properties of the filaments and the dissolution properties of the 3DP tablets. A physical mixture (API + polymer) was tumble-mixed using Maxiblend^{TM} (Globe- Pharma, New Brunswick, NJ, USA) at 25 rpm for 20 min, followed by sieving with a US#30-mesh screen to remove any aggregates in the mixture.

1.2.2.2. HME process

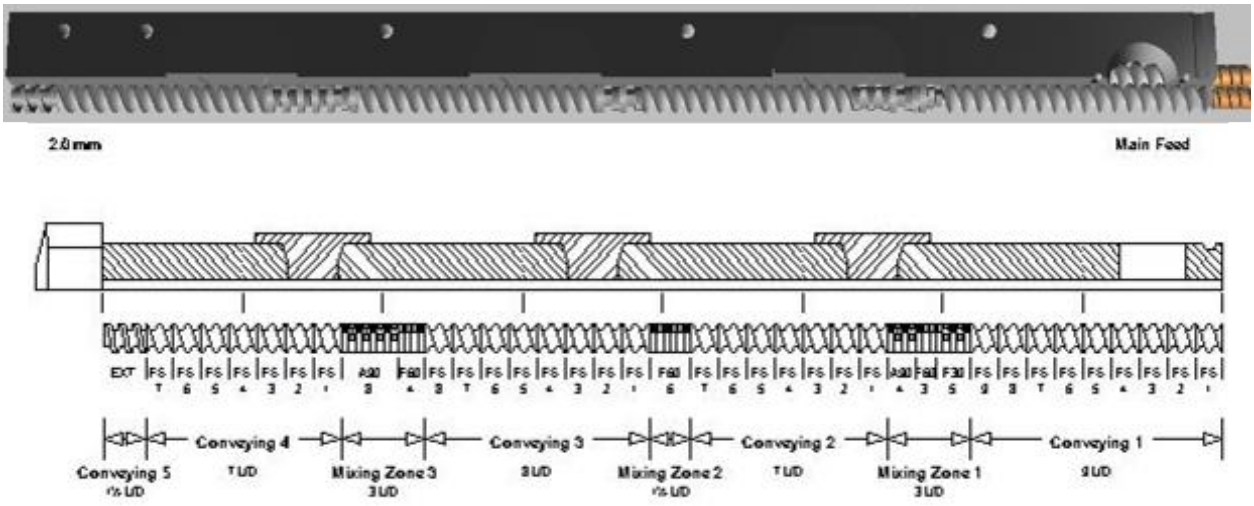

Figure 2. Standard screw configuration of Thermo Scientific 11mm twin screw co-rotating extruder.

The extruder (Thermo Fisher Scientific, Waltham, MA, USA) used in this work was a co-rotating, twin-screw extruder with 11- mm diameter screws. It had an L/D of approximately 40 and eight electrically heated zones. The feeding zone temperature was controlled by an external circulation heater. The HPMC formulations were extruded at 180 °C; however, all the other formulations were extruded at 140–160 °C in all the zones. The physical mixtures were extruded at a screw speed of 50 rpm with a standard screw configuration (Figure. 2). A 2-mm round-shaped die was used to extrude filaments for 3D printing. In addition, a conveyor belt was used to cool and straighten the filaments to feed them into the 3D printer. Extra filaments were collected and milled to compare 3DP tablets with tablets made by HME.

1.2.3. Filament characterization

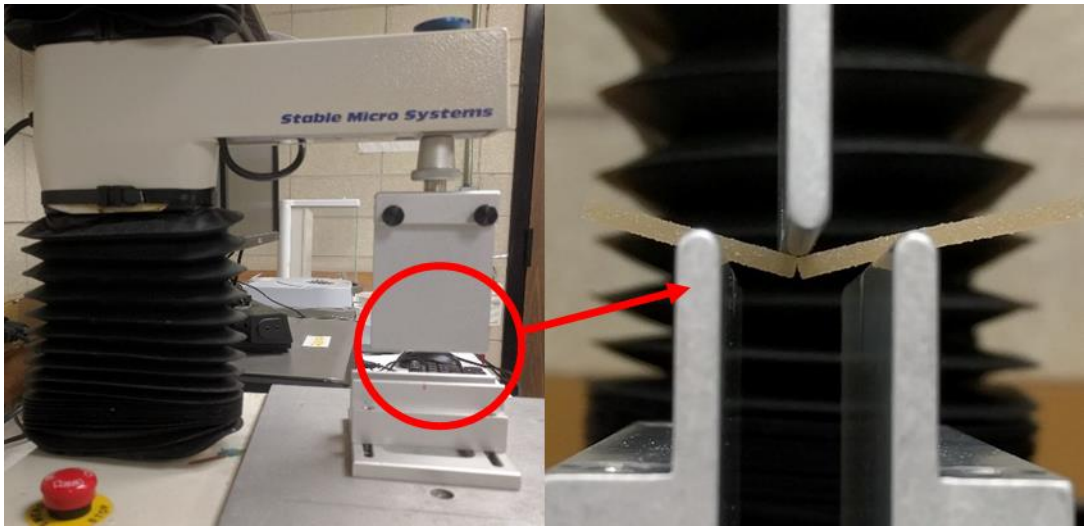

Figure 3. TA analyzer and 3-point bend test.

Samples of extruded filament were collected and cut into 5-mm segments. Next, a TA-XT2i analyzer (Texture Technologies, Hamilton, MA, USA) and a TA-95N 3-point bend probe set (Texture Technologies) were used to test the brittleness of the extruded filaments (Figure. 3). Each filament was placed on the sample holder of the 3-point bend tester with a 25-mm gap. The

moving speed of the blades was 10 mm/s until they reached 15 mm under the samples. Fifteen filaments of each formulation were tested and Exponent software version 6.1.5.0 (Stable Micro Systems, Godalming, UK) was used for data collection and analysis.

1.2.4. Differential scanning calorimetry (DSC)

A Diamond DSC system (PerkinElmer, Waltham, MA, US) was used to study drug crystallinity and characterize drug miscibility with the extrudates. Two to 5 mg of sample was hermetically sealed in an aluminum pan and heated from 40 to 200 °C at a rate of 10 °C/min. Ultra-purified nitrogen was used as the purge gas at a flow rate of 50 mL/min in all the DSC experiments. Data were collected and analyzed with Pyris software (PerkinElmer).

1.2.5. Thermogravimetric analysis (TGA)

TGA was performed by using a PerkinElmer Pyris 1 TGA calorimeter to determine the thermal stability of APAP and the polymers during the HME processing. The samples were placed in an open aluminum pan and heated from 30 to 300 °C at a rate of 20 °C/min. Ultra-purified nitrogen was used as the purge gas at a flow rate of 25 mL/min. Data were collected and analyzed using the Pyris software. Percentage mass loss and/or onset temperatures were then calculated.

1.2.6. 3D printing

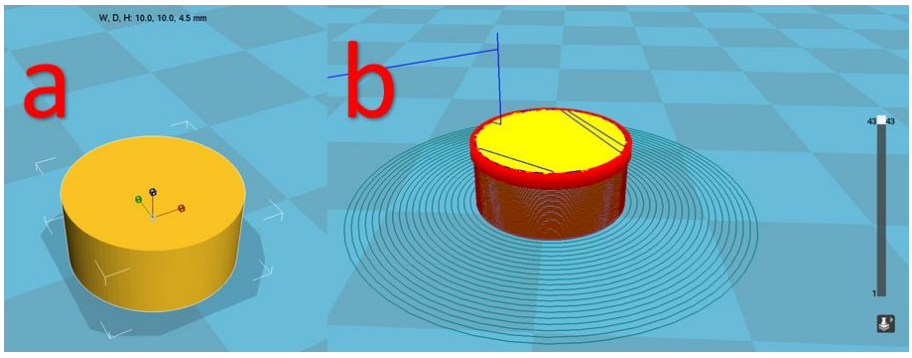

Figure 4. a) Dimensions of the 3D printing tablets; b) layer and printing path view of the tablets.

The model tablets were designed using Microsoft 3D Builder (Microsoft, Redmond, WA, USA) and converted to .gcode files using CURA software (version 15.04; Ultimaker, Geldermalsen, The Netherlands). Tablet dimensions (diameter, 10 mm; thickness, 4.5 mm) were determined based on the drug load (Figure 4). Tablets were fabricated with the extruded filaments using a commercial FDM-3D printer (Prusa i3 3D desktop printer, Prusa Research, Prague, Czech Republic) with an extruder, which had an E3D V6 hot end and a 0.4-mm nozzle (figure 5). The following printer settings were found to produce the best tablets: a standard resolution with the raft option activated and an extrusion temperature of 200 °C. The other settings used were as follows: bed temperature, 50 °C; printing speed, 50 mm/s; nozzle traveling speed, 50 mm/s; layer height, 0.10 mm; and outside shell thickness, 0.4 mm. The infill percentage was set at 100% to allow printing of tablets with optimum characteristics. The dimensions and weights of the 3DP tablets were then measured.

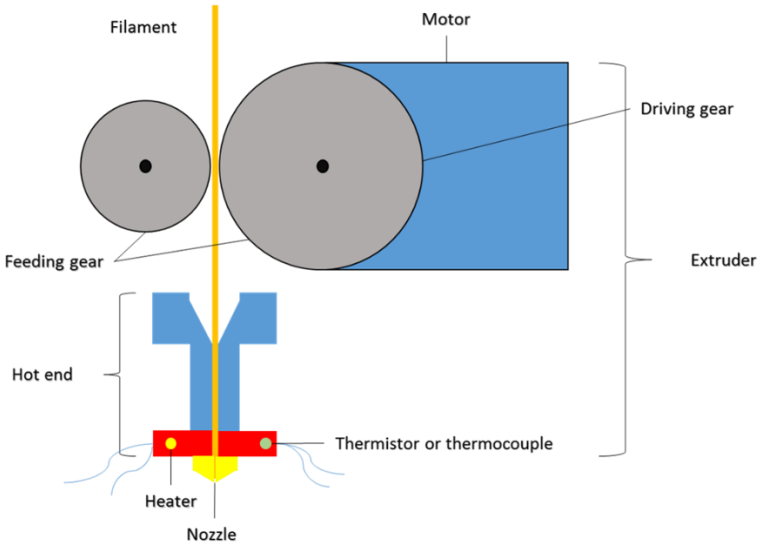

Figure 5. Schematic picture of 3D printer extruder.

1.2.7. Preparation of tablets by direct compression

Based on the weights of the 3DP tablets, 400 mg of physical mixtures of each formulation were compressed into tablets using a 0.375-in. die at 300 bar (PM tablets). On the other hand, the extruded filaments were milled and compressed into tablets under the same conditions (EXT tablets).

1.2.8. Tablet characterization

1.2.8.1. Assessment of tablet morphology

A VWR1 digital caliper (VWR1, PA, U.S.) was used to determine the diameters and thicknesses of the tablets and a Canon 60D camera was used to image the tablets (Canon, Tokyo, Japan). Cross- sectional images of the 3DP tablets, extrudate tablets, and directly compressed tablets were taken using scanning electronic micros- copy (SEM).

1.2.8.2. Determination of tablet strength

A standard tablet hardness tester (VK200; Agilent Technologies, Santa Clara, CA, USA) with a maximum force of 35 kp was used to measure tablet hardness. Six tablets from each group of tablets were tested.

1.2.9. *In vitro* drug release study

Drug release from the 3DP, EXT, and PM tablets was determined using a United States Pharmacopeia (USP)-II dissolution apparatus (Hanson SR8-plusTM; Hanson Research, Chatsworth, CA, USA). Dissolution tests were conducted as per the US Pharmacopeial standards using Simulated Intestinal Fluid TS (without pancreatin) (pH 6.8), which is representative of the small intestinal fluid of humans. Each experiment was carried out in triplicate using 900 mL of the dissolution medium at 37±0.5 °C for 24 h. The paddle speed was set at 50 rpm. Samples were taken at 0.5,1, 2, 4, 6, 8, 10, 12, and 24 h and analyzed. The amount of released APAP was

determined by HPLC (Waters Corp., Milford, MA, USA) at 246 nm and analyzed using Empower software (version 2, Waters Corp.).

1.3. Results and discussion

1.3.1. Preliminary study of raw materials

The TGA results showed that APAP and the physical mixtures degraded only at temperatures above 350 °C, which indicates that the drug and polymer matrix would not degrade at the HME processing temperature (140–180 °C) nor at the operating temperature (200 °C) of 3D printing (Figure 6). Although shear was applied during the HME process, it was not high and did not cause APAP degradation. This was because the die pressure and torque applied during the process were low.

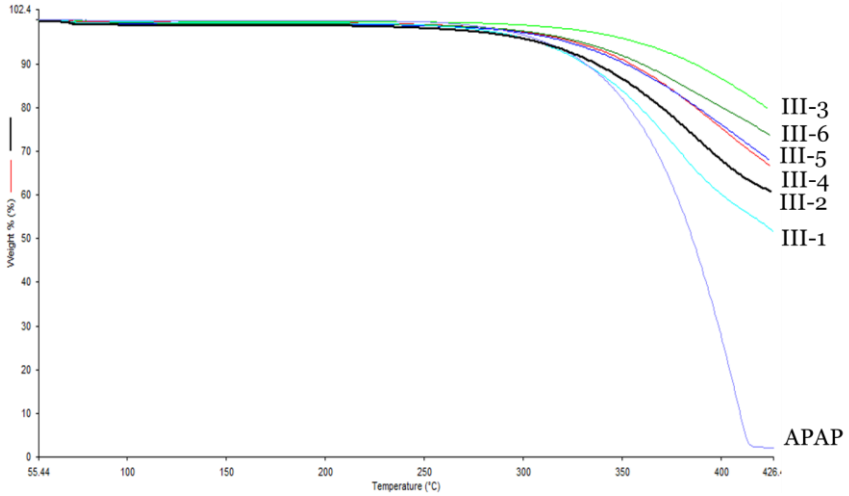

Figure 6. TGA results for raw materials and physical mixtures.

DSC is a thermoanalytical technique for measuring phase transitions in a sample as a function of temperature, when more heat flows to the sample than to the reference. The DSC curve for pure APAP showed a peak at 172 °C (Figure 7). A heating method was utilized for the physical mixtures in the DSC analysis. As expected, all the physical mixtures showed an obvious peak at

around 170 °C; however, there were peak shifts of approximately 2–3 °C, possibly owing to interactions between APAP and the polymers. During the heating process, all the extruded samples, except formulation III-6 (50% EC), had smaller peaks (or no peaks at all) than the physical mixtures did. This indicates that APAP dispersed or dissolved in the molten polymer matrix during the HME process to form a homogeneous solid dispersion. However, for formulation III-6, owing to the hydrophobic properties of EC N14 and, hence, its low miscibility with APAP, the APAP only partially dissolved in the EC polymer matrix. As a result, most the APAP was dispersed as its crystal form in the matrix.

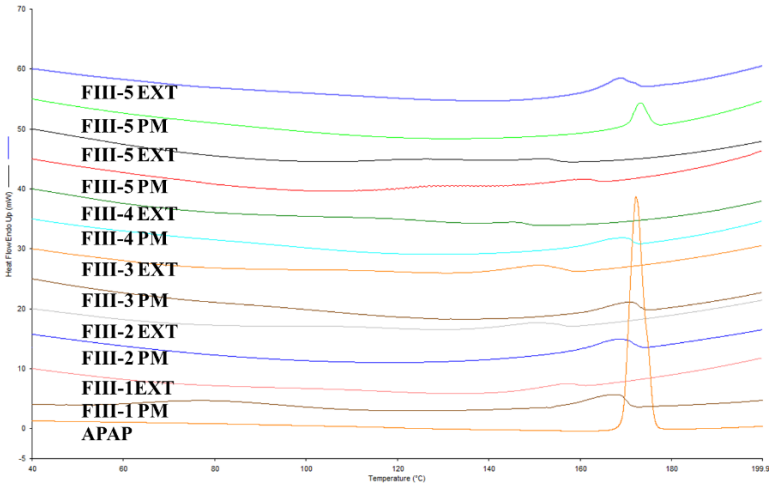

Figure 7. DSC results for physical mixtures and milled extruded filaments.

1.3.2. Fabricating 3D-printable filaments

As shown in Figure. 8 very brittle filaments were broken by the feeding gear. Similarly, filaments that were too soft were squeezed aside by the feeding gear. Viscosity is an important parameter to consider when formulating filaments for 3D printing. Therefore, we carried out optimization studies on the formulation composition and HME processing parameters. Most commercially available 3D printers were designed for the plastics industries. As a result, they mostly print plastic-like filaments, such as acrylonitrile butadiene styrene and PLA because they

possess proper stiffness, toughness, and melt viscosity. In the present study, we used PLA as a reference to compare the differences between commercially available filaments and extruded filaments.

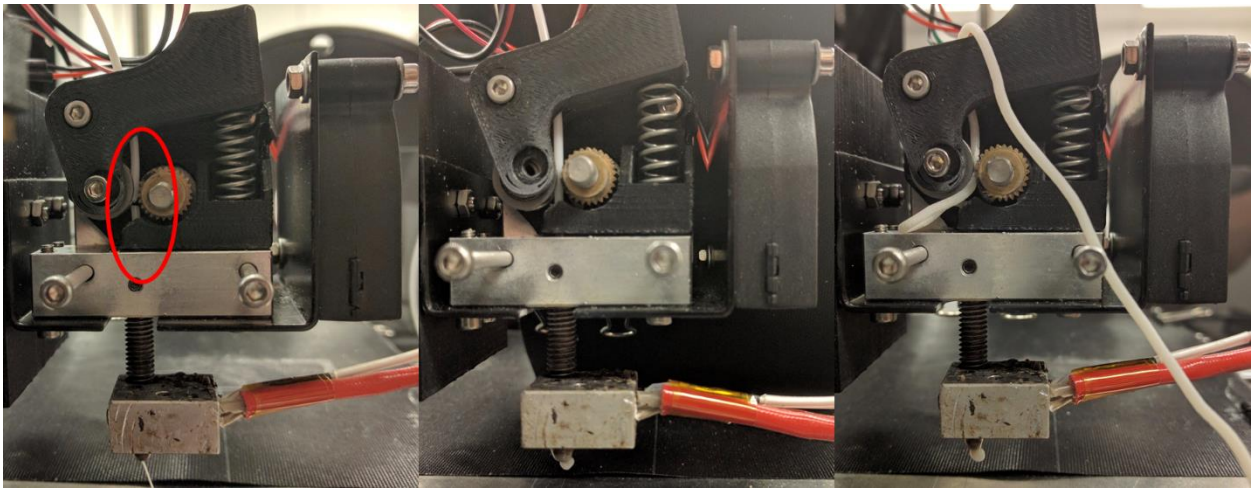

Figure 8. Filament properties during 3D printing process. a) Filaments too brittle; b) filaments good for printing; c) filaments too soft.

One of our goals was to fabricate filaments with adequate mechanical property using a pharmaceutical HME process suitable for use with most commercially available 3D printers. Stiffness is one of the most important parameters for judging whether a filament could be well fed into a 3D printer or not. It is used to describe the mechanical properties of a structure, as the "load" needed to achieve a certain "deformation".

$$\text{Stiffness} = \frac{Load}{Deformation}$$

There are varieties of possible configurations of the "load" (force, stress, arbitrary groups of forces, etc.) that acts on a structure. In addition, there is an infinite number of possible points in a structure, where deformation (displacement, angle, radius, curvature, etc.) can be measured [26].

A strong filament will require a high breaking force. However, the filaments we manufactured were not homogenized. In addition, their diameters varied because of the factors involved in the HME process (e.g., feeding rate and conveyor belt speed); therefore, stress (ratio of force to cross-sectional area) was taken to represent the actual stiffness of a filament. Furthermore, in this study, the Figure 7. DSC results for physical mixtures and milled extruded filaments. breaking stress was considered as "load" and the breaking distance was considered as "deformation".

Brittleness is another important parameter for judging filaments. The ability of a structure to deform plastically before it fractures is called its ductility. "Brittle" is the term used to describe a structure that has low ductility [27]. According to this definition, when force is applied to a brittle structure, it breaks without significant deformation (breaking distance). The 3-point bending flexural test is used to assess the breaking force, breaking distance or time (which is the time a blade touches a material to the time it breaks), and the flexural stress of a material. In this study, "stiffness" (breaking stress) and "brittleness" (breaking distance) were used to qualify the filaments. The stiffness of the extruded filaments was calculated from the breaking force and breaking distance values obtained from the 3-point test.

The aim of this study was to manufacture filaments with good mechanical and rheological properties, as well as tablets with desired drug dissolution and release properties. More than 10 batches of each filament type were printed and tested to ensure that they could be well fed into the printer and be printed for more than 6 times. Filaments that passed this test were referred to as being "Adequate" for 3D printing. Only 3DP tablets formulated using the third strategy were used the *in vitro* drug release study; therefore, only the necessary data are shown in this section to clarify the limitations of the 3DP operation.

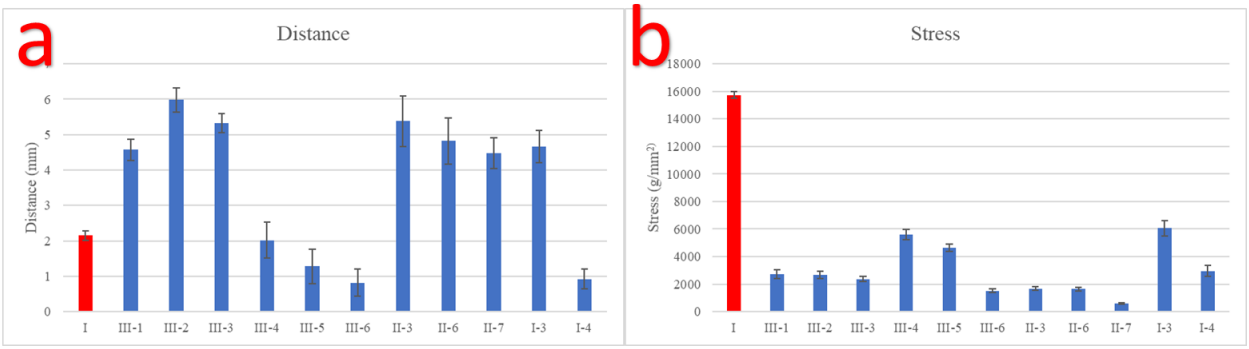

Figure 9. Filament 3-point bend test results of a) breaking distance and b) stiffness (breaking stress).

As shown in Figure 9, in the first stage of extrusion of single-polymer formulations, we found that the HPMC filaments displayed high stiffness (high breaking stress) and toughness (high breaking distance); however, the filaments had rough surfaces. The HPMC filaments could be fed into the printer; however, printing was difficult because of their rough surfaces and high melt viscosities. The EC filaments displayed good stiffness; however, they were very brittle (small breaking distance) and got easily broken by the feeding gear. The HPC LF and EF filaments were too soft and flexible to be fed into the printer. However, Soluplus1 and Eudragit1 L100 could not be extruded into filaments at high temperatures (140 °C), as they melted completely.

Table 2. Filaments 3-point bend test results. (n=10, mean±SD)

	Force (g)	**Distance (mm)**	**Stress (g/mm^2)**	**Strain (%)**	**Property**
I	1206.25±18.92	2.15±0.14	15740.58±235.69	80.54±0.23	Adequate*
III-1	445.73±30.80	4.58±0.30	2722.14±325.36	234.23±9.81	Adequate
III-2	183.99±45.13	5.98±0.35	2676.83±284.91	72.30±3.63	Adequate
III-3	243.75±18.19	5.32±0.27	2371.49±180.01	84.08±0.69	Adequate
III-4	584.62±49.27	2.02±0.50	5610.81±377.69	92.16±0.94	Brittle

III-5	621.86±36.05	1.28±0.49	4647.50±279.18	102.69±0.97	Brittle
III-6	283.42±21.67	0.82±0.38	1517.19±114.48	267.49±1.98	Adequate
II-3	320.13±26.64	5.38±0.72	1676.56±132.01	243.99±10.21	Soft
II-6	283.54±22.54	4.82±0.66	1633.29±129.26	236.92±3.72	Soft
II-7	98.65±6.67	4.48±0.44	578.83±48.31	233.97±3.35	Soft
I-3	673.86±61.66	4.66±0.46	6056.44±551.90	87.00±0.85	Adequate
I-4	323.29±45.14	0.92±0.28	2941.28±404.92	94.05±0.52	Adequate

*Adequate: 10 batches of each filament were tried during printing, if it can be printed without break or squeezed aside more than 6 times, we define the filaments is “adequate” for 3D printing.

For the second stage of the formulation screening, HPMC and EC were blended with HPC, Soluplus1, and Eudragit1 to prepare filaments for 3D printing. As seen in Figure 9 and Table 2 PLA had the highest force, stiffness, and stress values. In addition, filaments prepared from it were perfectly printed. Although the breaking distances of filaments II-3, II-6, and II-7 were high (>4.48±0.44 mm), their breaking stresses were approximately 1700 g/mm^2, which indicated that the filaments were too soft to be fed into the 3D printer. No high breaking stress limits were observed; however, for the HPMC formulation, the filaments were too hard and rough, which cause high friction during the feeding process. In 3rd stage study, 5% w/w Kollidon CL-F were added into the formulation, which can smooth the surface of the filaments, especially the HPMC based formulations, which can reduce the friction during feeding of the 3D printing process and made the filaments printable. In summary, a filament must simultaneously have high a breaking stress, a high stiffness, and a long breaking distance to allow for optimum printing.

During the printing process, all formulations prepared using the third strategy could be printed; however, formulation III-6 was somewhat brittle and was occasionally broken by the feeding gear. Formulations II-3, II-6, and II-7 were soft and had low breaking forces and stresses;

however, their breaking distances were large, which indicated softness of the filaments. Formulation I-3 produced the stiffest filaments and had favorable mechanical properties for 3D printing. The data indicate that, to fabricate extruded filaments for use with different models of 3D printers, the filaments should be adequately stiff (breaking stress > 2941 g/ mm^2) and brittle (breaking distance > 1 mm), as these can help in achieving optimal feeding and printing conditions.

Furthermore, the roughness and rheological properties of filaments can influence the printing process. High-melt viscosity can affect both extrusion and the 3D printing process. It can result in the production of filaments with rough surfaces, which can block the nozzle or disrupt extrusion during the printing process. However, further rheological studies on the filaments should be carried out.

1.3.3. Tablet morphology studies

In the formulation screening using the third strategy, all the formulations prepared were printed well; however, the tablets prepared from formulations III-4 and III-5 were much darker in color. This could have been due to degradation of the drug and/or the polymer(s) during the thermal processing. As a result, further work was not carried out on the two formulations. Images from the tablets morphology study and SEM analyses revealed that the 3DP tablets had smooth surfaces and a tight structure. Moreover, hardness testing and theoretical geometry calculations showed that the 3DP tablets had a higher density and hardness than the directly compressed tablets did. The mean hardness of tablets prepared from formulation III-1 was 24.7 ±4.2 kp. However, the hardness of 3DP tablets prepared from formulations III-2, III-3, and III-6 were above the upper limit of the hardness tester and much higher than the hardness of the directly compressed tablets (17– 28 kp). The volume of each cylindrical tablet was calculated as follows:

$$V = \frac{\pi D^2}{4} * h \qquad \text{Eq 1}$$

Where the D is the diameter of the tablets, and h is the thickness of the tablets. Thus, the theoretical density of a tablet was calculated according to the following equation:

$$\rho = \frac{m}{V} = \frac{4m}{\pi D^2 * h} \qquad \text{Eq 2}$$

Where the m is the weight of the tablet. As shown in Table 3, the theoretical density of 3DP tablets is much higher than that of directly compressed tablets. In addition, tablets with high hardness and density values show delayed disintegration and slow drug release after administration.

Table 3. Geometry study of the tablets. (n=6, arithmetic mean±SD)

Tablets		**Diameter (mm)**	**Height (mm)**	**Weight (mg)**	**Density (mg/mm^3)**	**Hardness (kp)**
I	3DP	10.15±0.09	4.50±0.04	375±27	1.029	>35
III-1	3DP	10.11±0.42	4.46±0.04	416±16	1.162	24.7±4.2
	EXT	9.53	4.79±0.01	~400	1.171	5.4±1.1
	PM	9.53	4.86±0.02	~400	1.154	18.0±1.4
III-2	3DP	10.03±0.45	4.42±0.10	436±12	1.248	>35
	EXT	9.53	4.62±0.01	~400	1.213	7.1±0.8
	PM	9.53	4.73±0.01	~400	1.185	14.4±0.9
III-3	3DP	10.22±0.21	4.47±0.02	440±9	1.199	>35
	EXT	9.53	4.58±0.03	~400	1.224	7.5±0.4
	PM	9.53	4.78±0.01	~400	1.173	20.9±1.1
III-6	3DP	10.24±0.18	4.21±0.19	408±14	1.178	>35
	EXT	9.53	5.83±0.02	~400	0.958	6.8±0.9
	PM	9.53	5.09±0.01	~400	1.102	13.6±0.9

As shown in Figure 10, the intensity of the yellow color of the formulations was in the order of 3DP > EXT > PM, which reflects changes in the crystalline state of the API after the thermal processes. According to the DSC results, most of the API dissolved in the molten polymer matrix. Physical mixtures contained the excipients in their amorphous states because of the mixing and high shear stress involved in the melt-extrusion process. Although no mixing and shear stress

are involved in the 3D-printing process, the high processing rate involved can cause the melting matrix to change to an amorphous state.

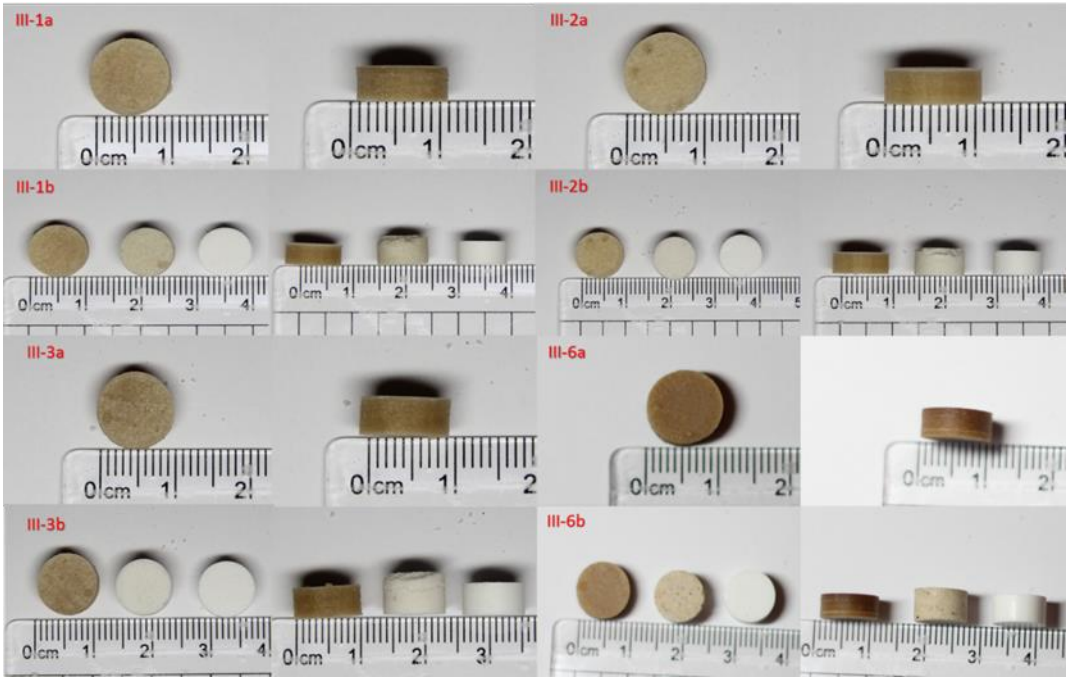

Figure 10. a) 3D-printed tablets; b) 3D-printed tablets (left), extrudate tablets (center), physical mixture tablets (right).

The different formulations contained similar components and therefore had similar structures. As a result, the SEM data for only one formulation have been presented (Figure 11). The upper images (Figure. 11a) show the internal layers of the tablets. Since the tablets were split for analysis, the single-layer structure was destroyed; therefore, an uneven layer is seen. The images at the center (Figure.11b) show a perfect layer structure of the tablets; however, the layers are not homogenous, which may have resulted from variations in filament diameter during the HME process. Constant processing parameters will get homogenous filaments, or a constant diameter of the filaments. The variations could have been due to the constancy of feeding speed, melt viscosity, or conveyor belt speed. The images in the lower panel (Figure. 11c) show some

spaces between the particles forming the tablets, which may have been caused by the high-melt viscosity of the materials. Furthermore, the spaces in the tablets could indicate that the 3D-printing process did not occur smoothly. Variations in the weights of the tablets were <0.6% and within the accepted range of <5% according to the USP 2091 guidance on weight variation of dietary supplements.

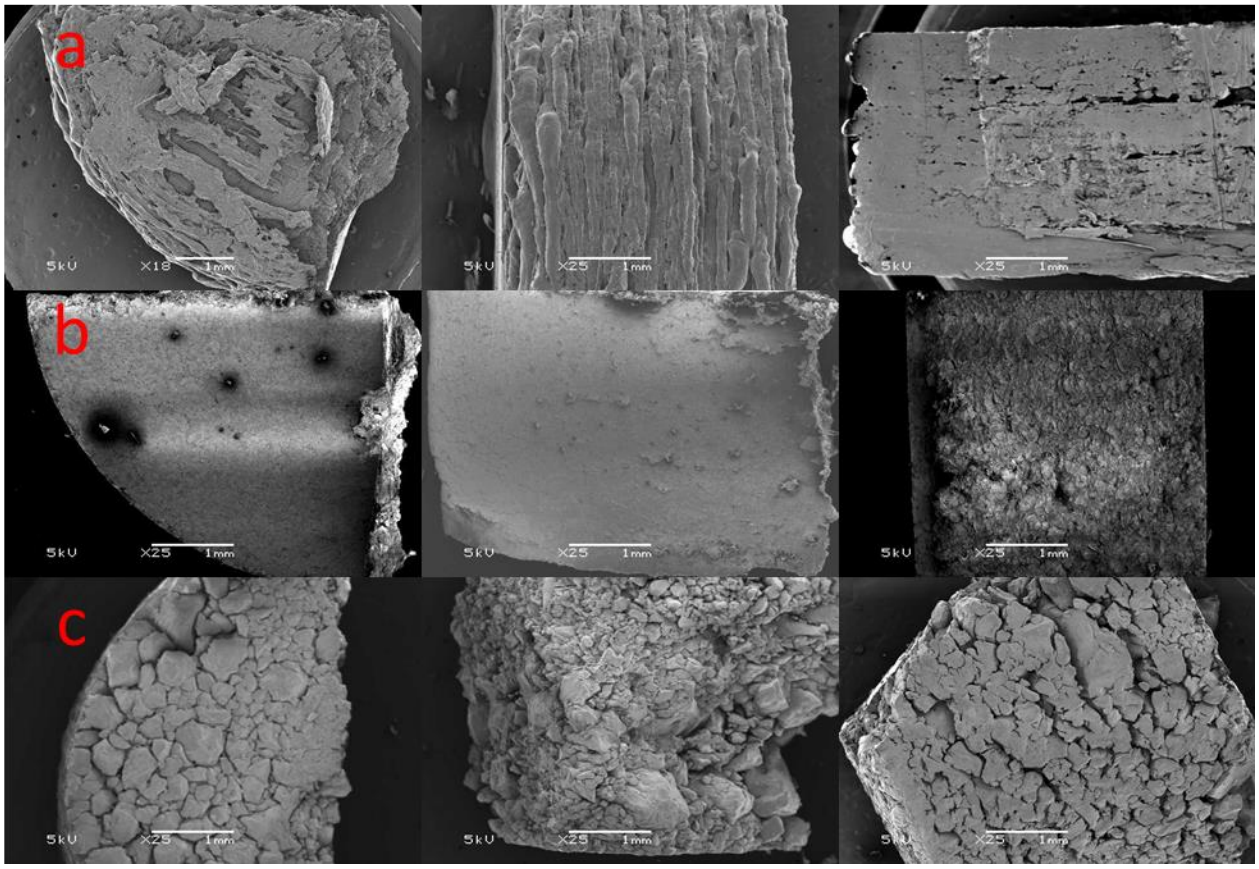

Figure 11. SEM images of formulation. a) 3D-printed tablets; b) direct-compressed physical mixture tablets; c) direct-compressed extrudate tablets.

According to the SEM images obtained for the PM and EXT tablets, no single particulate could be seen in the 3DP tablets, which indicate that the tablets were continuously structured and had homogenous compositions. Because of the special structure of the 3DP tablets, they

disintegrated at a slower rate than the other two types of tablets did, or perhaps the 3DP tablet can only dissolve, rather than disintegrate. It was observed that the particle size of the EXT tablets was larger than that of the PM tablets. Therefore, the expected order of tablet disintegration rate, and hence, drug release rate, was EXT > PM > 3DP.

1.3.4. *In vitro* drug release study

The 3DP, directly compressed EXT, and PM tablets were evaluated for their drug dissolution rates. Poorly water-soluble APIs can disperse or dissolve in polymer matrices to form solid dispersions or solutions during the HME process [28]. As expected, all the 3DP tablets showed good extended drug release rates because of their high density and hardness, which were due to their tight 3D structure (Figure 12). Faster drug release rates were observed with the directly compressed EXT and PM tablets. Formulations III-1, III-2, and III-3 showed 80% drug release within 6–10 h, whereas the 3DP tablets released APAP over a longer period (III-1: 87%, III-2: 63%, and III-3: 72% drug release after 10 h, respectively). The EXT tablets released APAP faster than the PM tablets did. This was because the APAP dissolved in the hydrophilic polymer matrix and formed a solid dispersion during the HME process. All the groups of tablets except those prepared from formulation III-6 (hydrophobic matrix) achieved 100% drug release within 24 h of the *in vitro* dissolution study. This proved that no API or excipient degradation occurred during the HME or 3D printing process.

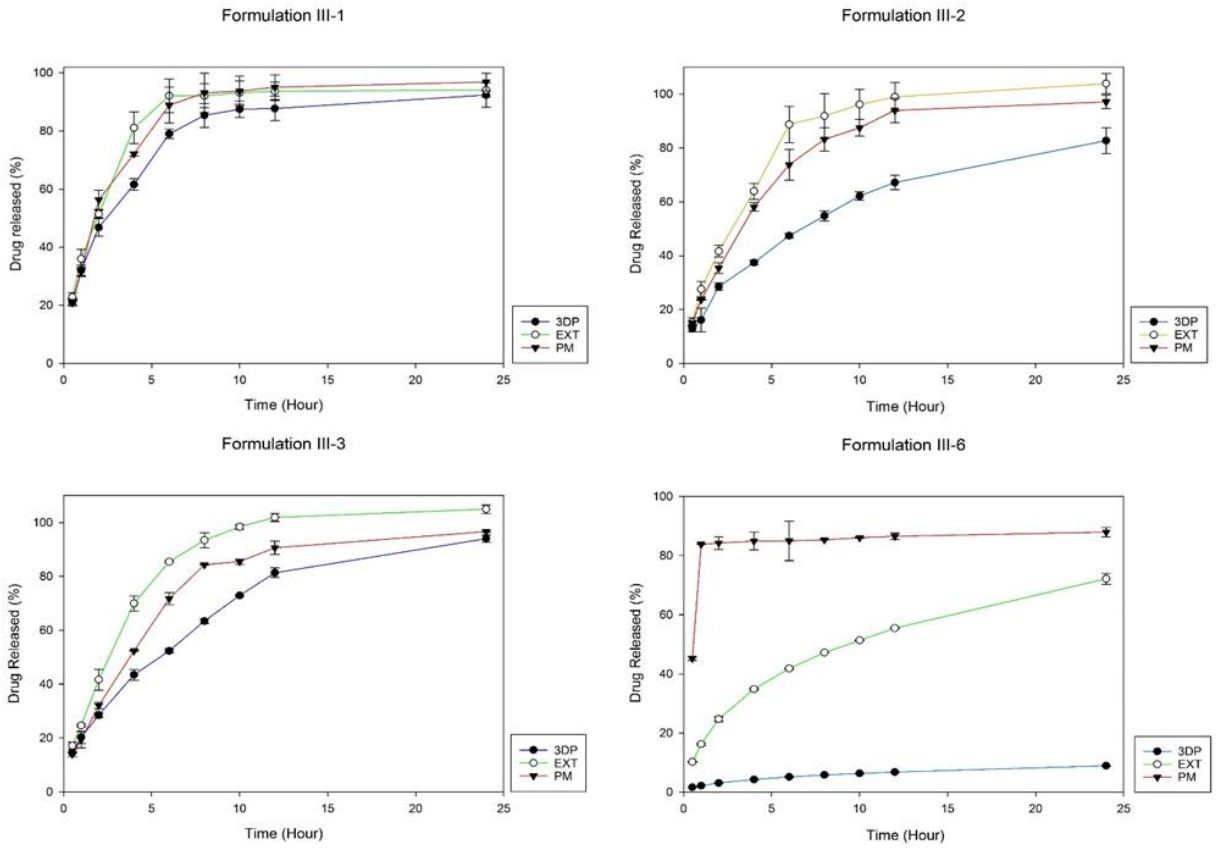

Figure 12. *In vitro* drug release study of 3D-printed tablets, direct-compressed extrudate tablets, and physical mixtures.

EC is soluble in various solvents but barely soluble in water. The PM tablets directly compressed from formulation III-6 showed an 80% drug release in 1 h, because the tablets disintegrated rapidly in the dissolution medium. However, the EXT tablets prepared from formulation III-6 showed an extended drug release rate (55.48% at 12 h and 72.19% at 24 h). Formulation III-6 can be considered as a partially solid dispersion. This is because, in that formulation, APAP was dispersed in an EC polymer matrix only partially due to the thermal processes. This is also evident in the DSC data for the milled extrudates prepared from formulation III-6 (Figure 7). The 3DP tablets from formulation III-6 released only 8.90% of APAP within 24 h because of its continuous and homogenous 3D structure. The tablets did not disintegrate easily

and as a result, APAP was barely released from the matrix. The release rate of APAP from the 3DP and EXT tablets was controlled due to its entrapment in the EC hydrophobic matrix.

As mentioned previously, the 3DP tablets barely disintegrated in the dissolution media because of their tight 3D structure. After the 24-h *in vitro* drug release study, formulations III-2 and III-3 dissolved; however, formulation III-1 produced some flocculent precipitates in the dissolution media. Moreover, formulation III-6 maintained its original shape almost throughout the study period.

Due to the structural design of the 3DP tablets, the printed tablets prepared from the different formulations displayed identical 3D structures and had approximately similar densities and hardness. The differences among the drug release rates from the various 3DP tablets were mainly attributable to the different formulation compositions.

The drug release profiles for all the 3DP tablets are shown in Figure 12. It was observed that drug release rate was in the order of III–1 > III–3 > III–2 > III-6. Formulation III-1 was a combination of hydrophobic and hydrophilic polymers and was expected to have a better extended drug release rate than formulations III-2 and III-3. This is because the API was dispersed mainly in the HPMC rather than in the EC polymer matrix, as was confirmed by the DSC results. The APAP peak was more notable in the thermogram for formulation III-6 than it was in the other thermograms (Figure 7). The total amounts of APAP released from formulations III-1, III-3, and III-4 were similar and were each much higher than the APAP amount released from formulation III-6, which supports the above hypothesis. HPMC E5 is more hydrophilic than HPC LF and EF are. In addition, HPC LF has a larger molecular weight (~95,000 Da) than EF has (~80,000 Da); thus, the drug release rates from the formulations were in the following order: III–1 > III–3 > III–2 > III-6.

1.4. Conclusions

In this study, we successfully fabricated solid-dispersion filaments with the API dissolved or dispersed in a polymer matrix by HME technology, which was suitable for FDM-based 3D printing. Extruded filaments prepared using binary polymer blends of HPMC E5 and EC N14 with either HPC EF and LF, Soluplus1, or Eudragit1 L100 were printed well. We also set up a preliminary standard to evaluate the physical and mechanical properties of the filaments that were suitable for 3D printing using a 3-point bend test. The 3DP tablets had a more consistent and elegant appearance, as well as better extended drug release profiles than the directly compressed tablets did. This study clearly demonstrates that coupling FDM-based 3D printing with HME offers a potential new method for manufacturing personalized-dose medicines and/or tablets, which can be prepared when needed.

CHAPTER 2

DEVELOPMENT AND EVALUATION OF THE PHARMACEUTICAL 3D PRINTABILITY OF HOT MELT EXTRUDED CELLULOSE-BASED FILAMENTS

2.1. Introduction

Nowadays, polymeric oral-controlled dosage development has been considered to be an economical and immediate consumption to reducing the inconvenience caused by the frequent dosing of conventional tablets, which can improve patients' quality of life (QOL) [29]. Furthermore, increasingly rising additive manufacturing (AM), also as known as 3D printing technology has provided a practical solution for individual, complex consumption for oral-controlled Drug delivery systems (DDSs). 3D printing is the layer-by-layer production of 3D objects from digital designs[11], and it is more efficiencies and economical compared with developing new active pharmaceutical ingredients or excipients, new manufacturing process, or protocols. 3D printing technology provides an alternative means of engineering release profiles by control of spatial distribution within a given polymer composition rather than creating a new host material[30].

Solid dispersions represent a promising formulation approach for overcoming today's major challenge in the pharmaceutical industry of developing bioavailable solid dosage form for more than 50% of drug candidates that are poorly water soluble[31][3][32]. Processing technologies such as spray drying (SD), hot-melt extrusion (HME), KinetiSol® dispersing (KSD), freeze-drying (FD), rotary evaporation (RE), co-precipitation (CP), centrifuge vacuum drying (CVD), and microwave technology [33] can be used for preparing the solid dispersions. Hot-melt

extrusion(HME) is the preferred option in pharmaceutical solid dispersion development because of the favorable powder properties generated from this technology, the absence of organic solvents in processing, the small footprint of the equipment, ease of increasing batch size, scalability from pilot to industrial setting, and suitability of continuous processing. [4][6]

HME is a term that the pharmaceutical industry adopted to differentiate it from traditional oral dosages manufacturing techniques, such as direct compression and tableting[5]. It involves the use of single- but mostly twin-rotor extruders for the processing of usually water-soluble polymeric excipients, mixing them while molten with APIs to affect partial or total API dissolution and pumping the homogeneous mixture through a die to form an extrudate, where the API exists in a totally or partially dissolved but (in both cases) stable form[34][10].

HME was firstly used to plastic and rubber industrial since the 1930s. Pharmaceutical hot melt extrusion (HME) is currently investigated by both industry and academia as a method for increasing the release rate of poorly water-soluble APIs and potentially enhance their bioavailability, by melt -mixing them with hydrophilic, water-soluble polymers[8]. HME helps to overcome poor bioavailability of active pharmaceutical ingredients (API), as well as creating new modified-release drug systems and can serve as a unit operation to taste mask the bitterness of a tablet. At the same time, an increasing body of literature is concerned with the production of controlled release dosages by melt-mixing readily water-soluble APIs with rate-controlling polymers[34].

Compared to the traditional pharmaceutical products manufacturing process, combine HME and 3D print technology as a continuous process will highlight each respective advantages: 1) increase the poorly water-soluble drugs solubility and bioavailability; 2) produce more complex structured dosages and personalized drug products. What`s more, combine this two technology

reduce the downstream process which will be more efficient and economical. In particular, the Food and Drug Administration (FDA) encouraged drug-makers to produce solid oral dosages that meet the increasing demands of oral drug delivery regarding bioavailability of the active pharmaceutical ingredients (API) and drug release characteristics, in a continuous and controlled process[22]. Several biodegradable polymers have been investigated by researchers, such as polyethylene oxide/polycyclooctene [23], ethyl cellulose (EC), hydroxypropyl methylcellulose (HPMC) E5[35], polyvinylpyrrolidone K30[24], and Eudragit® L100 [36], to print pharmaceutical dosage forms. Varieties of polymers and combination can be used for 3D printing. However, researchers rarely focus on the characterization and evaluation the filaments are suitable for 3D printing or not. This study aimed to characterize and the evaluate both physical and chemical properties of filaments designed for fuse depositional manufacturing additive manufacturing and produced by hot melt extrusion (HME) technology.

2.2. Materials and Methods

2.2.1. Materials

Acetaminophen (APAP) (Spectrum Chemicals, Gardena CA) was chosen as the model API. APAP is a crystalline BCS I drug with a melting point of 169°-170°C. AquaSolve™ hypromellose acetate succinate (HPMCAS) LG and HG, Benecel™ hydroxypropyl methylcellulose (HPMC) E5 and K100M, Klucel™ Hydroxypropyl cellulose (HPC) EF and HF, and Aqualon™ ethylcellulose EC N14 were donated by Ashland®. Diluted water was used for all formulations and solutions. All other reagents were of either HPLC or analytical grade.

2.2.2. Formulation

A variety of formulations have been tried and separated into 2 different stages in this study in total. Firstly, 7 different kinds and grades of pure polymer without drug-loaded polymer were

extruded. Then 7 formulations of single polymer with 30% W/W drug loading were tried. (Polylactic acid (PLA) without drug loading was used as reference) (table. 4) To get physical mixtures, raw materials were prepared and mixed by using Maxiblend™ (GlobePharma, New Brunswick, NJ, USA) at 25 RPM for 20 min, after passing through a US#30 mesh screen to remove any aggregates that may have formed.

Table 4. operation parameters and process trends for the 7 different formulations during HME process.

	T (°C)		Torque (N*m)		Pressure (bar)	
	without drug	PM	without drug	PM	without drug	PM
HPC EF	140	140	12	2.4	100	7
HPC HF	170	150	5.55	2	28.5	11.5
HPMC E5	190	150	8.4	4.26	47	23.5
HPMC K100M	N/A	190	N/A	6.7	N/A	77.5
HPMCAS LG	200	150	6.6	2.16	19	9
HPMCAS HG	200	150	4.6	4.32	6	10
EC N14	150	150	7.2	4	45	20

2.2.3. Pre-formulation Analysis

2.2.3.1. Thermogravimetric analysis (TGA)

All samples were prepared with open aluminum pans. A Perkin-Elmer TGA 1-Pyris (PerkinElmer, Inc, USA) were used to heat samples from 30 °C to 500 °C at 20 °C/min. Ultra-purified nitrogen was used as a purge gas with a flow rate of 25 ml/min. Data collection and analysis were performed using PerkinElmer Pyris™ software and % mass loss and/or onset temperature were calculated.

2.2.3.2. Differential scanning calorimetry (DSC)

All samples were prepared with TA aluminum pans and lids (Tzero) with an average sample mass of 5–10 mg. Measurements were performed on a TA Instruments Discovery DSC 25

(TA Instruments, USA) with a heating rate of 10 °C/min, a heat-cool-heat circle was used to for the conventional physical mixtures. Ultra-purified nitrogen was used as a purge gas with a flow rate of 50 ml/min for all the experiments. Data were collected and analyzed with TA Instruments Trios software. All melting temperatures were reported as extrapolated onset unless otherwise stated.

2.2.3.3 Polarized light microscopy (PLM)

Polarized light microscopy observations were conducted with a polarizing microscope LEICA DM 2500 P, equipped with a video-recorder camera and a hot thermostated stage TMS 94 (Linkam Scientific Instruments Ltd.) connected to the temperature programmer. All samples was heated from 25°C to 220°C at 10 °C/min, and videos were recorded from the start until cooling to room temperature.

2.2.4. Preparation of the 3D printable filaments

A Thermo Fisher Scientific twin screw co-rotating process 11 extruder with standard screw design and an Antaris II inline NIR probe inserted as a PAT tool was utilizing the 3D printable filaments preparation. All physical mixtures were extruded at 50 RPM, and the temperature setting for different formulations are listed in table 4. A 2 mm round shape die used for extrusion filaments for a 3D printer. A conveying belt was used to cooling and make the filaments straight in order to feed into the 3D printer.

2.2.5. Characterization and evaluation the filaments

2.2.5.1. Mechanical properties

Flexibility, brittleness and stiffness properties of the filaments were evaluated to represent the printability of the filaments. For Flexibility and brittleness analysis, extruded filament samples were collected and cut into 5mm in length. TA-XT2 analyzer (Texture Technologies Corp, New York, USA) and TA-95N 3-point bend probe set with 25mm supporting gape were used to test the

brittleness of the extruded filaments. The blades moving speed is 10 mm/s until reach 15mm below the samples. Each single formulation filaments were repeated 15 times. Breaking distance and load force/stress data were collected and analyzed by Exponents software. For stiffness analysis, filaments samples were collected and cut into 5 mm in length, the experiment set up was same as the 3-point bend test, but the sample holder was a solid flat metal. The blade will cut into the sample for 35 % shape change (0.6 mm), and breaking stress/force data were collected. Each single formulation filaments were repeated 15 times as well.

2.2.5.2. Crystallinity of the extruded filament

All the extruded samples were milled using a home-style coffee grinder and then sieved using 40 mesh. A single heat circle was used to check the melting properties of the milled extrusion samples.

2.2.5.3. Powder X-ray diffraction

XRPD analyses were performed on a Bruker D8 Focus™ diffractometer with Cu radiation. Diffracted radiation was detected by a LynxEye™ Position Sensitive Detector. The X-ray generator power was set to 40 kV and 40 mA. A silicon standard was analyzed to check instrument alignment. The sample was packed on a 25 mm poly(methyl methyacrylate) (PMMA) holder to form a disc-shaped specimen. The specimen was analyzed with a continuous scan from 4° to 40° 2θ.

2.2.5.4. Rheology analysis

Raw materials and milled extrudates were prepared for the rheology analysis. A dynamic viscosity rheometer was used for frequency sweep studies, which was running at 170 °C from 1-100 rad/s for all samples. A temperature sweep all conducted for all the samples at 1 rad/s from 100 °C to 180 °C.

2.2.6. 3D printing

The tablets were designed using Microsoft 3D Builder (Microsoft, Redmond, WA, USA) and converted to .gcode files using CURA software (version 15.04; Ultimaker, Geldermalsen, The Netherlands). Tablet dimensions (diameter, 10 mm; thickness, 4.5 mm) were determined based on the drug load. Tablets were fabricated with the extruded filaments using a commercial FDM-3D printer (Prusa i3 3D desktop printer, Prusa Research, Prague, Czech Republic) with an extruder, which had an E3D V6 hot end and a 0.4-mm nozzle. The following printer settings were found to produce the best tablets: a standard resolution with the raft option activated and an extrusion temperature of 200 ˚C. The other settings used were as follows: bed temperature, 50˚C; printing speed, 50 mm/s; nozzle traveling speed, 50 mm/s; layer height, 0.10 mm; and outside shell thickness, 0.4 mm. The infill percentage was set at 100% to allow printing of tablets with optimum characteristics. The dimensions and weights of the 3DP tablets were then measured.

2.2.7. Assessment of tablet morphology

A VWR1 digital caliper (VWR1, PA, U.S.) was used to determine the diameters and thicknesses of the tablets, and a Canon 60D camera was used to image the tablets (Canon, Tokyo, Japan). Cross-sectional images of the 3DP tablets, extrudate tablets, and directly compressed tablets were taken using electronic scanning micros- copy (SEM).

2.2.8. Determination of tablet strength

A standard tablet hardness tester (VK200; Agilent Technologies, Santa Clara, CA, USA) with a maximum force of 35 kp was used to measure tablet hardness. Six tablets from each group of tablets were tested.

2.2.9. *In vitro* drug release study

Drug release from the 3DP tablets was determined using a United States Pharmacopeia (USP)-II dissolution apparatus (Hanson SR8-plusTM; Hanson Research, Chatsworth, CA, USA).

Dissolution tests were conducted as per the US Pharmacopeial standards using Simulated Intestinal Fluid TS (without pancreatin) (pH 6.8), which is representative of the small intestinal fluid of humans. Each experiment was carried out in triplicate using 900 mL of the dissolution medium at 37±0.5 ˚C for 24 h. The paddle speed was set at 50 rpm. Samples were taken at 0.5,1, 2, 4, 6,8, 10, 12, and 24 h and analyzed. The amount of released APAP was determined by HPLC (Waters Corp., Milford, MA, USA) at 246 nm and analyzed using Empower software (version 2, Waters Corp.).

2.3. Result and discussion

2.3.1. Thermal stability of the materials

Thermal behavior of the pure APAP and each of the polymer matrix has been studied through TGA. The APAP presents a mass loss step starting around 260˚C which is attributed to the decomposition of the chemical structure of APAP. The mass loss recorded during the applied thermal protocol is continuous, and the final residue is 3.8%. All of the polymer excipients showed better thermal stability compared to the API, which won`t degrade until heat above 360 ˚C (figure 13). As mentioned in section 2.2.3 and Table 4, the process temperature was all below 200 ˚C, which means the high process temperature will not cause the degradation both of the API as well as the polymers.

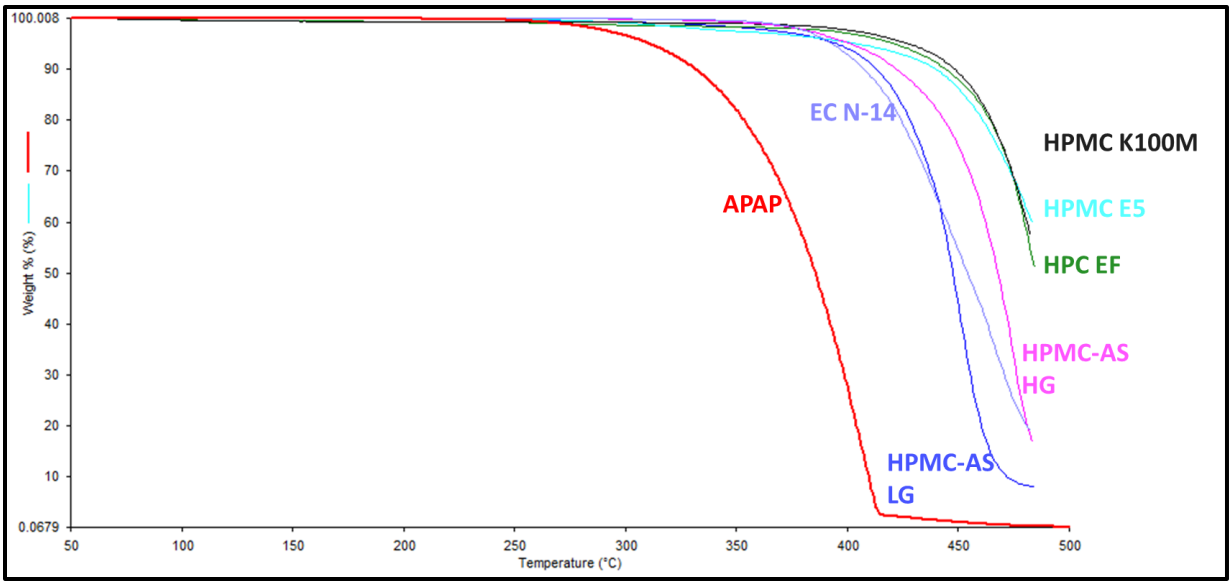

Figure 13. Thermal degradation graph of the APAP and polymer excipients.

2.3.2. Polarized light microscope (PLM)

PLM has been widely used to determine the melting behavior and crystalline transformation of all raw materials and physical mixtures[37]. Limited by the space, one of the same polymer matrix was shown in figure 14. The needle-shaped pure APAP shows the crystalline structure at room temperature, which is melted above 174 ˚C and completely transformed to the amorphous states. For HPC formulations, at the room temperature, the HPC matrix also showed crystalline structures as well, however, due to the particle size and crystalline shape we can easily tell the difference of APAP and HPC particles. Once heated above the melting point, the APAP can lose its crystalline structure but there still some HPC particles stayed in semi-crystalline shape, which indicating HPC matrix may have an issue to form an amorphous solid dispersion with APAP. For HPMC formulations, the polymer particles showed no crystalline structures, but there have some unmelted polymers after heating. In order to have the ASD, mixing zones (kneading blocks) are required to help the mixtures transfer from crystalline to amorphous. HPMCAS particles were not shown the crystalline structure, and the physical mixture can be completely molten while

APAP was dissolved and dispersed into the polymer matrix. For EC formulation, due to the thick and opaque molten mixtures, it is hard to visually confirm APAP was dispersed into the polymer matrix or not. DSC and PXRD studies were carried out to confirm the transformation and miscibility of the APAP with the polymer matrix.

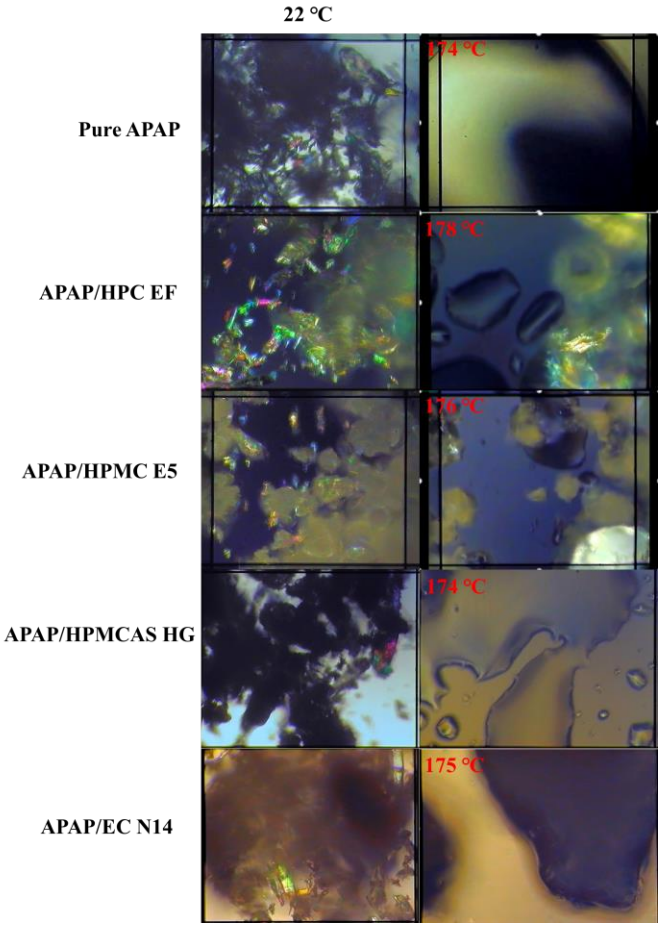

Figure 14. The melting behaviors and crystalline transformation under PLM.

2.3.3. Extrusion

Polymer without drug loading was extruded for reference objectives. However, due to the large molecular weight, HPMC K100M can`t be extruded below 220℃ with the standard screw design at 50 rpm. For the extrusion of the drug-loaded filaments, multiple in-line NIR spectra were collected continuously for monitoring the extrusion process. As shown in figure 15, multiple

spectra for each formulation except HPMC K100M grades were perfectly overlapped which proved the filaments were homogeneous and the high reproducibility of the extrusion process. Due to the massive molecular weight and high melt viscosity, the HPMC K100M grade formulation still hard to extrusion which also is confirmed by the high torque and die pressure during the extrusion process. Compared with the raw NIR spectrum with the pure API and polymers, we found that the peak area around 6000 cm^{-1} can be used to both qualify and quantify the APAP in the extrudates. The raw spectrum of extrudates showed that the signal at this range was decreased while the 2^{nd} derivative of the spectrum showed that peaks were slightly shifted to the lower energy side, which indicates the interaction between the APAP and the polymer matrix (figure 16). The APAP might act as the plasticizer and formed hydrogen bonds thus lowering the energy of the system during the extrusion process.

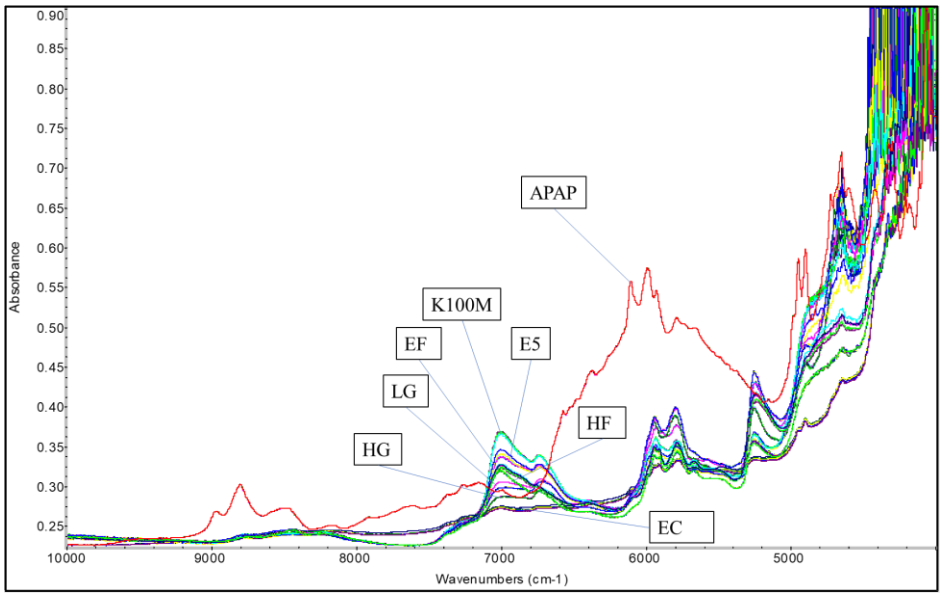

Figure 15. the raw inline NIR spectrum collected during the extrusion process.

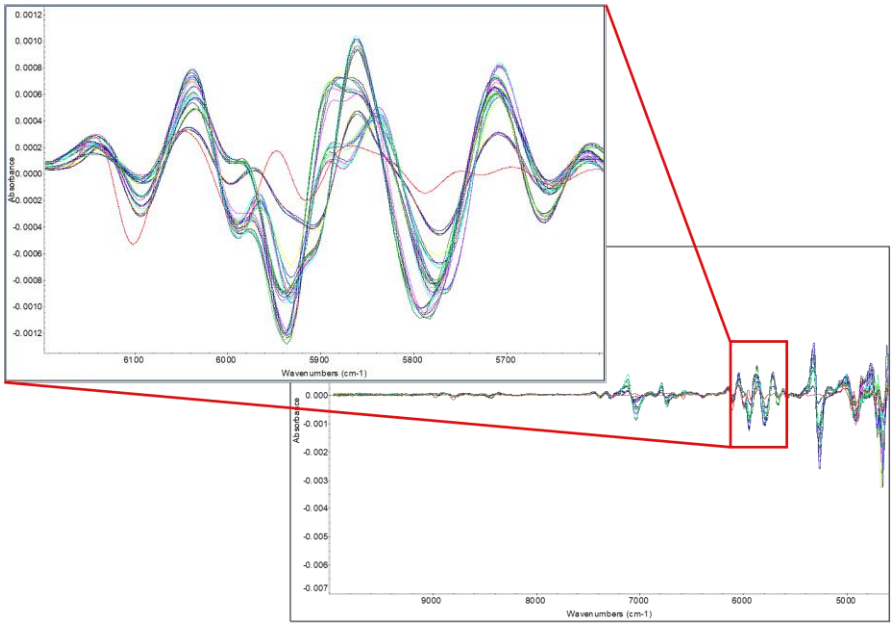

Figure 16. the 2nd derivative of the collected inline NIR spectrum during the extrusion process.

The extrusion parameters were recorded as well and presented in figures 17. Both the torque and die pressure, as well as the lowest extrudable temperature, will decrease when adding 30 % w/w APAP into the formulation, which indicating drug loaded physical mixtures represent good extrudability compared to the polymers without drug loading. AS observed from the mechanical characterization of the filaments, the extrudability and mechanical property were correlated. The higher extrusion torque and die pressure, the stronger and stiffer filaments will be obtained.

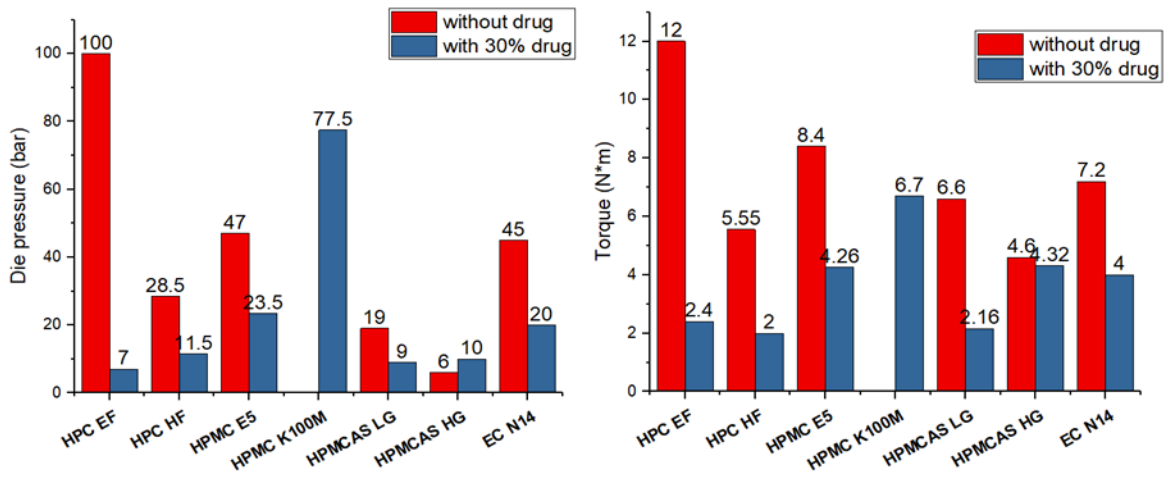

Figure 17 a) Process torque and b) die pressure of polymer without drug loading and with 30% APAP loaded formulations during HME process.

2.3.4. Filaments evaluation

The primary objective of this work is to manufacture the drug-loaded filament that can be widely used by a variety of FDM based 3D printers. Several physical and chemical characterizations were conducted in this work to determine the appropriate properties of the filaments can be printed. In the present study, we used PLA as a reference to compare the differences between commercially available filaments and extruded filaments.

2.3.4.1. Crystallinity

DSC studies were preformed to determine the crystallinity transformation during the thermal process. All the physical mixtures were heat and cool, then heated again, and apparently melting peak was observed during the first heating ramp which indicating the initial crystalline structures of the API. During the 2nd heating ramp, the melting peaks were disappeared except the HPC EF formulation showed the attenuated melting peak (figure 18 a)), which indicates the API was completely or partially dissolved or dispersed into the polymer matrix. All the extruded filaments were milled and applied for DSC analysis as well. As shown in figure 18 b), it showed

the similar results as the PM 2nd heating ramp. The HPC EF, HF and the EC formulation still showed the enthalpy of the melting which means there still consists the APAP crystalline, but it was attenuated compared to the melting enthalpy of their physical mixtures. All in all, the HME process allows conversion of API to amorphous form or dispersion of API in molecular level, which can result in enhanced bioavailability.

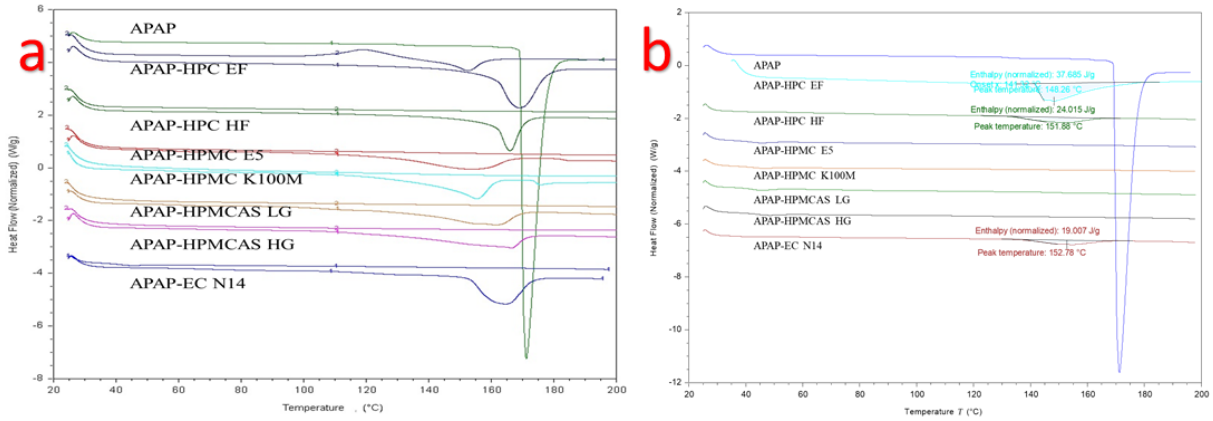

Figure 18. the DSC result of the a) physical mixtures and b) milled extruded filaments.

The FTIR techniques have been widely used in the analytical chemistry area especially in the organic compounds and the polymer analysis[38]. For APAP, it has the alcohol and amide functional groups which shall has the absorption peak around 3350 cm^{-1} and 3200 cm^{-1}, while the polymers has no nitrogen functional groups (figure 19 a)). As shown in figure 19 b), the APAP spectrum shows obviously the existence of the alcohol and amide groups. However, in the extrudates, HPC formulation still shown the -OH peak which means the APAP was just mixed with the polymer and in the other formulations, both the -OH and -NH peaks were decreased or disappeared which may due to the molecular level mixing or formation of the hydrogen bonds during the HME process.

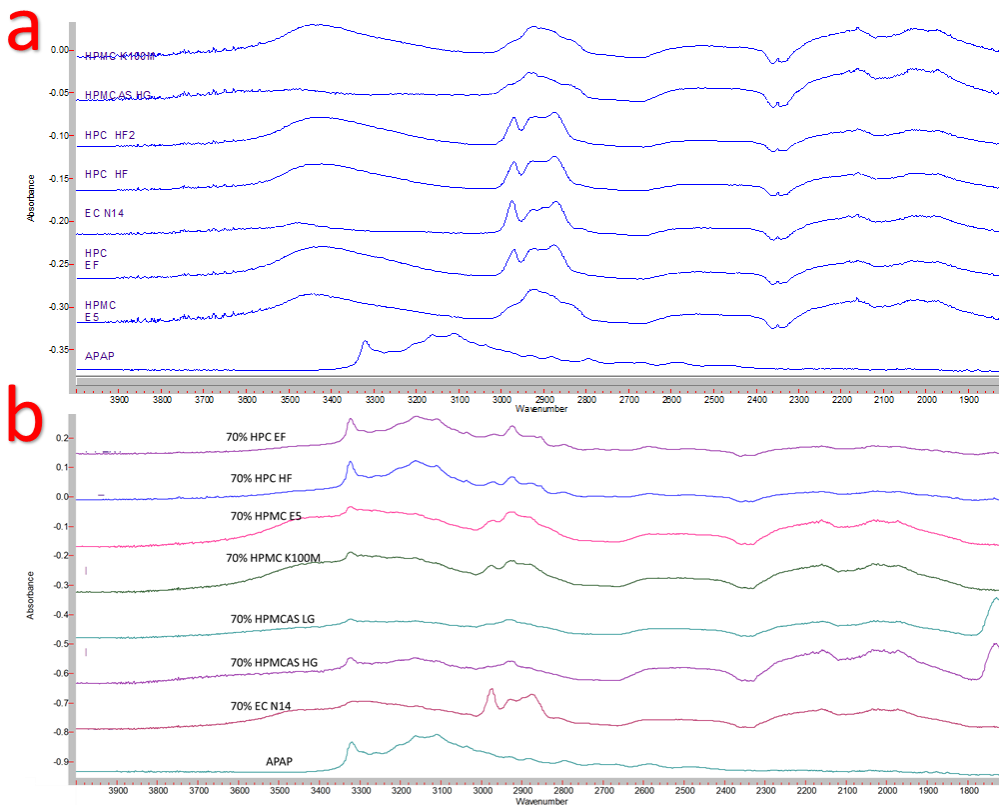

Figure 19. FTIR spectrum of the a) raw materials and b) milled extruded filaments.

X-ray powder diffraction (XRD) has been used for phase identification of crystallinity can provide information in unit cell level[39]. The extrudates were finely ground and homogenized. As shown in figure 20, the HPC EF, HF, and EC N14 formulation still show the crystalline structures of the APAP in the formulation, which indicating the poor miscibility of the APAP with such 2 matrixes. The XRD, FTIR and DSC data cross verified the crystalline transformation of the APAP during the HME process, APAP can be easily dissolved or dispersed into the HPMC and HPMCAS polymer matrix and form amorphous solid dispersions. On the other hand, APAP was hard to form an amorphous solid dispersion with HPC or EC matrix even with the help of the high temperature and mechanical force from the HME process.

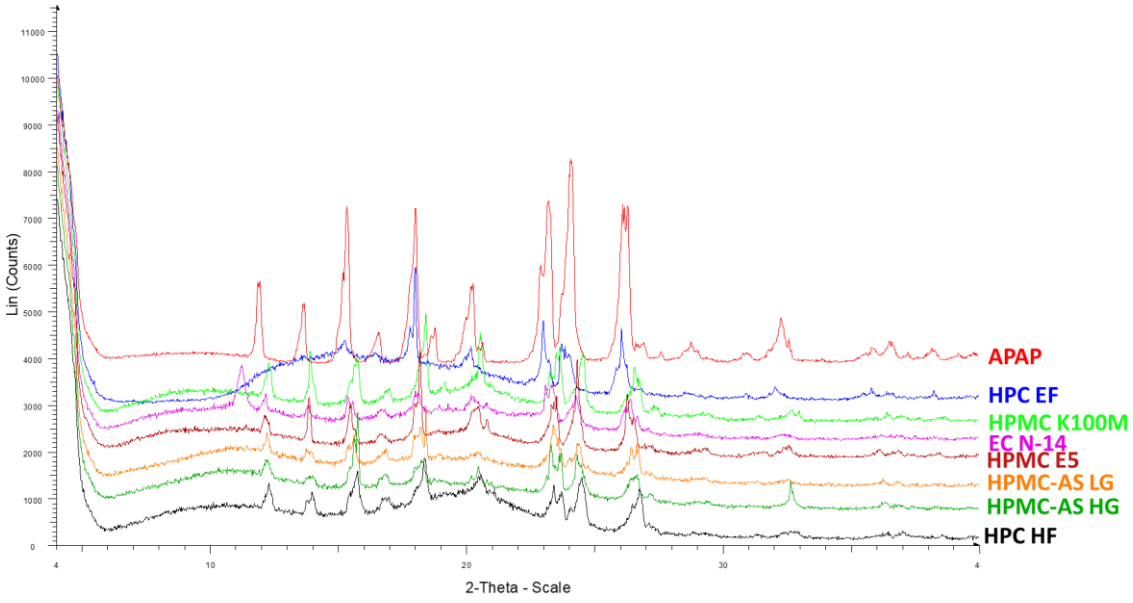

Figure 20. PXRD curve of the APAP and milled extruded filaments.

2.3.4.2. Mechanical properties of the filaments

The printability of different formulations were predominated by the mechanical and rheology properties of the extruded filaments. Filaments shall have adequate flexibility as well as strong enough to be printed. The FDM based 3D printing was developed from the plastic industry, and the PLA is one of the most widely used commercially available material on the market. In this work, PLA plastic was selected as the reference materials to evaluate the mechanical and rheological properties of the drug-loaded extruded materials.

The three-point bend test is a classic experiment in mechanics, used to measure Young's modulus of material in the shape of a strip, bar, or stick and so on. The material, of length L, rests on two supports and is subject to a concentrated load at its center[40].

Flexibility and toughness are two of the most critical parameters to determine the mechanical properties for judging whether a filament could be well fed into a 3D printer or not. In this work, flexibility can be defined that the tolerance of the filament the bending without breaking.

Moreover, the good toughness can be defined that when the filament subjected to the load, it breaks without significant plastic deformation. “toughness” is the term used to describe a structure that has high ductility[27]. The 3-point bend test is used to assess the breaking force, breaking distance or time (which is the time a blade touches a material to the time it breaks), and the flexural stress of a material. In this work, here the loading stress is used to represent the flexibility, and the breaking distance is used to represent the toughness of the filaments.

One of the primary purposes of this work was to produce filaments with adequate mechanical and rheological properties, as well as print tablets with expected drug release profiles. During 3D printing process, ten batches of each filament have been tried to ensure that they could be well fed into the hot end and be printed without more than six failures. Filaments that passed this test were referred to as being “Adequate” for 3D printing. In this work, it was observed that the HPC LF and HF filaments were too soft and flexible for the 3 point bend test as well as to be fed into the printer. Only HPMC E5, both HPMCAS HG and LG grades and EC N14 formulations can be successfully printed; therefore, only the necessary data are shown in this section to clarify the limitations of the 3DP operation.

As shown in Figure 21 a), all the listed filaments showed poor toughness compare to the reference materials; the HPMC filaments displayed similar flexibility while the other filament was not. The HPMC E5 filaments displayed proper flexibility (breaking stress>995.3 g/mm2) and toughness (breaking distance=1.389 mm); It seems HPMC K100M filaments showed proper mechanical properties and could be fed into the printer; however, printing was difficult because of the fraction caused by its rough surface and high viscosities at 200 ˚C. The EC filaments displayed neither flexible or robust (small breaking distance=0.341 mm) and got easily broken by the feeding

gear. Both HPMCAS grades were flexible than EC formulation but showed poor toughness, and these two filaments can be easily broken during the feeding process.

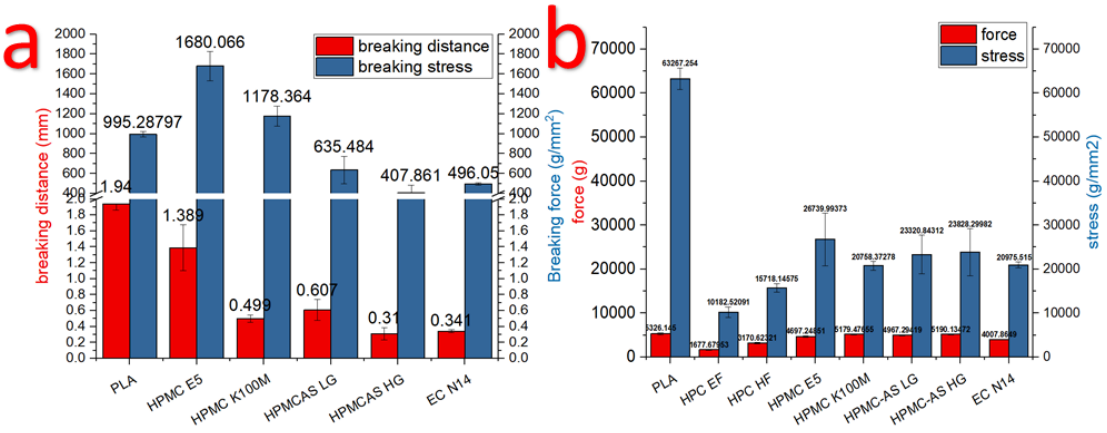

Figure 21. a) 3 point test results of the breaking distance and stress and b) stiffness test results of breaking stress and force of extruded filaments.

Stiffness is another critical properties to determine the printability of the filaments. It is used to describe the mechanical properties of a structure, as the “load” needed to achieve a certain “deformation.”

"Stiffness"= Load/Deformation

There are varieties of possible configurations of the “load” (force, stress, arbitrary groups of forces, etc.) that acts on a structure. In addition, there is an infinite number of possible points in a structure, where deformation (displacement, angle, radius, curvature, etc.) can be measured [26]. A strong filament will require a high breaking force; therefore, stress (ratio of force to cross-sectional area) was taken to represent the actual stiffness of a filament. Furthermore, in this study, the breaking stress was considered as “load,” and the blade move 0.6 mm after touching the filament was considered as “deformation.”

As shown in figure 21 b), the PLA plastic has excellent stiffness, and the extruded filaments were not as good as the reference material, which means they can be easily broken during the feeding process. As observed from the printing process, the HPC filaments were soft, and plastic deformation happened during the printing process, while the EC formulation shows very brittle and easily broken by the feeding gear. HPMC and HPMCAS showed proper stiffness, and there almost no plastic deformation or surface crack observed during the printing process.

From the observation, if the filaments intend to be widely used for a variety of 3D printers, it better has adequate flexibility (breaking stress >635.5 g/mm2), toughness (breaking distance >0.61 mm), and stiffness (20758.3 g/mm2). Alternatively, the other option is to adjust the force of the feeding system, make sure the force to convey the filament is smaller than 400.7 g.

2.3.4.3. Rheology characterization of the filaments

Furthermore, the roughness and rheological properties of filaments can influence the printing process. High-melt viscosity can affect both extrusion and the 3D printing process. It can result in the production of filaments with rough surfaces, which can block the nozzle or disrupt extrusion during the printing process. As shown in figure 22a, APAP showed plasticizer effect during the extrusion process, which results in the attenuation of the viscosity of the system when adding 30 % w/w APAP. In general, higher viscosity resulting in a rough surface and hard to extrusion and print. Here, drug-loaded EC N14 filaments have higher viscosity. However, the surface of this filament is smooth. Based on the observation and SEM pictures of each printed tablets, the HPMCAS tablets have fine appearance may due to the low viscosity of the formulation. Both HPMC tablets showed rough printing paths because of the relatively high viscosity compare to HPMCAS formulations. However, even though EC formulation has higher melt viscosity, the printed tablets still have a relatively fine appearance compare to the HPMC formulations.

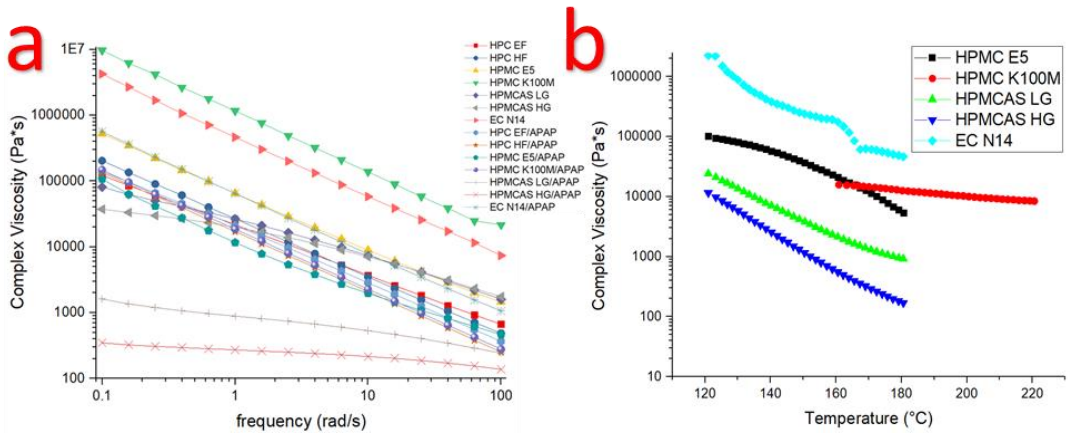

Figure 22. a) frequency sweep of the raw materials and drug-loaded extrudates; b) temperature sweep of the milled printable filaments.

2.3.5. 3D printing

From the characterization of the physical-chemical properties of the filaments, the printability of different formulations can be predicted. As expected, HPMC might be the perfect choice for FDM based pharmaceutical 3D printing because it can be smoothly printed without any failure. For the HPMC K100M grades, it cannot be printed through the printer because of the larger molecular weights which resulting in the high melting viscosity. Both HPC filaments were too flexible and soft to be printed, it was observed that the filaments would be pushed aside by the feeding gear, and the filament was not stiff enough to push the molten materials out of the nozzle. Both HPMCAS HG and LG formulations are a little bit brittle and lack of flexibility, which results in the breaking during feed into the hot end by the feeding gear. Even though, HPMCAS filaments can occasionally be printed, with average six failures per 10 prints. EC filaments also showed very brittly and some times can be printed, with average five failure per 10 prints. However, once the tablets successfully printed, it will have the smooth and homogeneous surface.

The appearance of the tablets was primarily affected by rheology properties of the materials. The printed EC tablets showed very smooth and homogeneous surface compare to the other tablets. Conjugation and adhesion were observed from the HPMCAS tablets, which due to the high melting viscosity. The HPMC E5 tablets were showed proper appearance and smooth surface (figure 23).

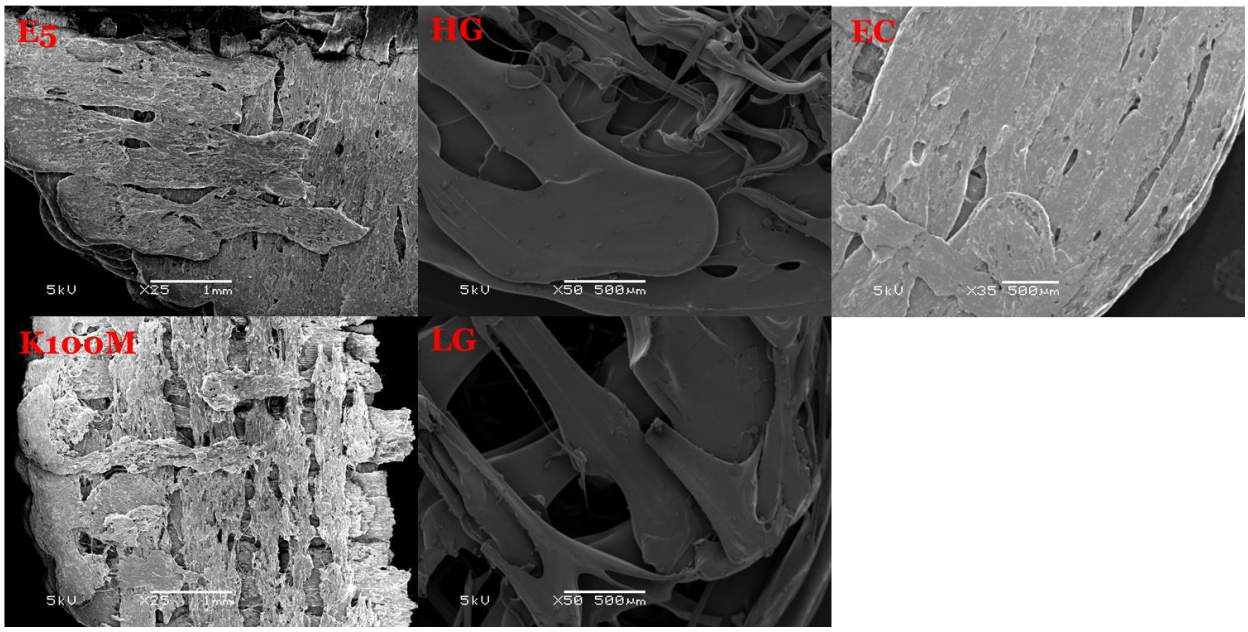

Figure 23. SEM pictures of the cross section of the 3D printed the tablets.

All the printed tablets seem “wider” and “shorter” than the designed dimensions, which may occur due to the cooling and solidification of the materials. The cooling and solidification take longer time resulting in the growing pressure from the just printed layer to the previous unsolidified layer. So the bottom part was slightly wider, and the height of the tablets was shorter than the designed dimensions. So further optimization of the printing speed and cooling time need to be done to grantee the quality of the 3D printed tablets. The weight is different for each formulation of the printed tablets wares between 4.5%-7.2% w/w. The weight variation may predominate by the rheology properties as well. As shown in table 5, the better flowability turns gives smaller variation (4.73% for EC and 4.77% HPMC E5 tablets), and vice versa, the higher

melt viscosity gives more considerable variation (6.54% for K100M, 7.11% for HG and 7.08% for LG tablets). So further studies on optimizing the formulations will be needed for pharmaceutical dosage development.

Table 5. Geometry study of the tablets. (n = 10, arithmetic mean±SD).

	Diameter (mm)	Thickness (mm)	Weight (mg)	Variation (w, %)	Hardness (kp)	Fail per 10 prints
HPMC E5	11.22±0.07	4.46±0.05	395.58±18.72	4.73	OV*	0
HPMC K100M	10.51±0.24	4.22±0.21	377.91±24.73	6.54	OV*	8
HPMCAS LG	10.33±0.28	4.40±0.22	366.93±26.12	7.11	32.8±5.6	6
HPMCAS HG	10.91±0.30	4.29±0.19	352.04±24.94	7.08	32.2±5.3	6
EC N14	10.47±0.16	4.42±0.05	354.19±16.92	4.77	23.8±6.5	5

**OV=over the limit.*

2.3.6. *In vitro* drug release

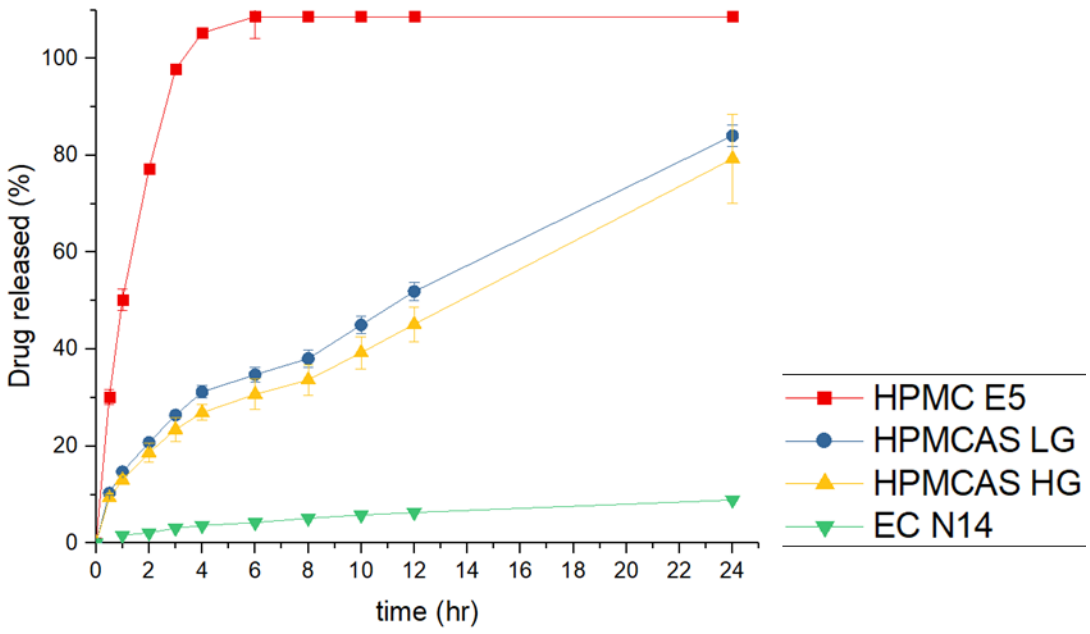

Figure 24. the *in vitro* drug release profiles of 3D printed tablets in SIF.

Dissolution tests were conducted in US Pharmacopeia Simulated Intestinal Fluid^{TS} (without pancreatin) (pH 6.8), more representative of human small intestinal fluid. It is apparent that the dissolution profiles show different behaviors. Poorly water-soluble API can disperse or

dissolve into the polymer matrix and form a solid dispersion or solution via HME process because of mixing of molten drug and polymers[41]. As expected, all HPMC E5 tablets have faster drug release rate because the HPMC matrix can form hydrogel rapidly and release the drug. Show 80% release after 2 h and reach 100% drug release in 4 h. The drug release from the matrix while the polymer matrix was also dissolved as well, so finally the tablet was dissolved entirely after 4 h.

AquaSolve^{TM} HPMCAS LG and HG tablets showed similar drug release profiles, and LG grade has faster drug release rates due to the high contents of the succinic groups (14-18%) compare to the HG grades (4-8%). Both LG and HG tablets can release APAP over an extended period (51% and 45% drug release after 12 h, respectively). The HPMCAS matrix also interacts with the water and formed a hydrogel, but not like the HPMC matrix, the drug can release from the matrix, but the polymer just absorbs the water and which can not completely dissolve in 24 h. So the drug released rates were predominated by the swelling speed and the matrix itself. As we can see from the drug release profiles, the drug released from the HPMCAS matrix was more steady compared to the drug released from the HPMC matrix. So the HPMCAS matrix was the better choice for the controlled released dosage development.

Aqualon EC is soluble in a wide variety of solvent but hardly soluble in water, which means the EC formulation may not cause erosion or swell in the dissolution media. The EC tablets just released 8.9% APAP at the end of the 24 h dissolution period. As mentioned in the previous discussion, most of the APAP has been dissolved or dispersed into the EC polymer matrix and formed a solid dispersion. So the polymer matrix stops the APAP release from the polymer matrix to the dissolution media, the drug released came from the undissolved APAP which was not entrapped in the polymer lattice or on the surface of the tablets. The tablets can not disintegrate as well, and APAP was hardly released from the matrix.

2.4. Conclusion

In this work, a variety of polymers have been tried for the manufacturing of the drug-loaded and 3D printable filaments. APAP was miscible with them and can dramatically improve the extrudability of the polymers. Also, the physical and chemical characterization showed that APAP could dissolve or dispersed into the HPMC and HPMCAS matrix and form the amorphous solid dispersions, while it can only partially disperse into the EC and HPC matrix. The mechanical characterization on the extruded filament showed that the HPMC E5 grades are good for 3D printing because it has proper flexibility, toughness, and stiffness. Both HPC filaments were soft even cannot feed into the 3D printer. EC filaments were very brittle and easily broken by the feed gear, it can be printed but need to be taken care during the printing process. Both HPMCAS filaments can be printed but not as good as the HPMC filaments. As predicted, the printed HPMC tablets showed fast drug release profiles while HPMCAS tablets were in controlled drug release rates. Moreover, EC formulation may good for the extend drug release dosage forms because the drug release rate was meager compared the other formulations. All in all, in this work, we successfully manufactured the drug-loaded filaments utilizing the pharmaceutical HME process. In addition, we also characterized the physical and chemical properties of the filaments for screening the filaments suitable for FDM based 3D printing or not. HPMC was a better selection for the new 3D print dosage development. This work also demonstrated the possibility of combining HME and 3D print technology as a continuous process. In future, optimizing the formulations such as combined two or more polymer matrixes, adding plasticizer or anti-plasticizer would be good direction for the 3D printable filaments developments.

CHAPTER 3

HYDROXYPROPYL METHYLCELLULOSE-BASED CONTROLLED RELEASE DOSAGE BY MELT EXTRUSION AND 3D PRINTING: STRUCTURE AND DRUG RELEASE CORRELATION

3.1. Introduction

Drug delivery systems (DDSs) are methods of administering active pharmaceutical ingredients (APIs) to achieve a therapeutic effect in humans or animals. They aim to ensure optimal drug distribution and absorption and improve efficacy and safety by controlling the rate, time, and target of drug release in the body [42]. Approaches for effective DDSs include controlled release formulations, in which the drug is released at a controlled rate over a set period of time and targeted delivery [44][43] in which the drug is only active in a targeted area of the body, such as in cancerous tissues [45][46]. Controlled release technologies can be broadly categorized into liposomal [47], electromechanical [48], and polymeric types [15]. The use of liposomes for controlled delivery has been widely studied, but *in vivo* instability and entrapment by the reticuloendothelial system are two major obstacles to be overcome [49]. The use of pumping devices to control the amount of drug released is in principle the most direct and sophisticated approach; however, osmotic pump systems are much more expensive and may be subject to dose dumping if the membrane breaks [50]. Polymeric controlled release systems, which use biodegradable, non-biodegradable, and soluble polymers as drug carriers, can be administered via parenteral, implantation, oral, insert, and transdermal routes [51]. Nowadays, polymeric oral-controlled release technologies are considered economical and immediately applicable in drug

development, improving patients' quality of life by reducing the inconvenience caused by the frequent dosing of conventional tablets [29]. Furthermore, the increased use of additive manufacturing, also known as 3D printing technology, provides an effective solution for individual, complex production of oral-controlled DDSs [52]. 3D printing is the layer-by-layer production of 3D objects from digital designs [11]. Compared with developing new materials for drug delivery, the development of new material fabrication tools and protocols is more efficient and economical. 3D printing technology provides an alternative means of engineering release profiles, by controlling the spatial distribution within a given polymer composition rather than creating a new host material [30].

Hot-melt extrusion (HME) is a manufacturing technique that, unlike traditional oral dosage manufacturing techniques, such as direct compression and tableting [5], generally involves the use of twin-rotor extruders that process water-soluble polymeric excipients, mixing them with APIs while molten to cause partial or total API dissolution, and pump the homogeneous mixture through a die to form an extrudate containing the API in a stable form [10].

HME has been used in the plastic and rubber industries since the 1930s. Pharmaceutical HME is currently being investigated by both industry and academia as a means to increase the release rate of poorly water-soluble APIs by melt-mixing them with hydrophilic, water-soluble polymers [8]. HME can help overcome poor API bioavailability, create new modified-release drug systems, and mask bitter tastes [53]. At the same time, an increasing body of literature exists on the production of controlled release dosages by melt-mixing readily water-soluble APIs with rate-controlling polymers.[54]

Compared to traditional pharmaceutical manufacturing processes, combining HME and 3D print technology as a continuous process highlights their respective advantages to 1) increase the

solubility and bioavailability of poorly water-soluble drugs; and 2) produce more complex structured dosages and personalized drug products. In addition, combining the technologies reduces the required downstream processing, making it more efficient and economical. The Food and Drug Administration (FDA) has recently encouraged the production of oral solid dosages that meet the increasing demands of oral drug delivery in terms of API bioavailability and drug release characteristics, in a continuous and controlled process [22].

The basic steps involved in continuous pharmaceutical HME/3D printing dosage production are 1) dosage design and conversion to a printer-readable format; 2) raw material preparation (powders, particulates, granules, pastes, etc.); 3) HME to produce filaments; 4) filament cooling; 5) 3D printing; and 6) removal and downstream processing (such as cooling, drying, and packing, etc.) In continuous pharmaceutical HME/3D printing, extrusion of the 3D printable filaments is a very important step, along with dissolving poorly water-soluble APIs into molten polymeric excipient and mixing, which improves the final dosage bioavailability[55].

The aim of this novel study was to couple fused deposition modeling (FDM) 3D printing with HME technology to print hydroxypropyl methylcellulose (HPMC)-based controlled release tablets with various structural designs and drug release profiles.

3.2. Material and methods

3.2.1. Materials

Acetaminophen (APAP; Spectrum Chemical, New Brunswick, NJ, USA) was selected as a model API. APAP is crystalline, and in the Biopharmaceutics Classification System is considered a borderline compound between class I (high permeability, high solubility) and class III (low permeability, high solubility), with a melting point of 169–170°C [56]. Benecel™ HPMC E5 was donated by Ashland Inc. (Covington, KY, USA). HPMC has been investigated for the preparation of oral drug delivery systems and is one of the most widely used hydrophilic matrix materials [57][58]. It can significantly affect the release kinetics of APAP due to its high swellability [59]. Once the tablets contact the dissolution media, the polymer chain will have relaxed with volume expansion, thus it diffuses into the matrix [60], then, the APAP diffuses out of the system [61]. HPMC E5 has an average molecular weight of 34,500 Da and normal viscosity of 4.0–6.0 mPa・S. Soluplus® was donated by BASF (Ludwigshafen, Germany) and is a co-polymer of polyethylene glycol, polyvinyl acetate, and polyvinylcaprolactam-based graft with an amphiphilic chemical structure, particularly developed for solid dispersions, which acts as a polymeric solubilizer. Due to its functional groups, it can both solubilize poorly water-soluble APIs in aqueous media and act as a matrix polymer in solid dispersions[62]. All other reagents were either HPLC- or analytical-grade.

3.2.2. Methods

3.2.2.1. Formulation

APAP, Soluplus®, and HPMC E5 were combined at a weight ratio of 1:2:7 and tumble-mixed on a Maxiblend™ (GlobePharma, New Brunswick, NJ, USA) at 25 rpm for 30 min, after filtration through a US #30 mesh screen to remove any aggregates that may have formed.

3.2.2.2. Hot melt extrusion (HME)

The extruder used in this study was a co-rotating, twin screw extruder with 11 mm diameter screws, a length/diameter ratio of 40, and eight electrically-heated zones (Thermo Fisher Scientific, Waltham, MA, USA); feeding zone temperature was controlled by an external circulation heater. Physical mixtures were extruded at 160°C for all zones with a standard screw configuration at a screw speed of 50 rpm. A 2 mm-round die was used to extrude filaments for the 3D printer. A conveyor belt was used to cool and straighten the filaments for feeding into the 3D printer.

3.2.2.3. Differential scanning calorimetry (DSC)

A Diamond DSC system (PerkinElmer, Waltham, MA, US) was used to study drug crystallinity and characterize drug miscibility in the extrudates. Samples (2–5 mg) were hermetically sealed in an aluminum pan and heated from 40–200°C at a rate of 10°C/min. Ultra-purified nitrogen was used as the purge gas at a flow rate of 50 mL/min in all DSC experiments. Data were collected and analyzed with Pyris software (PerkinElmer).

3.2.2.4. Thermogravimetric analysis (TGA)

During HME processing, a PerkinElmer Pyris 1 TGA calorimeter was used to determine the thermal stability of APAP and the polymers. The samples were placed in an open aluminum pan and heated from 30–300°C at a rate of 20°C/min. Ultra-purified nitrogen was used as the purge gas at a flow rate of 25 mL/min. Data were collected and analyzed using Pyris software, and percentage mass loss and/or onset temperatures were calculated.

3.2.2.5. 3D printing

The model tablets were designed using Microsoft 3D Builder (Microsoft, Redmond, WA, USA), sliced using CURA software (version 15.04; Ultimaker, Geldermalsen, The Netherlands), and then converted to .gcode files. Nine tablets were designed, with the same overall tablet dimensions (diameter, 10 mm; thickness, 4.5 mm), but with different outside shell thicknesses or

core fill densities (Figure 25). Tablets were fabricated from the extruded filaments using a commercial FDM-3D printer (Prusa i3 3D desktop printer, Prusa Research, Prague, Czech Republic) with an extruder, which had an E3D v6 HotEnd and a 0.4 mm nozzle. The best tablets were produced using standard resolution with the raft option activated, and an extrusion temperature of 200°C. Other settings used were as follows: bed temperature, 50°C; printing speed, 50 mm/s; nozzle traveling speed, 50 mm/s; layer height, 0.10 mm. The dimensions and weights of the 3D printed (3DP) tablets were then measured. To determine the dissolution kinetics, empty tablets (1.6 mm and 0.4 mm outside shell) were also printed.

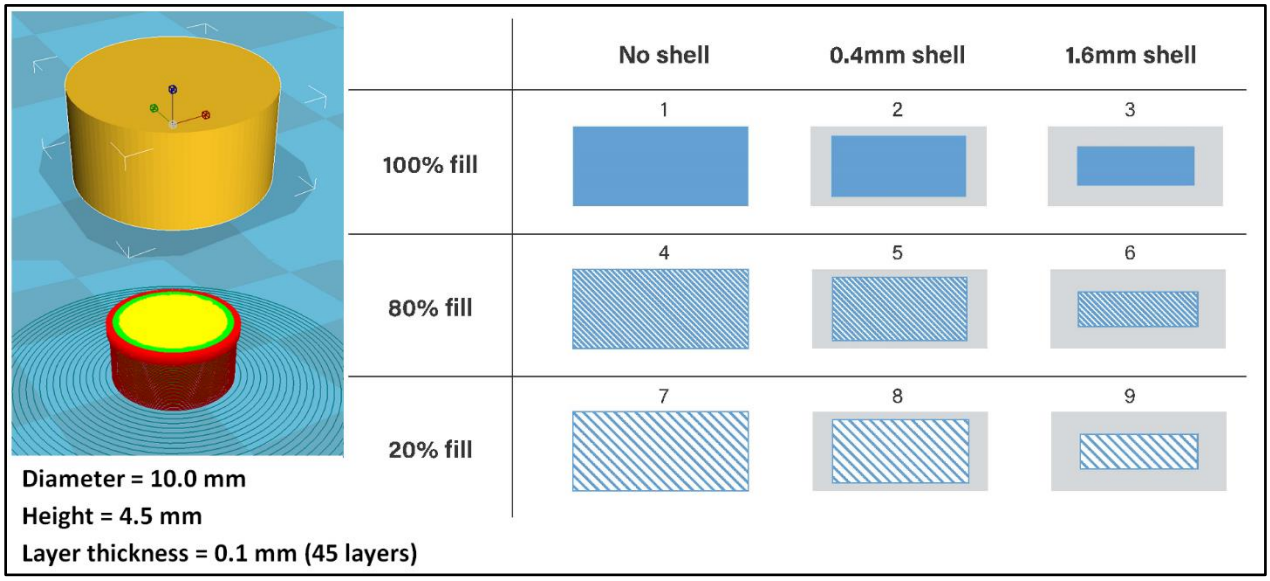

Figure 25. 3D tablet designs with varied outside shell thicknesses and inner core fill densities.

3.2.2.6. Assessment of tablet morphology

A digital caliper (VWR®, PA, USA) was used to determine the diameters and thicknesses of the tablets, and cross-sectional images of the 3DP tablets were acquired using a JOEL JSM 5610LV scanning electron microscopy (SEM) (JOEL, MA, USA).[63]

3.2.2.7. Determination of tablet strength

A standard tablet hardness tester (VK200; Agilent Technologies, Santa Clara, CA, USA)

with a maximum force of 35 kp was used to measure tablet hardness. Six tablets from each group were tested.

3.2.2.8. *In vitro* drug release

Drug release from different 3D structured tablets was determined using a United States Pharmacopeia (USP) dissolution apparatus II (Hanson SR8-plus™; Hanson Research, Chatsworth, CA, USA). Dissolution tests were conducted as per US Pharmacopeia standards using Simulated Intestinal Fluid^{TS} (without pancreatin, pH 6.8), which is representative of the small intestinal fluid of humans. Each experiment was carried out in triplicate using 900 mL of dissolution medium at 37 ± 0.5°C for 24 h. The paddle speed was set at 50 rpm. Due to their porous internal structures, tablets #8 and 9 floated; therefore, sinkers were used to keep the tablets submerged in the dissolution vessel. Samples were analyzed at 0.5, 1, 2, 4, 5, 6, 8, 10, 12, and 24 h. The amount of released APAP was determined by HPLC (Waters Corp., Milford, MA, USA) at 246 nm and analyzed using Empower software (version 2, Waters Corp.).

3.2.2.9 Dissolution kinetics studies

One of the main objectives was to combine the HME and 3D print to produce zero-order release dosages through the optimization of the 3D structure. In order to investigate the dissolution kinetics, the dissolution data were fitted to several mathematic models, including the Higuchi, Ritger-Peppes, Peppes-Sahlin, and zero-order models, and a correlation coefficient (R^2) was used to evaluate the accuracy of the individual models.

3.3. Results and discussion

3.3.1. Preliminary study of raw materials

TGA can provide information about decomposition or drug degradation [64]. According to the TGA results, mass loss of APAP and the physical mixtures emerged at temperatures above 350°C, indicating that the drug and polymer matrix would not degrade during melting extrusion at

160°C and 3D printing at 200°C. Extruded filaments were fed into the 3D printer HotEnd by feeding gears at 14 ºC, and then melted in the HotEnd hose, avoiding drug decomposition or degradation during the printing process. Though a standard screw configuration with 3 different mixing zones was utilized during HME processing, which would have a high shear force resulting in drug decomposition or degradation, drug content result was confirmed with final *in vitro* drug release studies.

DSC is a thermoanalytical technique to detect phase transitions in samples, with the premise that when the sample undergoes a phase transition, more heat will be required than that required by a reference sample.[7] The APAP DSC curve exhibited a peak at 172°C. A heat-cool-heat method was utilized for DSC analysis of the physical mixture. As expected, the physical mixture showed an obvious peak at approximately 170°C during the first heating process and no peak during the second heating process. This result indicated that APAP can disperse or dissolve into the molten polymer matrix during HME processing, forming an amorphous solid dispersion.

3.3.2. Tablet morphology study

3.3.2.1. 3D structure

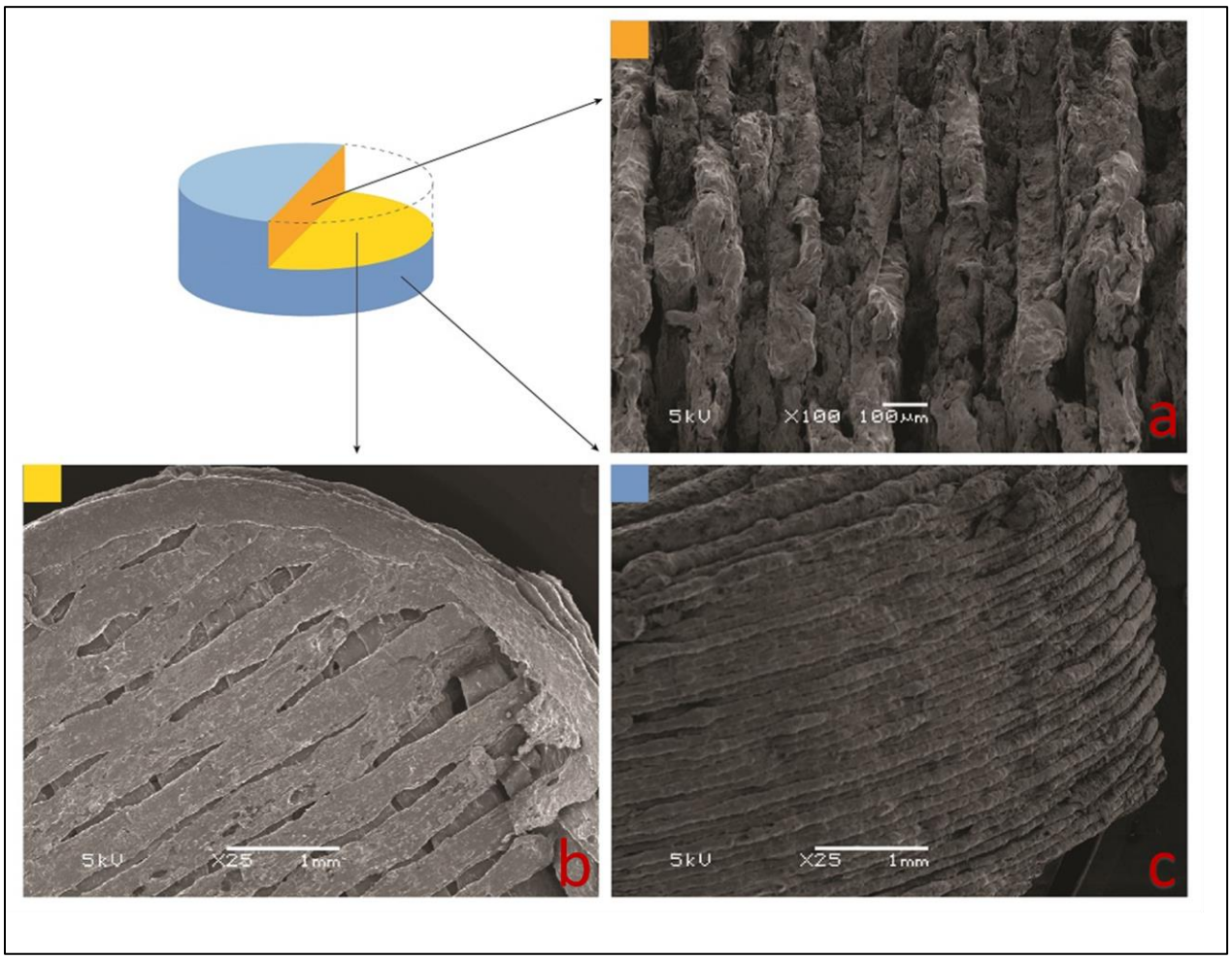

Figure 26. 3D structure of tablet #5, with a 0.4 mm shell and 80% inner fill.

All tablets were successfully printed with designed 3D structures. Due to space limitations, one sample (tablet #5, with a 0.4 mm shell and 80% inner fill) is shown in Figure 26. Tablets were broken and split apart rather than cut, as the blade would destroy the inner 3D structures. Figure 26a shows the clearly layered structure of the 0.4 mm shell and inner fill. Figure 26b shows a cross section of porous structure of the inner fill. Figure 26c demonstrates the layered structure of the tablet shell.

As shown in Figure 27a, in tablets without an outside shell, the porous inner fill structure

is in direct contact with the medium, while in the 0.4 mm and 1.6 mm shell tablets, the outside shell acts as a barrier for the inner porous structure, preventing the core from direct contact with the medium. Due to the erosion and swelling effects of HPMC and Soluplus®, the tablets slowly dissolve in dissolution medium rather than disintegrate[65]; therefore, tablets with 16 mm shell thickness should dissolve not only much slower but also at more constant rates than the other tablets

As shown in figure 27b, tablets with 100% core fill density have a very solid structure with limited surface area, and were expected to have the slowest drug release rates. Tablets with 80% and 20% fill density exhibited porous structures with larger surface areas. However, low inner fill density will also affect the hardness of the tablets.

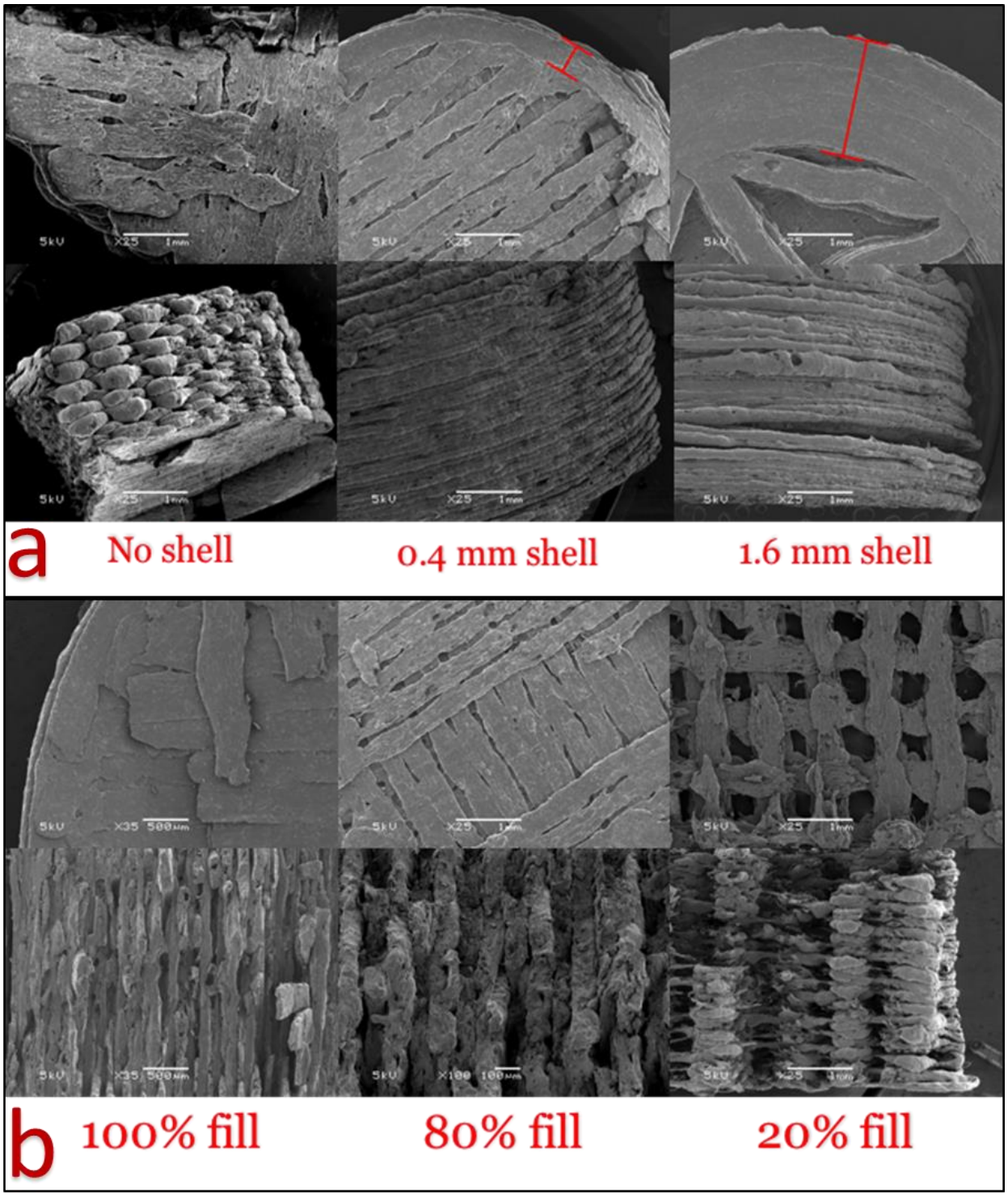

Figure 27. a) 3D structures of tablets printed with no shell or with shells of 0.4 and 1.6 mm thickness; b) Tablets with 100, 80, and 20% inner core fill density.

3.3.2.2. Tablet morphology

Images from the tablet morphology study and SEM analyses revealed that the 3DP tablets had smooth surfaces and a tight structure. Generally, tablets with a higher core fill density or thicker shells had higher density and hardness than tablets with lower core fill and thinner shells (Table 6). The hardness of tablets designed with 100% fill exceeded the detection limit of the hardness tester, and tablets with 80% fill were harder than tablets with 20% fill. The outside shell thickness also affected hardness, as tablet #9, with a 1.6 mm shell, was much harder than other tablets with same fill density. The hardness test can only measure stress towards the tablets; however, in the vertical direction, the structure was loose and easy to split, even when the hardness exceeded the limit of detection.

The volume of each cylindrical tablet was calculated as follows:

$$V = \frac{\pi D^2}{4} * h \qquad \text{Eq 3}$$

where D and h are the diameter and thickness of the tablets, respectively. Thus, the theoretical density of a tablet was calculated according to the following equation:

$$\rho = \frac{m}{V} = \frac{4m}{\pi D^2 * h} \qquad \text{Eq 4}$$

where m is the weight of the tablet. The density of the HME-generated filaments was calculated using the same equation. As shown in Table 6 the theoretical density of 3DP tablets was much higher than that of unprinted filaments. In addition, tablets with high hardness and density values are expected to have delayed dissolution and slow drug release after administration. In the geometric study, the tablets had only small variations in weight (the largest is T7, at ~7%) and dimensions, which demonstrate the good reproducibility of the 3D printing process. Based on the weight of the tablets and shell without inner fill, the 0.4 mm shell was approximately 47.99% of

the overall weight of T2, 53.04% of T5, and 79.31% of T8. The weight of the 1.6 mm shell was approximately 80.09% of the overall weight of T3, 82.42% of T6, and 96.77% of T9.

Table 6. Geometric characteristics of the 3D printed tablets

	Shell (mm)	Fill %	Diameter (mm)	Thickness (mm)	Weight (mg)	Density (mg/mm^3)	Porosity (%)	Hardness (kp)
T1	0	100	11.22±0.07	4.46±0.05	435.45±15.21	0.988	0	OV*
T2	0.4	100	10.51±0.24	4.22±0.21	377.91±24.73	1.030	0	OV*
T3	1.6	100	10.33±0.28	4.40±0.22	366.93±26.12	0.992	0	OV*
T4	0	80	10.91±0.30	4.29±0.19	352.04±24.94	0.877	20	OV*
T5	0.4	80	10.47±0.16	4.42±0.05	354.19±16.92	0.931	13.97	32.8±5.6
T6	1.6	80	10.36±0.19	4.47±0.02	395.58±18.72	1.050	2.71	32.2±5.3
T7	0	20	10.28±0.18	4.35±0.16	176.51±12.65	0.489	80	2.7±1.4
T8	0.4	20	10.21±0.16	4.48±0.05	197.19±11.62	0.538	55.82	5.3±4.2
T9	1.6	20	10.39±0.25	4.41±0.22	319.34±10.46	0.854	10.51	23.8±6.5

*OV= over detection limit

3.3.2.3. Porosity study of the tablets

The SEM images (not shown) indicated that the extrudate filament was robust, the structure was not porous, and the materials were extruded from the nozzle of the printer, so all the porosity is generated from the tablet 3D structure design. The porosity of the 3D printed tablets can be expressed by using the following equation [66]:

$$P = \frac{V_{void}}{V_{geometric}} \qquad \text{Eq 5}$$

where V_{void} is the total volume of the empty space inside the tablets and $V_{geometric}$ is the volume of the tablets as a whole object. As shown in Figure 3, 100% filled tablets can be considered as solid with no porous structure and the porosity of tablets #4 and #7 can be considered as the designed fill density. Based on the geometric measurements and tablet designs, the calculated

porosity of the tablets is listed in Table 6. Tablets #7 and #8 showed faster release rates than the other tablets with the same shell, because of both the thin shell and porous structure. For the other tablets, owing to the robust shell structure and swelling of the matrix, the inner core porous structure had a limited impact on the dissolution kinetics.

3.3.3. *In vitro* drug release

3.3.3.1. Drug release profiles

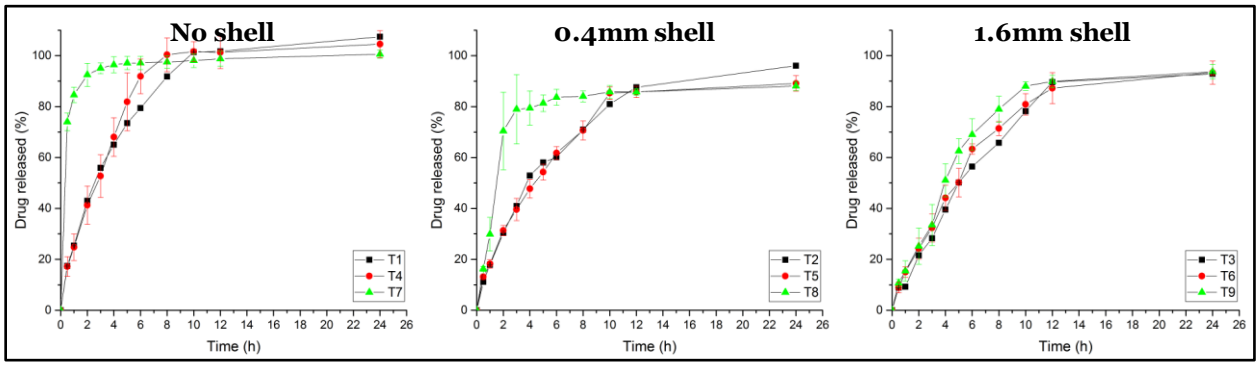

Figure 28. *In vitro* drug release profiles of tablets (T) with no shells and with shells of 0.4 and 1.6 mm thickness.

As shown in Figure 28, tablets with 1.6 mm shells had extended drug release rates due to the 3D structure of the thicker shell, while tablets without shells exhibited fast release profiles, because the inner structures were loose and direct contact with the dissolution media. The 0.4 mm shell was totally dissolved within 4 h, which was confirmed by drug release studies, showing 100% drug release in 4 h. Based on the tablet geometry study, the calculated weight ratios of 0.4 mm shells were 47.99%, 53.04%, and 79.31% for T2, T5, and T8, respectively, and the percentage of drug released after 4 h was 52.91%, 54.27%, and 79.41%, respectively, suggesting that the inner core releases the drug after the shell is dissolved. Tablets with 1.6 mm shells released APAP over a longer period, with 71%, 79%, and 66% of drug released after 8 h from T6, T7, and T8, respectively. In the 100% fill tablets, the drug release rate from T1, which had no shell, was higher

than those for T2 and T3, which indicated that the inner core with 100% fill has a looser structure than the shell. T7 (20% inner fill, no shell) exhibited 74% drug release within 0.5 h and 85% drug release in 1 h, and all tablets without shells had released at least 70% of the drug within 4 h. The linear regression of no shell tablets was lower than 0.88. As expected, the released rate was 100%< 80%< 20%.

The drug dissolution rates of tablets with each designed 3D structure were evaluated. Poorly water-soluble APIs can disperse or dissolve in polymer matrices to form solid dispersions or solutions during the HME process [28]. As mentioned in the DSC results, APAP was completely dissolved into the polymer matrix, forming an amorphous solid dispersion. The observed dissolution and drug release rates from the HPMC based matrix were influenced by the 3D geometric structure and composition, and the following phenomena were observed in the *in vitro* drug release study:

1) Once the tablets contacted the dissolution media, a steep concentration gradient formed at the media/tablet interface. Here, water acted as a plasticizer and reduced the glass transition temperature (T_g) of the system. Once the system reached the T_g during the *in vitro* study, the matrix transformed to hydrogel [59].
2) The HPMC-based matrix swelled and formed hydrogel while the media were penetrating, which changed the drug concentration at the media/tablet interface. Matrix imbibition of the media through the tight shell structure was the most important rate-controlling step during the dissolution study. The media took longer to penetrate through the thicker shell than through the thinner shell and inner core.
3) The concentration gradients led the APAP to diffuse from the media/tablet interface to the hydrogel, and thus into the dissolution media.

4) The more porous lower fill density was less restrictive for drug diffusion upon drug depletion, meaning that APAP dissolved and diffused more rapidly from the HPMC chain. Conversely, due to the tight structure of the high fill density and thicker shell, the APAP was slowly released from the matrix.

All groups of tablets achieved ~100% drug release within 24 h, confirming that no API or excipient degradation occurred during the HME or 3D printing processes. There are various mathematical kinetic models that can be applied to describe *in vitro* drug release kinetics, such as Higuchi [67], Ritger-Peppas [68], Sahlin-Peppas [69], first order, and zero order, which help researchers understand release mechanisms and optimize formulations. Drug release can be considered either Fickian or non-Fickian diffusion. In Fickian diffusion, the drug release rate is independent of the drug concentration in the matrix [70].

3.3.3.2. Dissolution kinetic studies

Higuchi equation is developed by Higuchi in 1961, which is one of the most famous and most often used mathematical model to describe the drug release rate from the matrix systems [71]. The original equation of Higuchi model is:

$$\frac{M_t}{A} = \sqrt{D(2 * C_0 - C_s) * C_s * t} \qquad \text{Eq 6}$$

here M_t is the accumulative drug released in time t; A is the overall contact surface of the matrix to the medium; D is the drug diffusivity in the polymer; C_0 and C_s are the drug concertation at beginning time and solubility in the polymer. Such equation can be simplified as following:

$$\frac{M_t}{M_\infty} = k_H * t^{1/2} \qquad \text{Eq 7}$$

where the cumulative amount of the drug in the system, k_H is a constant contains the information of the structure and geometry of the matrix [72]. The Higuchi model initially only

applicable for planer systems and then was modified and extended by researchers for variety of matrix [73][74][75]. The accumulative released drug is proportional to the square root of time. Researchers point out the original equation can only be used for "ideal" controlled released matrix because it was derived under pseudo-steady states and it validity is dependent upon the following assumptions [76]:

i. The initial drug concentration is much higher than the drug solubility.
ii. Drug diffusion is one-dimensional, making edge effects negligible.
iii. The suspended drug micro- or nanoparticles are much smaller than the thickness of the system.
iv. Swelling or dissolution of the polymer carrier can be neglected.
v. The drug diffusion coefficient is constant.
vi. Perfect sink conditions prevail and are maintained.

Higuchi model was not applicable for this work because the 3D printed matrix may diffusion multidimensional and the swelling of the matrix is unneglectable, the initial drug concentration of *in vitro* study can`t meet the assumptions listed above as well.

We applied the data from the *in vitro* drug release study to the Ritger-Peppas model (also as known as "power law"), a simple model that exponentially relates the drug release to the fractional release of the drug, developed by Peppas et al. in 1983. The Ritger-Peppas model can be described as the following:

$$\frac{M_t}{M_\infty} = k * t^n \qquad \text{Eq 8}$$

where M_t is the cumulative amount of drug released at time t, M_∞ is the total amount of drug, k is a constant incorporating structural and geometric characteristics of the device, t is the

time at which drug release is calculated or measured, and n is the release exponent, indicative of the mechanism of drug release [77].

Table 7. *In vitro* dissolution parameters of the 3D printed tablets

	Ritger-Peppas model		Linear model		Peppas-Sahlin model			
	Exponent, n	R^2	Slope, k	R^2	k_1	k_2	m	R^2
T1	0.59	0.9872	7.14	0.8881	0.29014	-0.0277	0.8509	0.9975
T2	0.69	0.9924	5.28	0.9254	0.20396	-0.0145	0.8348	0.9956
T3	0.78	0.9808	5.46	0.9790	0.06398	0.0732	0.4685	0.9861
T4	0.71	0.9968	6.02	0.8472	0.18201	0.0746	0.5061	0.9949
T5	0.64	0.9973	4.97	0.9399	0.18909	0.0074	0.6001	0.9968
T6	0.82	0.9968	5.82	0.9585	0.11352	0.0314	0.6168	0.9979
T7	0.10	0.8971	1.41	0.2995	-	-	-	-
T8	0.67	0.9801	2.36	0.5606	-	-	-	-
T9	0.79	0.9900	5.00	0.9271	0.12184	0.0437	0.5939	0.9869

*T7, T8 parameters were not calculated because their released rate too fast (over 60% in 2 h).

Ritger and Peppas's work shows this model has good ability for fitting before reaching approximately 60% total amount of drug release, and the equation has two distinct physical realistic meanings in the special cases of 0.45 (Fickian diffusion) and 0.89 (Case II transport). The Case II transport mechanism is a very near approximation of a normal Fickian diffusion process. If 0.45< n< 0.89, it indicates the superposition of both phenomena (anomalous transport). These two extreme values for the exponent n are only valid for cylinder geometry [68].

All the calculated data are listed in Table 7. Though the shape were cylindrical, the tablets has different density along the axial direction from the core due to the specific 3D structure design, and T3 (n=0.78, R^2=09808), T6 (n=0.82, R^2=0.9968), and T9 (n=0.79, R^2=0.9900) can be considered Case II transport, which can be defined to approximate Fickian diffusion. The drug release rate from HPMC-based matrix with a shell design can be dominated by the swelling kinetics of the polymer, resulting in Case II transport. For T2, n=0.10, indicating Fickian diffusion, but the tablet dissolved too quickly, with 74% of drug released by the first sample collection point

at 0.5 h, and R^2=0.8971 indicates that there was limited accuracy when applying the model to T2. For other tablets, the exponent n varied from 0.59–0.71, indicating that both the swelling and diffusion kinetics controlled the drug release rate from the matrix. Peppas and Sahlin also developed a model to analyze anomalous transportation:

$$\frac{M_t}{M_\infty} = k_1 * t^m + k_2 * t^{2m} \quad \text{Eq 9}$$

where k_1, k_2, and m are constants. The first term on the right-hand side represents the Fickian diffusional contribution, whereas the second term the Case II swelling contribution. The coefficient m is the purely Fickian diffusion exponent which has same meaning with the n in Ritger-Peppas model. The percentage of drug released due to the Fickian mechanism, F, is calculated as:

$$F = \frac{1}{1 + \frac{k_2}{k_1} t^m} \quad \text{Eq 10}$$

The ratio of both contributions can be calculated as follows:

$$\frac{R}{F} = \frac{k_2 * t^m}{k_1} \quad \text{Eq 11}$$

Such equations were applied to investigate the effect of the differently designed 3D structures on drug release; however, significant effects on the resulting R/F-ratios were found with the investigated 9 different tablets and shells (Table 7). Here the Fickian contribution can be expressed as a function of t^m, then the relaxational contribution can be expressed as a function of t^{2m}. Compared with the n in equation 5 and m in equation 6, $m \neq n$, thus the relaxational mechanism is not negligible [69]. For tablets T1 and T2, though the R^2 values were good, the k_2 was negative when applying the Peppas-Sahlin model, making the data nonsensical and indicating that the drug releasing mechanism were anomalous transport. For tablets T7 and T8, the drug

release reached 60% in 2 h, which lacking data for calculating the k_1, k_2, and m. It is difficult to determine the importance of the Fickian or Case II mechanisms without using equations 7 and 8. Figure 29 shows that along with the time or the drug released from the matrix, the Fickian diffusion domination decrease for the first 6 h or 60% of drug released from tablet T5, and the tablet T3 R/F curve indicating that the drug release was dominated by the swelling mechanism. Tablets T4, T6, and T9 were predominated by Fickian diffusion then the swelling mechanism. In this study, the domination of the diffusion mechanism was decrease along with the time or the dissolution of the matrix. Both the diffusion and swelling mechanism indicating the constant and steady drug release rate. Summarize the result of Ritger-Peppas and Peppas-Sahlin model, tablets T3, T5, T6, and T9 can be a proper candidate for zero order drug release.

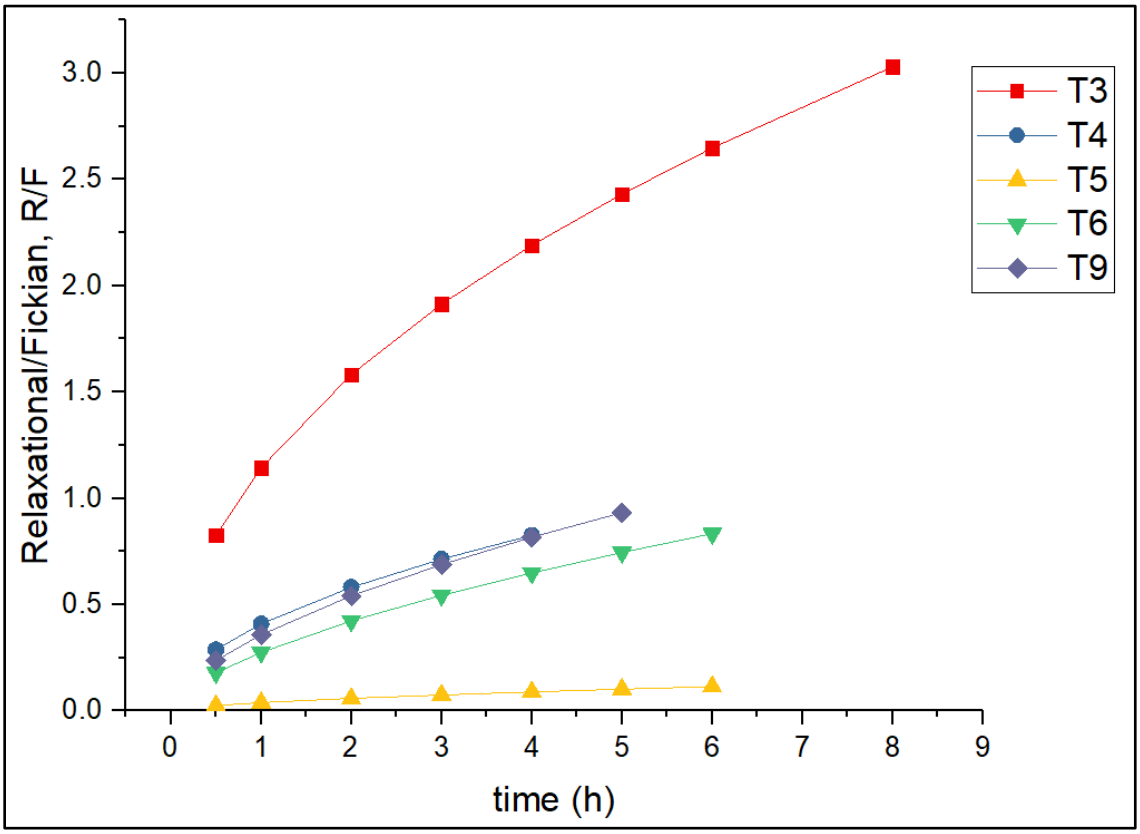

Figure 29. Swelling contribution, R to diffusion contribution, F ratio from tablets #3, 4, 5, 6, and 9.

3.3.3.3. Zero order drug release

Zero order release, in which the drug release rate is constant over a period of time, is the ultimate goal of all controlled release DDSs. The equation for zero-order release is as follows:

$$M_t = M_0 + k * t \quad \text{Eq 12}$$

where $\boldsymbol{M_t}$ is the cumulative amount of drug released at time t, $\boldsymbol{M_0}$ is the initial amount of drug, $\boldsymbol{k}$ is the release kinetic constant, and $\boldsymbol{t}$ is the time at which the drug release is calculated or measured. As all the tablets reached 80% drug release within 10 h, linear fitting of *in vitro* drug release data from all 9 tablet types are listed in Table 7. Due to the tight structure of the shell, the 1.6 mm shell was totally dissolved within 24 h, and the drug release from the 1.6 mm shell (linear regression R^2=0.9950), T3 (linear regression R^2=0.9790), T6 (linear regression R^2=0.9585), and T9 (linear regression R^2=0.9271) was steady and constant (Figure 30), meaning that the tight structure of the shell resulted in nicely controlled (zero order) drug release rates. T4 (linear regression R^2=0.8472) was almost zero order released, however when plot the first 6 h release data, that the T4 (linear regression R^2=0.9966) and can be considered as zero order release, which confirmed the diffusion mechanism and swelling mechanism dominated the T4 contributes to the constant and steady 60% drug release. The linear fitting results were consistent with the fitting of the Ritger-Peppas and Peppas-Sahlin models, in which drug release from T3, T5, T6, and T9 was constant and steady.

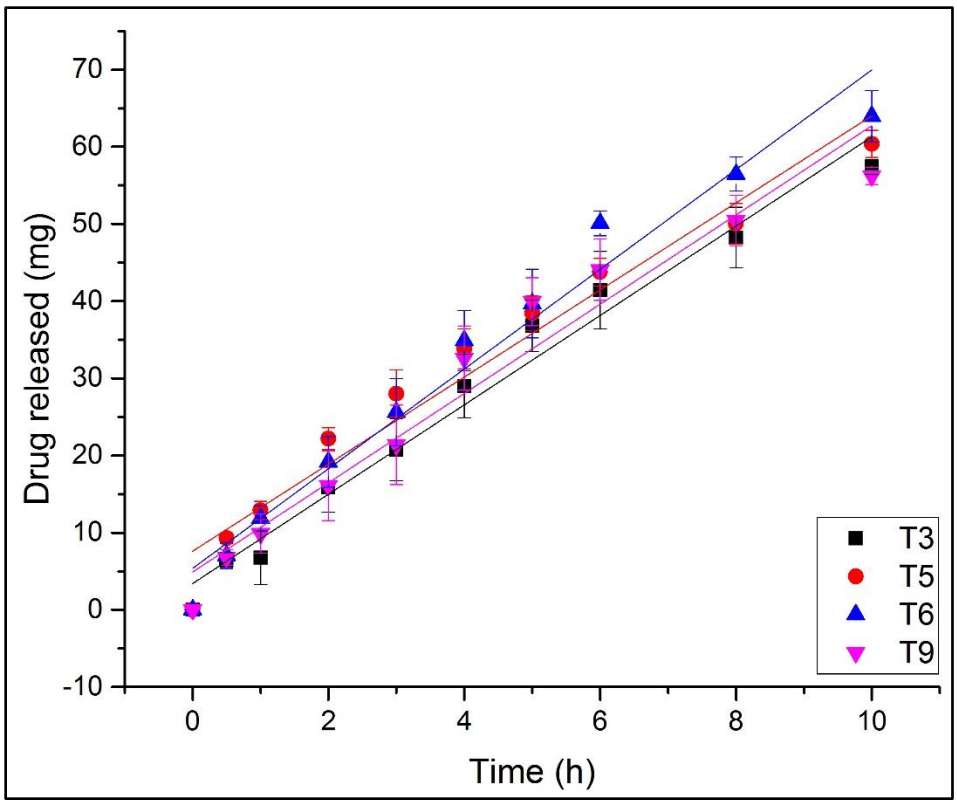

Figure 30. Linear fitting of drug release from tablets #3, 5, 6, and 9 over 10 h.

3.4. Conclusions

In this study, we successfully fabricated solid-dispersion filaments with the API dissolved in a polymer matrix via HME technology. Extruded filaments prepared based on HPMC were printed with optimized 3D printing parameters, producing controlled release tablets with different 3D structures. Based on Ritger-Peppas model fitting, drug release from HPMC-based matrix tablets T3, T6, and T9 may be considered Case II transportation diffusion, indicating that the rate of drug release is independent of time and concentration. Based on the Peppas-Sahlin model, T3, T4, T5, T6, and T9 were dominated by either diffusion or swelling mechanisms. T3, T6, and T9 also had constant and steady drug release rates by linear fitting, confirming that the diffusion model can be considered sustained (zero order) release. In other words, compared to changing the formulation, polymer, or further processes, such as coating, 3D structure design is effective and

efficient for optimizing controlled drug release rates. In this work, the thick and tight outside shell structure act as a "barrier" during the *in vitro* drug release study, which contributes to the slow forming hydrogel and constant control of the drug release rate from the HPMC based matrix. Even though the inner fill tablet is 100% (T1), it cannot perform as well as the outside shell tablets (T3, T6, and T9). This study clearly demonstrates that coupling FDM-based 3D printing with HME offers a novel, economical, and efficient method for manufacturing complex, personalized dosage forms and better controlled release profiles dosages that can be prepared as required for individuals.

CHAPTER 4

DEVELOPMENT OF CONTROLLED RELEASE ORAL DOSAGES WITH CORE-SHELL STRUCTURE USING 3D PRINTING TECHNOLOGIES

4.1. Introduction

For a long time, drugs have been used to treat disease and improve health. Drug delivery systems (DDSs) refers to a method or process to achieve a therapeutic effect by transporting active pharmaceutical ingredients (APIs) in humans or animals body [42]. An effective DDS can be described as the API is released in a controlled rate over a period of time [78]. Targeted delivery can be also defined as the controlled release formulation where the drug is active in the specific target of the body such as, in cancerous tissues[45][46]. There are serval approaches can be used to achieve the controlled release such as polymeric matrix [66], electromechanical delivery [48], and polymeric matrix[47]. The two major issues for Liposome-based controlled formulation are poor long term *in vivo* stability and reticuloendothelial system entrapment [49]. Using of pumping devices for is the most sophisticated but extremely expensive approach controlled drug released. In addition, the membrane breaking of the osmotic pump system may subject to dose dumping [50].

Oral drug administration has been developed for a long time and proved is the most acceptable route, which is cost-friendly and easily accessed[79], however, there still the inherent limitations exist. As shown in figure 31, general single oral dose administration will take effects

slowly and just effective for a short period of time. In order to extend the therapeutic time, multiple dose can be given which inevitably cause the patient compliance [80]. Recently, polymeric oral-controlled release technologies have gained a lot interest from both industrial and academic area because of the potential to improve patients' quality of life (QOL) by reducing the inconvenience of frequent dosing in an economical and immediately approach [29]. The polymeric controlled release utilize hydrophilic, amphiphilic, or hydrophobic polymers (biodegradable, or non-biodegradable) as drug-carriers, in which the APIs entrapped in the matrix and the polymer matrix controls the drug release rates[51]. Hot melt extrusion (HME) technologies have been developed and applied in pharmaceutical manufacturing for 2 decades and might be optimal for preparation of the polymeric formulations [5]. It mostly using twin-rotor extruders for the processing of soluble polymeric excipients and poor soluble APIs, mixing them while molten, thus, the APIs partially or totally dissolved into the polymer matrix and formed amorphous solid dispersions with improved bioavailability and stability [10]. However, due to the uniformity of the polymeric oral-controlled release dosages, the drug release kinetics from the polymer matrix is slow.

In addition, an significant issue researchers has to face during optimization of the oral administration is the individual variation, because of the patients has different races, genders, ages, pharmacogenetics, and pharmacokinetic characteristics and so on. Developing new molecular entity (NME) is complex, expensive, and time-consuming [81][82][83], so optimizing the currently available drugs to improve their bioavailability, or therapeutic effect could be effective and economical solutions [84][85][86]. Increasingly rising additive manufacturing (AM), also as known as 3D printing technology, is an optimal solution because it provides an effective solution for individual, complex consumption with the assistance of the computational design for oral-controlled DDSs [87][88]. 3D printing is the layer-by-layer production of 3D objects from digital

designs[11], it also allows engineering release profiles by control of spatial distribution within a given polymer composition rather than creating a new host material [89].

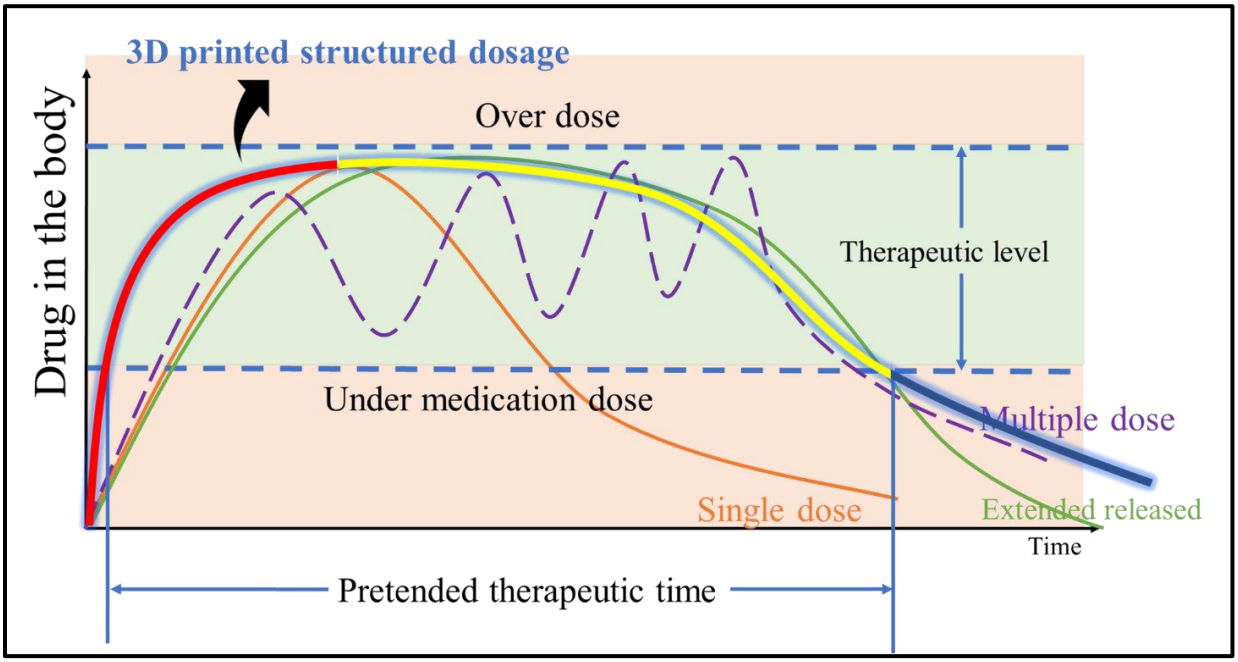

Figure 31. Optimization of oral drug administration via HME/3D printing technologies.

Compared to the traditional pharmaceutical products manufacturing process, combine HME and 3D print technology together will highlight each respective advantages: 1) increase the poorly water soluble drugs solubility and bioavailability; 2) produce more complex structured dosages and personalized drug products.

Based on the advantages offered by coupling 2 technologies, the aim of this study was to couple fused deposition modeling (FDM) 3D printing with hot melt extrusion (HME) technology to enable Additive Manufacturing (AM) to print a core-shell structured controlled release tablets with dual mechanism drug release performance in the USP SIF media. A series of physical

chemical evaluation of the tablets as well as the comparation between direct compressed and 3D printed tablets were also conducted in this study.

4.2. Material and methods

4.2.1. Materials

Acetaminophen (APAP) (Spectrum Chemical, New Brunswick, NJ, USA), a typical drug used to treat pain and fever, is selected as the model API. APAP is a crystalline and considered a borderline compound between Class I Biopharmaceutics Classification System (BCS) drug (high permeability, high solubility) and class III, with a melting point around 170-172°C [56].

Benecel™ HPMC K4M (donated by Ashland Inc, Covington, KY, USA) with weight average molecular weight ≃34,500 and melt viscosity ≃ 8.43×10^4 Pa・S at 160 C and 1 rad/s, is used as the shell matrix. It is one of the most widely used hydrophilic matrix material which has been investigated for the preparation of oral drug delivery systems[58]. The APAP release mechanisms and kinetics from the HPMC based matrix has been studied [59]. The high swellability allows the polymer chain relaxed with volume expansion when the matrix contacts with dissolution media, thus, the APAP diffuses out of the system[60].

Aquosolve^{TM} HPMCAS HG (donated by Ashland Inc, Covington, KY, USA) weight average molecular weight ≃18,000 and melt viscosity ≃ 4.62×10^4 Pa・S at 160 C and 1 rad/s, is selected as the core matrix. It is insoluble in stomach but will swell and dissolve rapidly in upper intestine, which commonly used as a solid-dispersion carrier to improve the poorly soluble API bioavailability[90]. All other reagents were either HPLC- or analytical-grade.

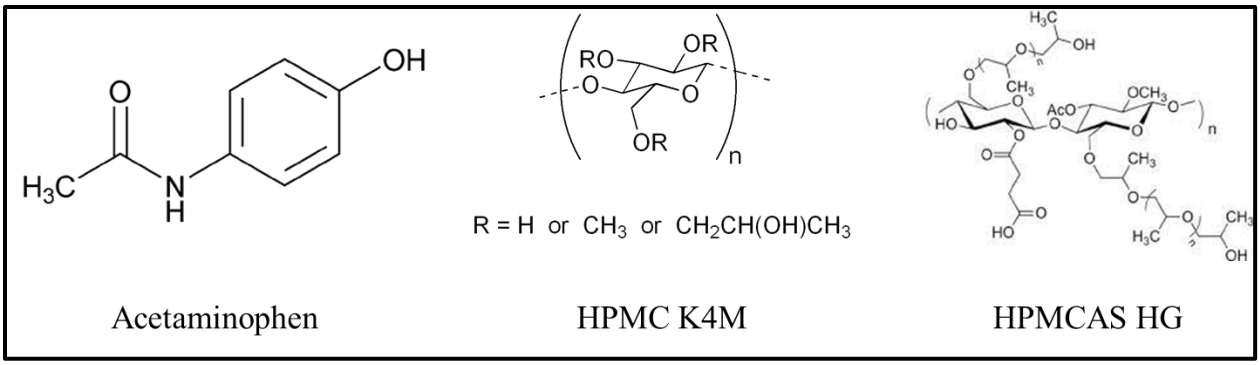

Figure 32. the chemical structure of the API and polymer matrix.

4.2.2. Methods

4.2.2.1. Formulation

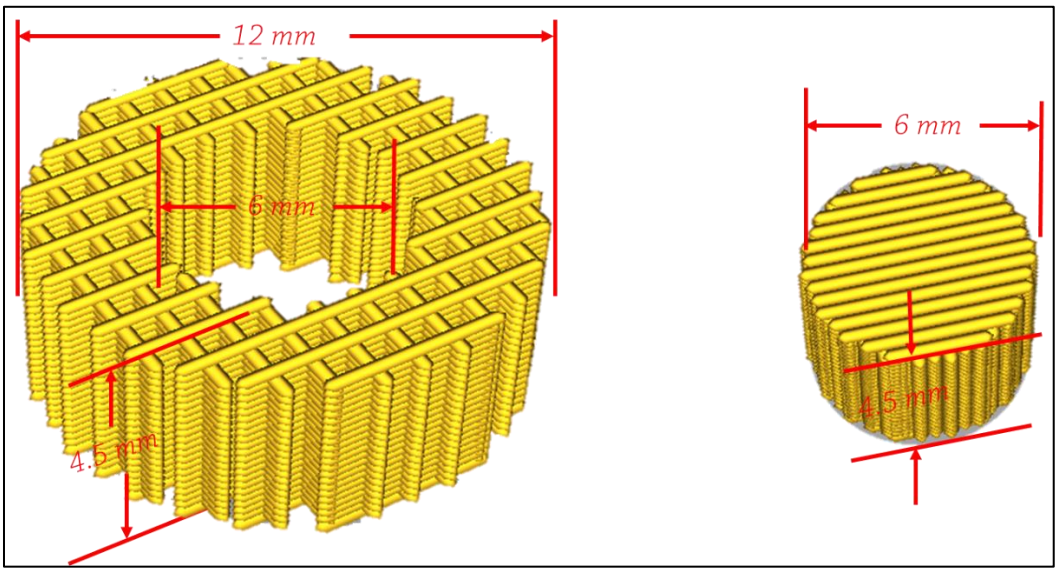

Figure 33. the 3D structure of porous fast release shell and condense extend release core.

The overall tablets contains two parts, the porous fast release shell and condense extended release cores (figure 33). For the shell, 30% w/w drug were mixed with 70% HPMC K4M, while the core was 30% drug with 70% HPMCAS HG. The physical mixture (API+polymer) was

tumble-mixed using Maxiblend^{TM} (GlobePharma, New Brunswick, NJ, USA) at 25 RPM for 30 min, after passing through a US#30 mesh screen to remove any aggregates that may have formed.

4.2.2.2. Preparation of the filaments

A co-rotating, twin screw extruder with 11 mm diameter screws, L/D of 40, and eight electrically-heated zones (Thermo Fisher Scientific, Waltham, MA, USA) was used in this work; feeding zone temperature was controlled by an external circulation heater. Physical mixtures were extruded at 160°C for all zones with a standard screw configuration at screw speed 50 RPM. The molten materials was extrude through a 2 mm round shape die with an in -line NIR probe inserted as the PAT to monitoring the quality and homogeneity of the filaments, and a conveyor belt was used to cool and straighten the filaments to feed into the 3D printer. Polymer matrix without drug loading were also extruded at 200 C to evaluate the polymer-API interaction during the extrusion process.

4.2.2.4. Differential scanning calorimetry (DSC)

A TA DSC25 system (TA Instruments, New Castel, DE, USA) was used to study drug crystallinity and characterize drug miscibility with the extrudates. 8-10 mg of sample was hermetically sealed in an aluminum pan and heated from 25 to 200°C at a rate of 10°C/min. Ultra-purified nitrogen was used as the purge gas at a flow rate of 50 mL/min in all the DSC experiments. Data were collected and analyzed with Trios software (TA).

4.2.2.5. Thermogravimetric analysis (TGA)

TGA was performed by using a PerkinElmer Pyris 1 TGA calorimeter to determine the thermal stability of APAP and the polymers during the HME processing. The samples were placed in an open aluminum pan and heated from 30 to 300 °C at a rate of 20 °C/min. Ultra-purified

nitrogen was used as the purge gas at a flow rate of 25 mL/min. Data were collected and analyzed using the Pyris software. Percentage mass loss and/or onset temperatures were then calculated.

4.2.2.6. 3D printing

The model tablets were designed using Microsoft 3D Builder (Microsoft, Redmond, WA, USA) and sliced by CURA software (version 15.04; Ultimaker, Geldermalsen, The Netherlands) then convert to .gcode file. Tablets were not only prepared using different polymer matrix for core and shell, but also designed to have a gradually decreasing internal density gradient which the core is 80% fill density and the shell is 50% fill density. Tablets were fabricated with the extruded filaments using a commercial FDM-3D printer (Prusa i3 3D desktop printer, Prusa Research, Prague, Czech Republic) with an extruder, which had an E3D V6 hot end and a 0.4-mm nozzle. The following printer settings were found to produce the best tablets: a standard resolution with the raft option activated and an extrusion temperature of 200°C. The other settings used were as follows: bed temperature, 50°C; printing speed, 50 mm/s; nozzle traveling speed, 50 mm/s; layer height, 0.10 mm. The dimensions and weights of the 3DP tablets were then measured. The printed shell and core were manually assembled as the core-shell structured tablets.

4.2.2.7. Assessment of tablet morphology

A VWR® digital caliper (VWR®, PA, U.S.) was used to determine the diameters and thicknesses of the tablets. Cross-sectional images of the 3DP tablets, and direct compressed extrudate tablets were taken using a JOEL JSM 5610LV scanning electronic microscopy (SEM).

4.2.2.9. *In vitro* drug release study

Drug release from the core-shell structured tablets, shell only, core only, and direct compressed extrudates tablets was determined using a United States Pharmacopeia (USP)-II

dissolution apparatus (Hanson SR8-plus™; Hanson Research, Chatsworth, CA, USA). Dissolution tests were conducted as per the US Pharmacopeial standards using Simulated Intestinal Fluid TS (without pancreatin) (pH 6.8), which is representative of the small intestinal fluid of humans. Each experiment was carried out in triplicate using 900 mL of the dissolution medium at 37 ± 0.5°C for 24 h. The paddle speed was set at 50 rpm. Samples were taken at 5, 10, 15, 30, 60, 120, 180, 240, 300, 360, and 420 min for analysis. The amount of released APAP was determined by HPLC (Waters Corp., Milford, MA, USA) at 246 nm and analyzed using Empower software (version 2, Waters Corp.)

4.3. Results and discussions

4.3.1. Thermal analysis

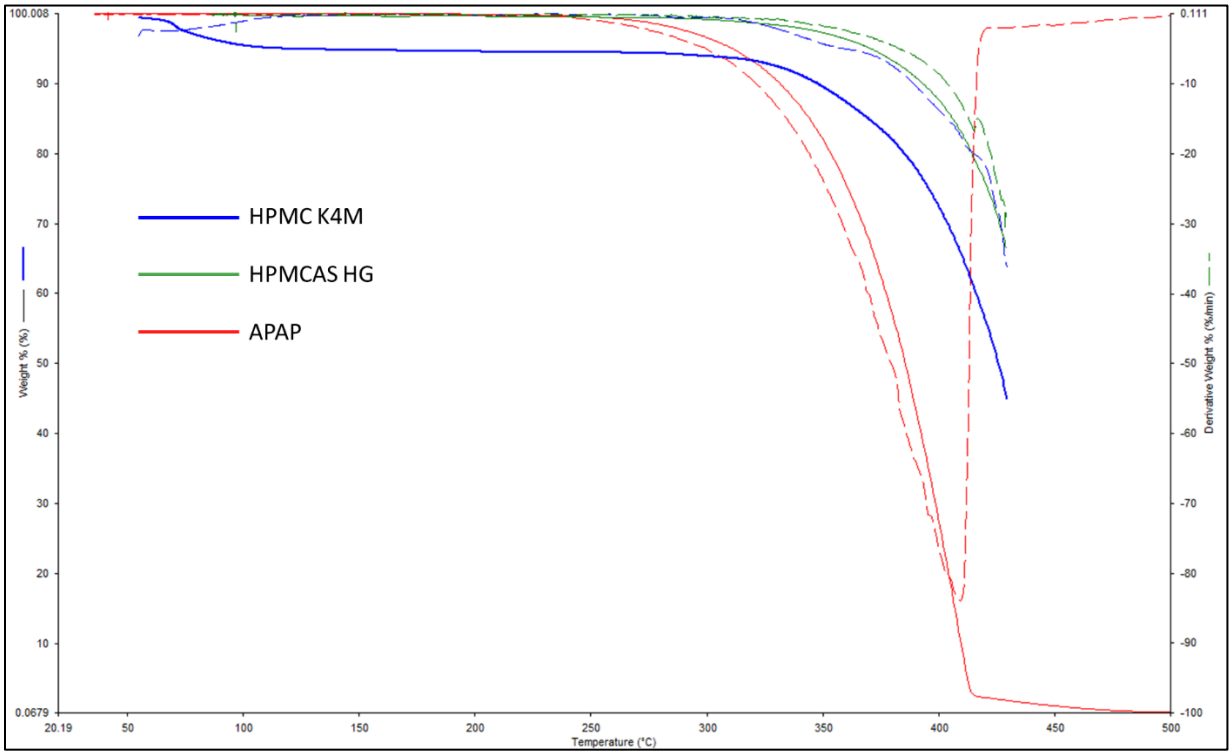

Figure 34. the TGA graph of the raw materials: APAP, HPMC K4M, and HPMCAS HG.

Thermogravimetric analysis (TGA) is a measurement indicating the change in the physical properties and chemical properties of a material as the temperature (equal heating rate) or time (loss of isothermal and/or mass conservation) increases[91]. In this study, the TGA graph will show the moisture contents and the degradation of the raw materials. 1st derivative was plotted to show change of the thermal curves. As shown in figure 34, APAP and HPMCAS HG showed no moisture or crystalline water in the matrix, and they all have one degradation steps when heating above 350 °C. The HPMC K4M curve showed a 5% weight loss before reaches 100 °C, which indicating the water contents in the polymer. In addition, the torque was not high (2.88-4.32 Nm) during the extrusion process, which indicating there not much mechanical energy added into the extrusion process. So the extrusion process should not cause the degradation of the materials. The *in vitro* drug release study also showed cross verified there no degradation happened during the HME and 3D printing process.

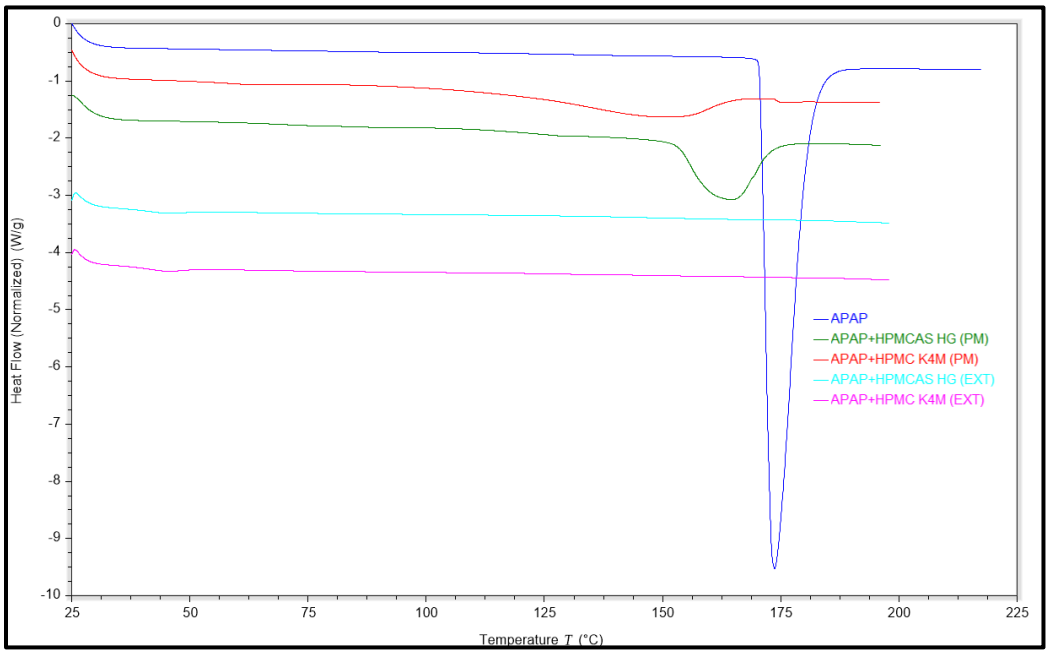

Figure 35. the DSC graph of the APAP, physical mixed (PM) formulations, and extruded (EXT) formulations.

Differential scanning calorimetry (DSC) is a thermal analysis technique that uses a compensator to measure the heating rate and temperature required to bring a sample and reference to the same temperature [92]. As the temperature rises, the crystallized structure begins to melt and the compensator measures the phase change necessary to increase the heat flow to overcome the melting, so as to maintain the consistent temperature, which results in an endothermic peak appears on the DSC curve [93]. As shown in figure 35, APAP showed a obvious melting peak around 172 °C, while physical mixtures showed a attenuated enthalpy around 150 °C and 160 °C, which indicating the APAP can be dissolve into the molten polymer matrix. The extrudates showed no peaks at all because with the help from the extrusion process, the crystalline API all dispersed or dissolved into the molten polymer matrix form amorphous solid dispersions. The polarized light hot stage microscopy can also confirm the formation of the ASDs, as shown in figure 36, APAP crystal can be clearly seen in the microscope, while heat to 160 °C, the polymer matrix melt and the API starts to dissolve in to the polymer matrix. As heat to 180 °C the APAP crystal can not be seen under the microscope and the physical mixtures transfer to the amorphous solid dispersions.

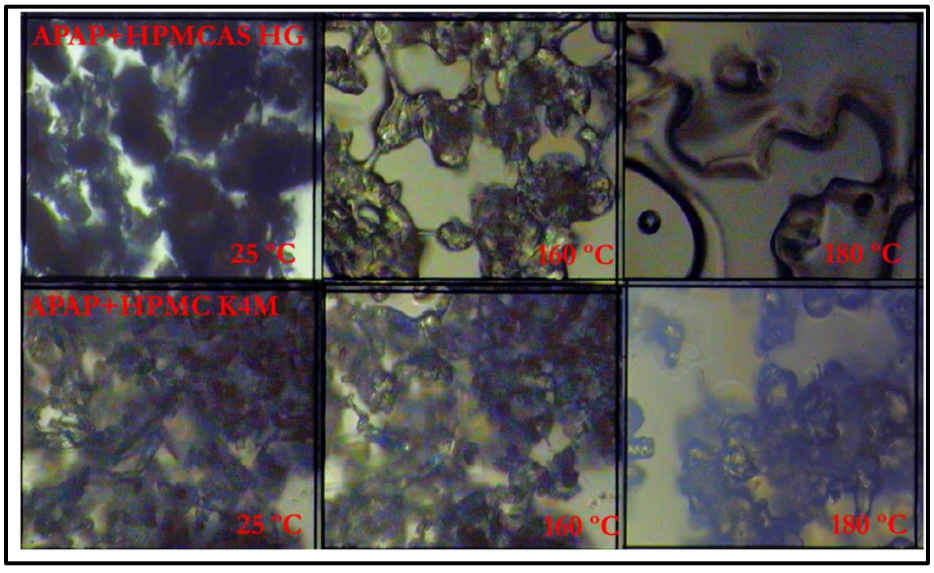

Figure 36. polarized light hot stage microscopy pictures of heating the physical mixtures to 180 °C.

4.3.2. Preparation of the filaments

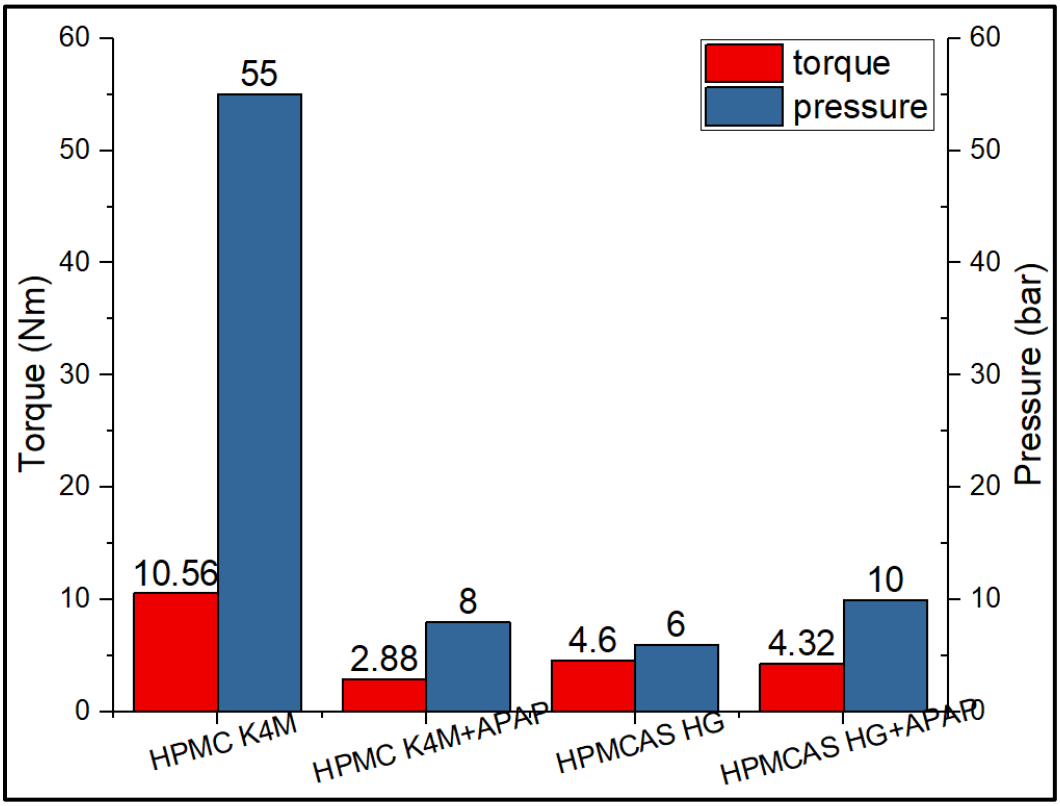

Figure 37. the extrusion torque and die pressure for different extrusion formulations.

In this work the standard screw design was applied for all the material extrusion process, which allows the balance between the distributive and dispersive extrusion to grantee the transformation of crystalline form to amorphous solid dispersion as well as the uniformity. The extrusion torque and die pressure were recorded and shown in figure 37. The torque represent extrudability of the materials and also indicating the miscibility of the API and polymer matrix, as mentioned in the DSC analysis part, the APAP should be more easily mixed with the

Filaments with adequate physicochemical and mechanical properties were successfully produced by the HME process. The diameter of the filaments were around 1.75 mm. The process temperature, torque and die pressure was recorded when the extrusion reaches the steady states.

The torque was used to evaluate the extrudability of the materials and can also represent the flexibility of the materials. As observed, the drug loaded filaments were flexible compared to the filament without drug loading; In addition, the HPMC filaments are more flexible than the HPMCAS filaments. And the die pressure in this work can be used to represent the hardness of the filaments, and similar observation obtained as the torque studies: filaments without drug loaded are harder and HPMCAS filaments are harder than HPMC formulation.

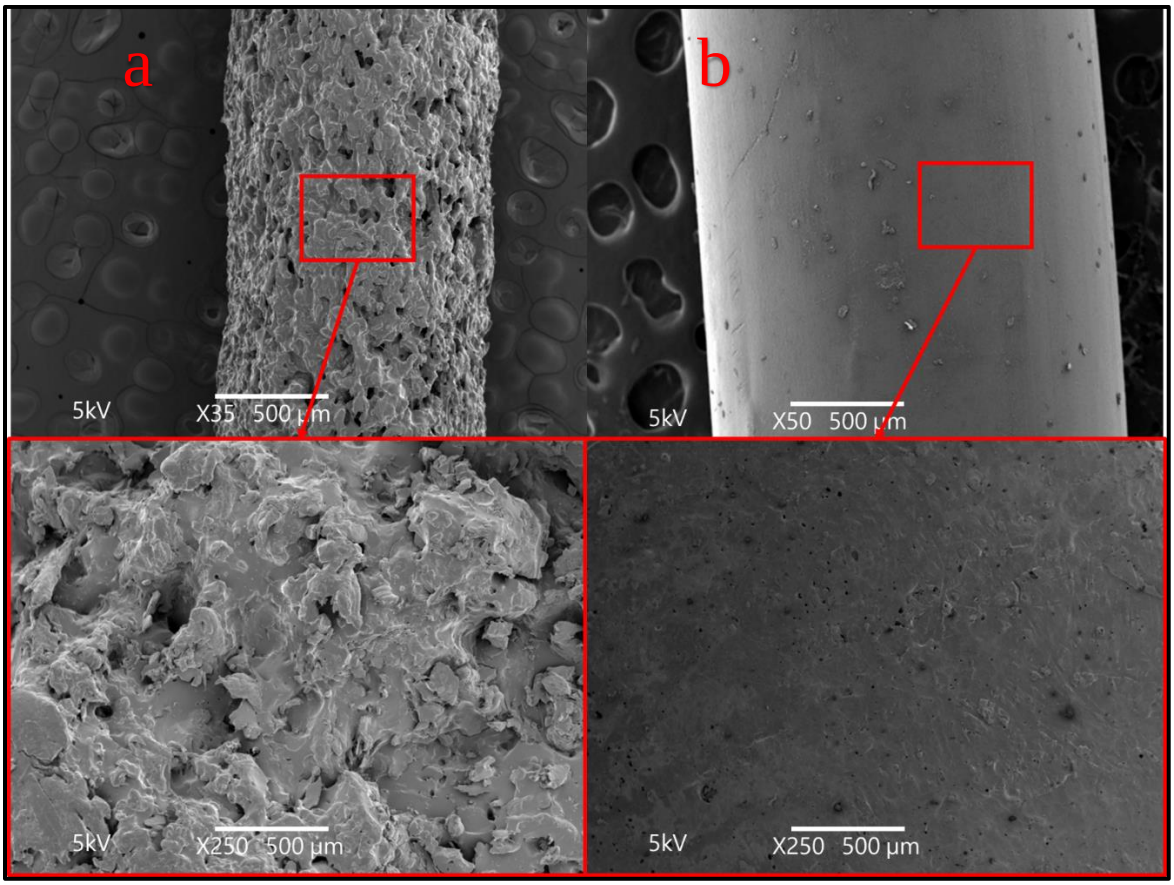

Figure 38. the SEM graphs shows the surface of the a) HPMC and b) HPMCAS filaments.

From the figure 37, it seems the HPMC matrix is more extrudable than the HPMCAS formulations, however, the rough surface and porous structure are observed from the SEM pictures (figure 38). It may because of the moisture contents in the HPMC formulation which cause the air

bubbles during the extrusion process. The rough surface of the filaments also affects the 3D printed structures as will and the shell also observed has rough surface and micro porous structures (figure 38a).

As shown in figure 37, the lowest extrudable temperature, extrusion torque and die pressure of drug loaded matrix were reduced compared to the polymer only. It may because of the APAP interact with the polymer matrix and formed a hydrogen bonds and act as the plasticizer during the extrusion process, which reduced the glass transition temperature (T_g) of the system. As mentioned in section 4.3.1 of this chapter, the APAP was dissolve or dispersed into the polymer matrix and transform from the crystalline to amorphous can be proved by the DSC studies.

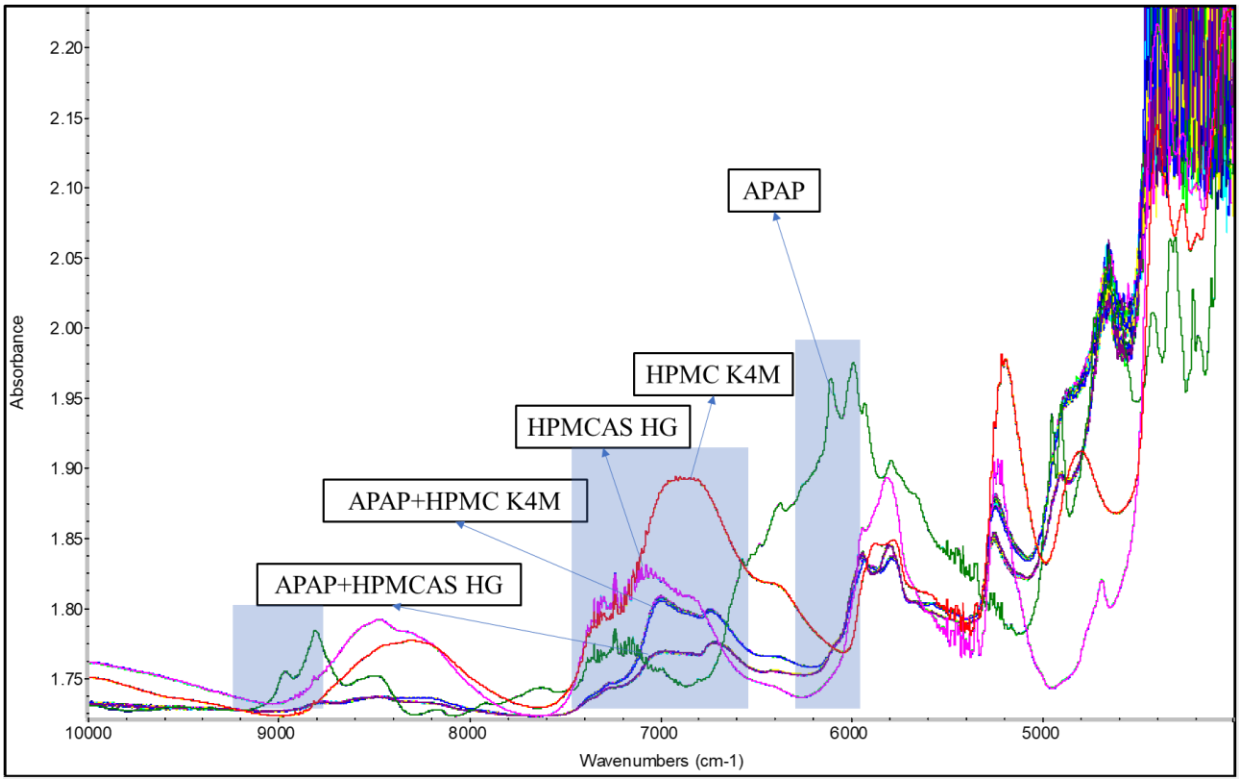

Figure 39. the raw in-line NIR spectra collected during the extrusion process.

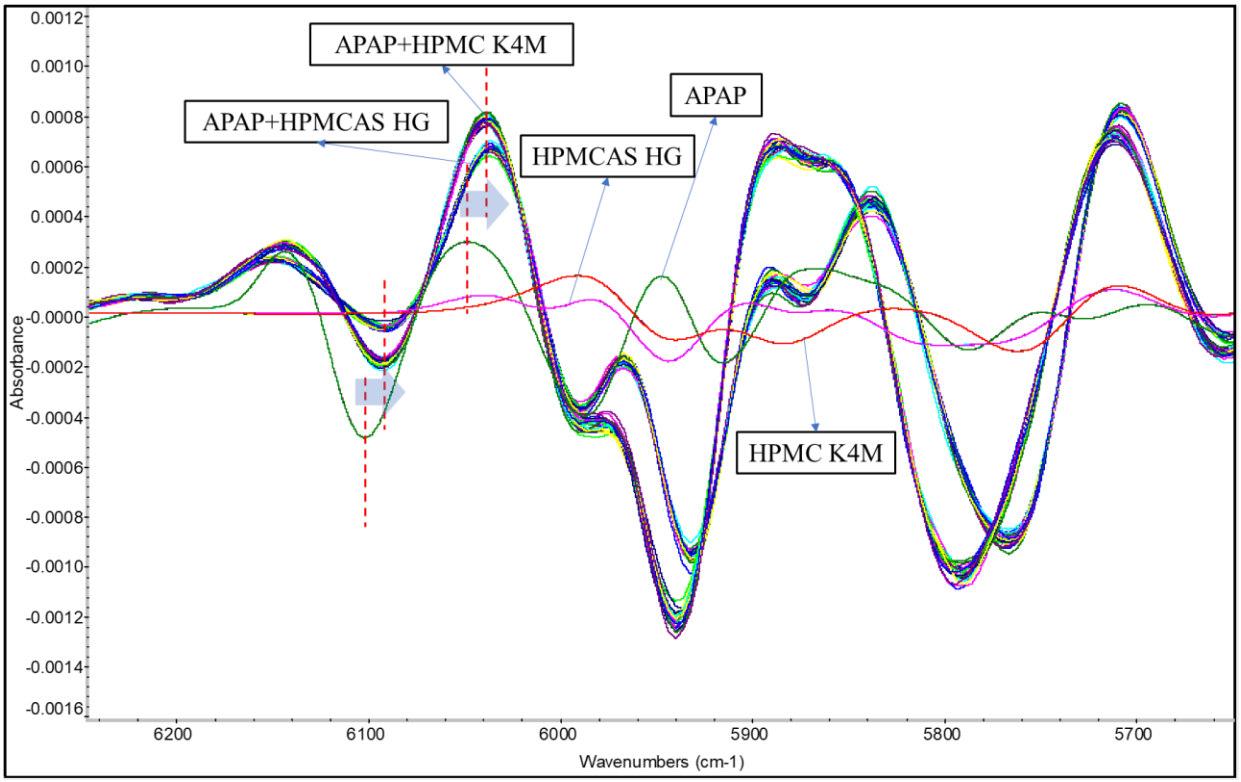

Figure. 40. The 2nd derivative of the raw spectra collected during the extrusion process.

As an invaluable in-process analytical tool, Fourier transform near-infrared (FT-NIR) spectroscopy in conjunction with multivariate analysis (MVA) techniques, such as partial least squares (PLS) in this work, has been used to provide near real-time chemical information. The extrudates spectra are continuously collected by the in-line fiber optical probe while the pure API and polymers were collected using the integer sphere. All the spectra are present in figure using a common scale.

According to the previous work, the FT-NIR signal response to the HME parameters changing, which shows on the spectra graph is that the signal intensity is different under different process parameters or drug loading[94]. The spectra collected during extrusion of each formulation were perfectly overlap which indicating the homogeneity of the extruded filaments.

As showing in figure 39, materials showed different peaks and three potential wavenumber range (8780-9230 cm^{-1}, 6500-7430 cm^{-1}, and 5850-6250 cm^{-1}) can be identified as the APAP signature peaks, because the APAP shows high signal intensity while the polymers did not. It can be used to analysis the interaction of the APAP and polymer matrix during the HME process. The identical peak area can be used to isolated the APAP peaks from the molten mixtures to represent the signal of the APAP. In order to, see the interaction during the HME process clearly, second order derivative of all curves were adopted. The 6500-7430 cm^{-1} was demonstrated in figure, for an example, peaks around 6100 cm^{-1} and 6030 cm^{-1} can be considered as the signal from the APAP, however, the peak of the spectra of the molten mixtures are both shifting to the lower energy side, which could possibly be the formation of the hydrogen bonds leads to the attenuation of the glass transition T of the system.

4.3.3. Tablet morphology studies

Due to the second thermal process, 3D printed tablets showed different physiochemical properties compare to the direct compressed milled extrudates tablets. As showing in figure 41, the particulates can be observed from the direct compressed tablets, especially the HPMCAS HG tablets. However, due to the hygroscopicity of the HPMC formulation, the particulates were compressed and more uniform than the HPMCAS HG tablets. According to the SEM results, compared with PM tablets, there is no single particulates can be seen in 3dp tablets, which can be considered as a continuous structured object with homogenized composition. As discussed in section before, the HPMC has rough surface which affects the appearance of the 3D printed tablets as well. On the contrary, the 3D printed HPMCAS HG tablets showed more smooth surface and better appearance.

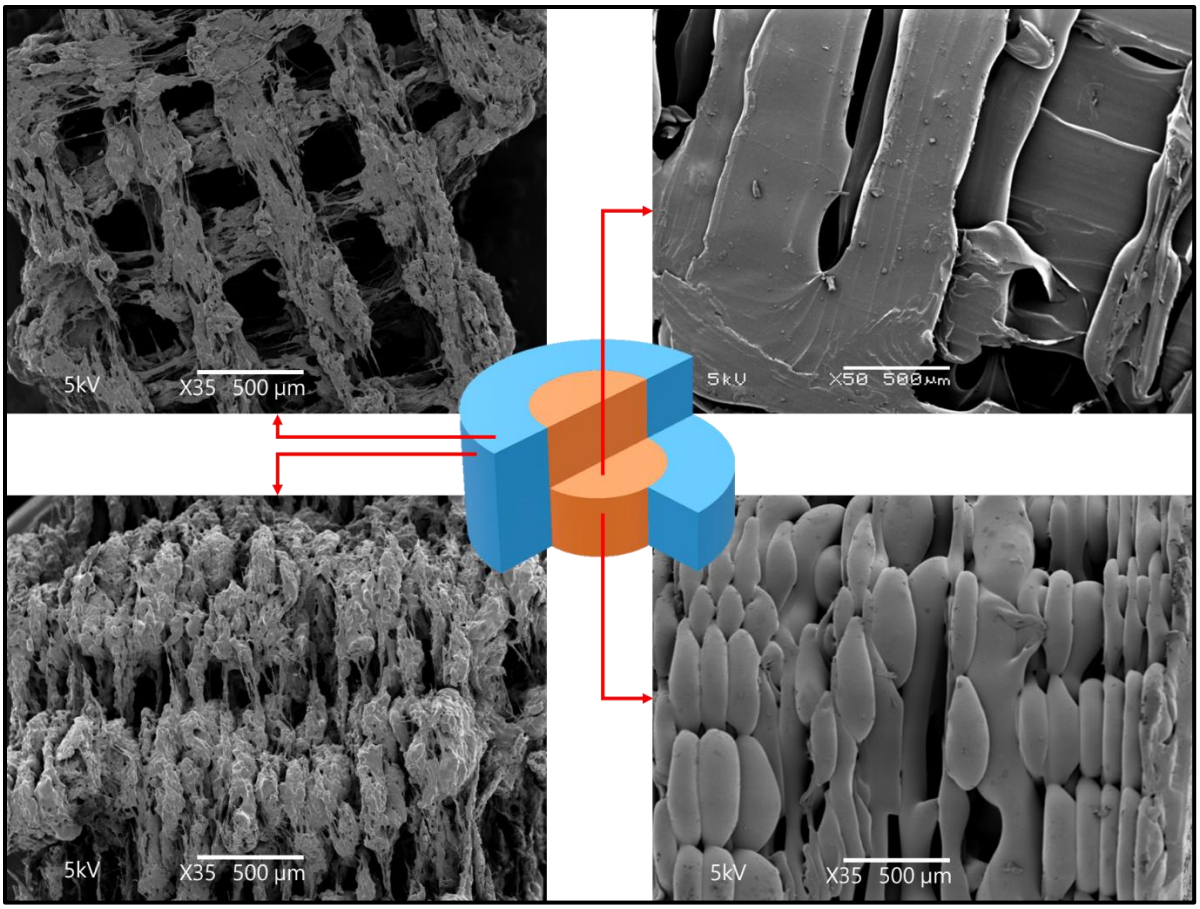

Figure 41. the SEM pictures of the 3D printed tablets shown the porous structure of the shell and the condense core.

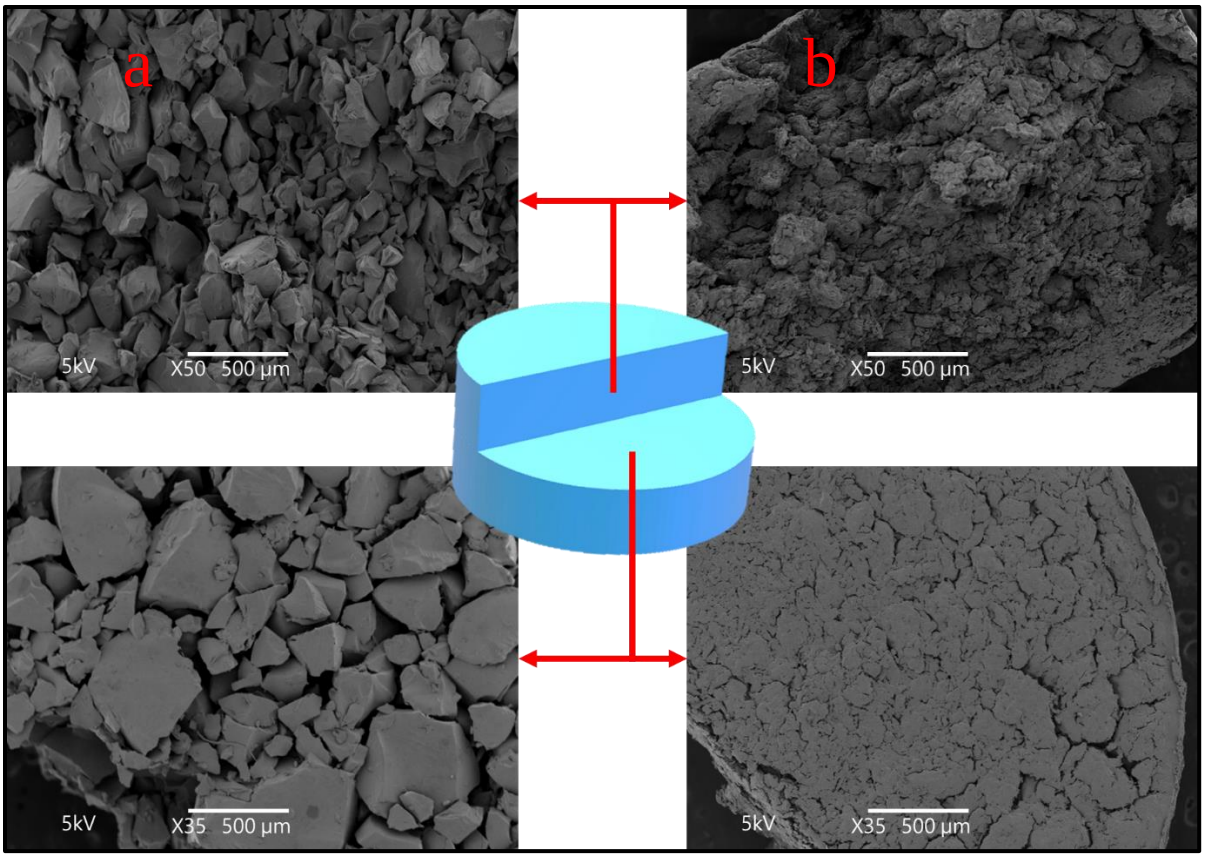

Figure 42. the SEM pictures of direct compressed a) HPMCAS matrix and b) HPMC matrix tablets.

Table 8. the weight, dimensions and density of the 3D printed and direct compressed tablets.

	Weight (mg)	Diameter (mm)	Height (mm)	Density (mg/mm^3)
Core-shell	286.13±1.73	12.39±0.12	4.53±0.04	0.9253
3DP shell	198.46±2.65	12.27±0.11 (5.84±0.03)*	4.51±0.02	0.9545
3DP core	100.01±7.00	5.84±0.06	4.40±0.08	1.0566
DC HPMC	197.33±3.06	8.00±0.01	3.65±0.07	1.0737
DC HPMCAS	197.67±2.08	8.00±0.00	4.37±0.09	0.9005

*the inner diameter of the shell

The cylinder shaped tablets volume can be calculated as follows:

$$V = \frac{\pi D^2}{4} * h \qquad \text{Eq 13}$$

where D and h are the diameter and thickness of the tablets, respectively. Thus, the theoretical density of a tablet was calculated according to the following equation:

$$\rho = \frac{m}{V} = \frac{4m}{\pi D^2 * h} \qquad \text{Eq 14}$$

where m is the weight of the tablet. The density of the HME-generated filaments was calculated using the same equation. The 3D printed tablets has specific 3D structure, which all have porous structure or combine two totally different parts. The shell tablets is tube shaped with 50% infill, so the density was calculated using equation 3:

$$V = \left(\frac{\pi D^2}{4} * h - \frac{\pi d^2}{4} * h\right) * 50\ \% \qquad \text{Eq 15}$$

where D is the outside diameter and d is the inside diameter. The core structure was 80 % filled, so the volume is:

$$V = \frac{\pi D^2}{4} * h * 80\% \qquad \text{Eq 16}$$

The core-shell structured tablets has 77.8% volume is shell with 50 % infill density and 22.2% volume is core with 80% infill density, so the theoretical volume is:

$$V = \frac{\pi D^2}{4} * h * (77.8\% * 50\% + 22.2\% * 80\%) \qquad \text{Eq 17}$$

The volume of the 3D printed shell, core and core-shell tablets obtained from the equation 15-17 was then substituted into equation 17 for the density estimation.

As shown in Table 8 the theoretical density of 3DP tablets was much higher than that of unprinted filaments. In addition, tablets with high hardness and density values are expected to have delayed dissolution and slow drug release after administration. In the geometric study, the tablets had only small variations in weight and dimensions, which demonstrate the good reproducibility of the 3D printing process.

4.3.4. *In vitro* drug release studies

According to the previous work, both HPMC and HPMCAS matrix will formed hydrogel which can control the drug release rates. In this work, the shell (HPMC) has more porous structure which should formed the hydrogel faster than the condense core (HPMCAS HG) structures. In order to maintain the same size and weights, the direct compressed tablets were prepared with high pressure. Even though there has particulates in the direct compressed tablets, they are not disintegrate during the dissolution studies and the high density which will dramatically slow down the formation of the hydrogel.

The drug dissolution rates of tablets prepared by 3D printing and direct compression were evaluated. As discussed in section 3.1, the APAP was dispersed or dissolved into the polymer matrices and formed solid dispersions or solutions during the HME process. The drug release rates from tablets prepared by different techniques influenced by the 3D geometric structure and composition, and the following were happened during the *in vitro* drug release study:

- The dissolution mechanism of both 3D printed and direct compressed tablets were swallow and erosion, neither of them can disintegrate due to the cellulose polymer matrix. So, a steep concentration gradient formed at the media/tablet interface once the tablets contacted the dissolution media. Here, water acted as a plasticizer and reduced the glass transition temperature (T_g) of the contact interface section. Once the system T_g reached the temperature of *in vitro* study, the matrix transformed to hydrogel [59].
- The HPMC and HPMCAS matrix swelled and formed hydrogel while the media were penetrating, which changed the drug concentration at the media/tablet interface. Media penetrate through polymer matrix was the most important rate-controlling step during the dissolution study. The media took longer to penetrate through the direct compressed tablets

because they and the core because they have high density than through the porous shell structures.

- The APAP to diffuse from the media/tablet interface to the hydrogel due to the concentration gradients, and thus into the dissolution media. HPMC has higher solubility than the HPMCAS matrix in the pH 6.8 SIF, which indicating the drug release rates from the HPMCAS matrix would be slower than from the HPMC matrix.
- In addition, the more porous structure was less restrictive for drug diffusion upon drug depletion, the APAP will release rapidly from the HPMC shell; conversely, due to the condense structure and HPMCAS matrix, the APAP was slowly released from the core.

As expected, all direct compressed tablets has extend drug release rate because its high density. Faster drug release was observed with shell structure, which released 80% drug in 2 h, while the core structure tables release APAP over an extended time period (<80% after 7 h, respectively).

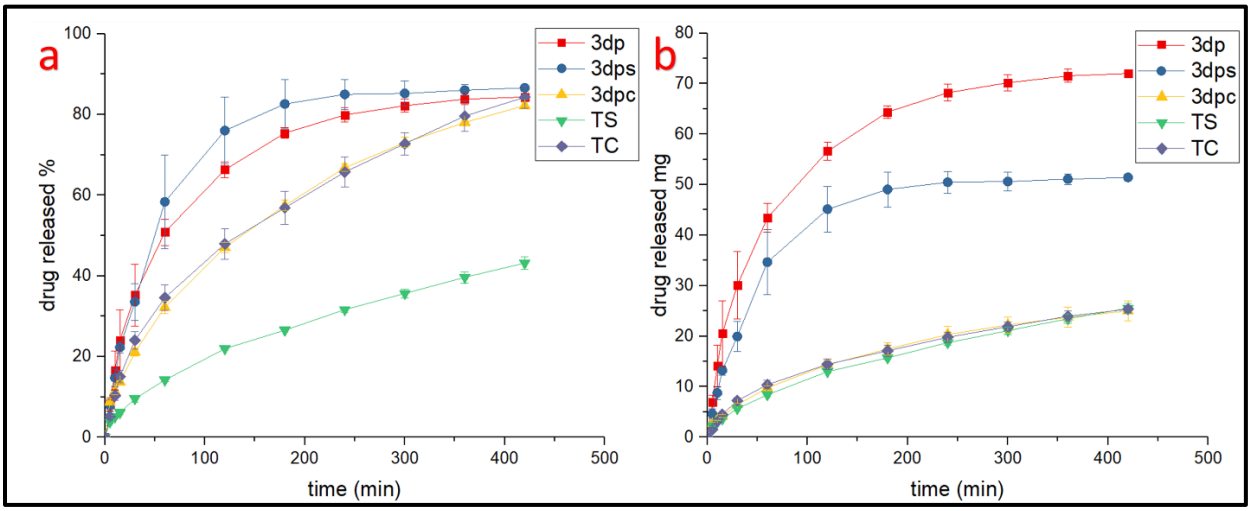

Figure 43. the drug release profiles of the 3D printed tablets and direct compressed tablets.

In order to see the drug release rates changes along with the time, the dissolution cure were showed in the total amount released (mg) to the time (figure 43b). As shown in the curve, the core-shell structured tablets released drug more than the shell and core only because both the shell and core contributes to the total amount drug released from the core-shell tablets. There is no doubt that shell structure release drug faster and more than the core structure during the 420 min drug release studies.

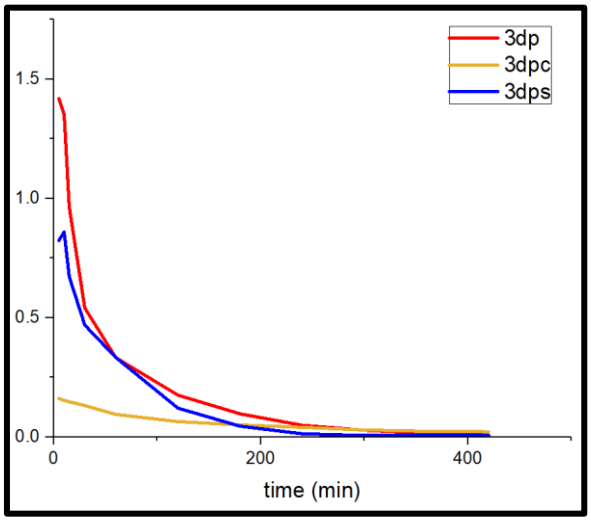

Figure 44. the drug release rates of the 3D printed tablets, shell structure and core.

To have a clear vision of the drug release rates, the 1st order of dissolution curve was deriveted and shown in figure. The drug release rates from the core-shell tablets was fast at beginning, and the rates decrease due to the amount of the APAP released from the tablets and the decrease of the concentration gradients. When the shell structure reaches the equilibrium the drug release rate becomes slow and steady, which contributes to the extended therapeutic effects. The shell only structure releases drug fast at the beginning as well, but it becomes zero when the hydrogel reaches the equilibrium. The core only structure releases drug slowly but in a constant rates always.

4.4. Conclusion

In this work, the 3D printable amorphous filaments were successfully prepared and evaluated. Also the 3D core-shell structured tablets were acquired by both HME and FDM based 3D printing technologies. The *in vitro* dissolution profiles demonstrated that the drug release from the core-shell structured tablets was fast at the first 1h which contributes to fast effectives when the oral dosage was administrated, then the drug release rate decrease and become constant due to the condense extend core structure which contributes to the long effectiveness for the oral dosages. The work also demonstrated that the bright future of combining the HME and 3D printing technology for personalized dosages preparation.

Conclusion

As an emerging technology in the pharmaceutical industry, there are many challenges to 3D printing. Some review articles have already raised points worthy of consideration. Liaw *et al*. reviewed the FDA regulations and challenges of 3D printing [102]. Preis *et al*. systematically reviewed the current status of the 3D-printed drug for children and the challenges encountered [103]. Our current research focuses on the challenges of the materials, equipment, and processes of 3D printing for personalized drug delivery systems.

Most 3D printing platforms were initially developed for applications in industries other than pharmaceutical, and most materials used in the printing were not pharmaceutical grade. To develop personalized drug delivery systems using 3D printing technologies, pharmaceutical scientists have two important considerations: 1) find appropriate materials for the different types of 3D printing, and 2) maintain the desired properties after the printing process.

This thesis was organized systematically to present the combination of hot melt extrusion and additive manufacturing in development of pharmaceuticals. The additive manufacturing/3D printing is an emerging technology at infancy but has a tremendous potential in development of pharmaceutical products. This promising potential to develop the personalized medication is a revolutionary change in compounding the dosage forms with tailored dose, especially for narrow therapeutic drugs. This would have profound effect on society and industry. However, the appropriate regulations and policies must be developed for future research in this arena. 3D printing has provided new prospects for various industries in production paradigm and range of

manufacturing industrial to retail and decentralized manufacturing. This additive manufacturing has exceptional applications which need to be exploited in manufacturing sector. Nevertheless, the usage of different 3D printing technologies has increased in various industries in the recent past, it requires advancements (reducing production time, printers cost and printer materials) to replace the conventional production methods. Wohler's report in 2014 reveals that revenue for additive manufacturing globally rise four folds from $5 billion in 2016 to $21 billion in 2021. This suggests a huge market potential for additive manufacturing in near future.

In this thesis, we successfully conjugated the HME and 3D printing technology as an efficient and economical platform for personalized or patient focused dosages development. Moreover, a considerable work has been done to screen the 3D printable filaments for such formulation development. And also the comprehensive understanding the 3D printed structures with their in vitro drug release profiles were obtained. Based on these achievements, the optimization of the oral drug administration has been achieved by specific core-shell structure design. This thesis clearly demonstrated that the promising future of combining HME and 3D printing technologies for the future novel drug delivery system development.

List of References

1. Baghel S, Cathcart H, O'Reilly NJ. Polymeric Amorphous Solid Dispersions: A Review of Amorphization, Crystallization, Stabilization, Solid-State Characterization, and Aqueous Solubilization of Biopharmaceutical Classification System Class II Drugs . J. Pharm. Sci. Elsevier; 2016 p. 2527–44. Available from: https://www.sciencedirect.com/science/article/pii/S002235491500009X

2. Popescu C. Enhanced Dissolution Efficiency of Zaleplon Solid Dispersions via Modified β-Cyclodextrin Molecular Inclusion Complexes. J. Pharma Pharm. Sci. 2015;1:12–21. Available from: https://doi.org/10.24218/vjpps.2015.04.

3. Vasconcelos T, Sarmento B, Costa P. Solid dispersions as strategy to improve oral bioavailability of poor water soluble drugs. Drug Discov. Today. Elsevier; 2007;12:1068–75.

4. Sareen S, Joseph L, Mathew G. Improvement in solubility of poor water-soluble drugs by solid dispersion. Int. J. Pharm. Investig. 2012; 2:12. Available from: http://www.ncbi.nlm.nih.gov/pubmed/23071955

5. Sarode AL, Sandhu H, Shah N, Malick W, Zia H. Hot melt extrusion (HME) for amorphous solid dispersions: predictive tools for processing and impact of drug–polymer interactions on supersaturation. Eur. J. Pharm. Sci. Elsevier; 2013;48:371–84.

6. Thiry J, Krier F, Evrard B. A review of pharmaceutical extrusion: Critical process parameters and scaling-up Int. J. Pharm. 2015. p. 227–40. Available from: http://www.ncbi.nlm.nih.gov/pubmed/25541517

7. Feng X, Ye X, Park J-B, Lu W, Morott J, Beissner B, et al. Evaluation of the recrystallization kinetics of hot-melt extruded polymeric solid dispersions using an improved Avrami equation.

Drug Dev. Ind. Pharm. Taylor & Francis; 2015;41:1479–87.

8. Repka MA, Langley N, DiNunzio J. Melt extrusion. Mater. Technol. Drug Prod. Des. Springer; 2013;4:5.

9. Patil H, Feng X, Ye X, Majumdar S, Repka MA. Continuous production of fenofibrate solid lipid nanoparticles by hot-melt extrusion technology: a systematic study based on a quality by design approach. AAPS J. Springer; 2015;17:194–205.

10. Stanković M, Frijlink HW, Hinrichs WLJ. Polymeric formulations for drug release prepared by hot melt extrusion: application and characterization. Drug Discov. Today. Elsevier; 2015;20:812–23.

11. Gross BC, Erkal JL, Lockwood SY, Chen C, Spence DM. Evaluation of 3D printing and its potential impact on biotechnology and the chemical sciences. ACS Publications; 2014.

12. Tiwari R V., Patil H, Repka MA. Contribution of hot-melt extrusion technology to advance drug delivery in the 21st century. Expert Opin. Drug Deliv. 2016;13:451–64. Available from: http://www.tandfonline.com/doi/full/10.1517/17425247.2016.1126246

13. Ye X, Patil H, Feng X, Tiwari R V, Lu J, Gryczke A, et al. Conjugation of hot-melt extrusion with high-pressure homogenization: a novel method of continuously preparing nanocrystal solid dispersions. AAPS PharmSciTech. Springer; 2016;17:78–88.

14. Ashour EA, Kulkarni V, Almutairy B, Park JB, Shah SP, Majumdar S, et al. Influence of pressurized carbon dioxide on ketoprofen-incorporated hot-melt extruded low molecular weight hydroxypropylcellulose. Drug Dev. Ind. Pharm. 2016;42:123–30. Available from:

http://www.ncbi.nlm.nih.gov/pubmed/25997363

15. Vo AQ, Feng X, Morott JT, Pimparade MB, Tiwari R V, Zhang F, et al. A novel floating controlled release drug delivery system prepared by hot-melt extrusion. Eur. J. Pharm. Biopharm. Elsevier; 2016;98:108–21.

16. Goyanes A, Wang J, Buanz A, Martínez-Pacheco R, Telford R, Gaisford S, et al. 3D Printing of Medicines: Engineering Novel Oral Devices with Unique Design and Drug Release Characteristics. Mol. Pharm. American Chemical Society; 2015;12:4077–84. Available from: http://pubs.acs.org/doi/10.1021/acs.molpharmaceut.5b00510

17. Goyanes A, Buanz ABM, Hatton GB, Gaisford S, Basit AW. 3D printing of modified-release aminosalicylate (4-ASA and 5-ASA) tablets. Eur. J. Pharm. Biopharm. Elsevier; 2015;89:157–62. Available from: http://www.sciencedirect.com/science/article/pii/S0939641114003580?via%3Dihub

18. Melocchi A, Parietti F, Maroni A, Foppoli A, Gazzaniga A, Zema L. Hot-melt extruded filaments based on pharmaceutical grade polymers for 3D printing by fused deposition modeling. Int. J. Pharm. Elsevier; 2016;509:255–63.

19. Norman J, Madurawe RD, Moore CM V, Khan MA, Khairuzzaman A. A new chapter in pharmaceutical manufacturing: 3D-printed drug products. Adv. Drug Deliv. Rev. Elsevier; 2017;108:39–50.

20. Sachs E, Cima M, Cornie J. Three-Dimensional Printing: Rapid Tooling and Prototypes Directly from a CAD Model. CIRP Ann. - Manuf. Technol. Elsevier; 1990;39:201–4. Available from: http://www.sciencedirect.com.umiss.idm.oclc.org/science/article/pii/S000785060761035X

21. Goole J, Amighi K. 3D printing in pharmaceutics: a new tool for designing customized drug delivery systems. Int. J. Pharm. Elsevier; 2016;499:376–94.

22. OConnor T, Lee S. Emerging technology for modernizing pharmaceutical production: Continuous manufacturing. Dev. Solid Oral Dos. Forms Pharm. Theory Pract. Second Ed. 2016. p. 1031–46.

23. Wu BM, Borland SW, Giordano RA, Cima LG, Sachs EM, Cima MJ. Solid free-form fabrication of drug delivery devices. J. Control. Release 1996;40:77–87. Available from: https://dmse.mit.edu/publications/solid-free-form-fabrication-drug-delivery-devices

24. Yu DG, Yang XL, Huang WD, Liu J, Wang YG, Xu H. Tablets with material gradients fabricated by three-dimensional printing. J. Pharm. Sci. Elsevier; 2007;96:2446–56.

25. Khan S, Boateng JS, Mitchell J, Trivedi V. Formulation, Characterisation and Stabilisation of Buccal Films for Paediatric Drug Delivery of Omeprazole. AAPS PharmSciTech New York: Springer US; 2015;16:800–10. Available from: http://www.ncbi.nlm.nih.gov/pmc/articles/PMC4508285/

26. Baumgart F. Graphical statics a forgotten tool for solving plane mechanical problems. Injury. Elsevier; 2000;31:24–85.

27. Rösler J, Harders H, Baeker M. Mechanical behaviour of engineering materials: metals, ceramics, polymers, and composites. Springer Science & Business Media; 2007.

28. Serajuddin A. Solid dispersion of poorly water-soluble drugs: Early promises, subsequent problems, and recent breakthroughs. J. Pharm. Sci. Wiley Online Library; 1999;88:1058–66.

29. Kojima H, Yoshihara K, Sawada T, Kondo H, Sako K. Extended release of a large amount of highly water-soluble diltiazem hydrochloride by utilizing counter polymer in polyethylene oxides (PEO)/polyethylene glycol (PEG) matrix tablets. Eur. J. Pharm. Biopharm. Elsevier; 2008;70:556–62.

30. Moulton SE, Wallace GG. 3-dimensional (3D) fabricated polymer based drug delivery systems. J. Control. Release. Elsevier; 2014;193:27–34.

31. Verweij JP, Moin DA, Mensink G, Nijkamp P, Wismeijer D, van Merkesteyn JPR. Autotransplantation of Premolars With a 3-Dimensional Printed Titanium Replica of the Donor Tooth Functioning as a Surgical Guide: Proof of Concept. J. Oral Maxillofac. Surg. 2016;74:1114–9. Available from: http://www.sciencedirect.com/science/article/pii/S0278239116001221

32. Baghel S, Cathcart H, O'Reilly NJ. Polymeric Amorphous Solid Dispersions: A Review of Amorphization, Crystallization, Stabilization, Solid-State Characterization, and Aqueous Solubilization of Biopharmaceutical Classification System Class II Drugs J. Pharm. Sci. 2016. p. 2527–44. Available from: http://www.ncbi.nlm.nih.gov/pubmed/26886314

33. Janssens S, Van den Mooter G. Review: physical chemistry of solid dispersions. J. Pharm. Pharmacol. 2009;61:1571–86. Available from: http://www.ncbi.nlm.nih.gov/pubmed/19958579

34. Islam MT, Scoutaris N, Maniruzzaman M, Moradiya HG, Halsey SA, Bradley MSA, et al. Implementation of transmission NIR as a PAT tool for monitoring drug transformation during HME processing. Eur. J. Pharm. Biopharm. Elsevier; 2015;96:106–16.

35. Zhang J, Feng X, Patil H, Tiwari R V., Repka MA. Coupling 3D printing with hot-melt

extrusion to produce controlled-release tablets. Int. J. Pharm. 2017;519:186–97.

36. Rathbone MJ, Hadgraft J, Roberts MS, Lane ME. Modified-Release Drug Delivery Technology, Volume 1, 2nd edition. 2008.

37. Moanţă A, Ionescu C, Rotaru P, Socaciu M, Hărăbor A. Structural characterization, thermal investigation, and liquid crystalline behavior of 4-[(4-chlorobenzyl)oxy]-3,4′-dichloroazobenzene. J. Therm. Anal. Calorim. Springer Netherlands; 2010;102:1079–86. Available from: http://link.springer.com/10.1007/s10973-010-0899-1

38. Ewing A V., Biggart GD, Hale CR, Clarke GS, Kazarian SG. Comparison of pharmaceutical formulations: ATR-FTIR spectroscopic imaging to study drug-carrier interactions. Int. J. Pharm. Elsevier; 2015;495:112–21. Available from: https://www-sciencedirect-com.umiss.idm.oclc.org/science/article/pii/S0378517315301654

39. Huskić I, Christopherson J-C, Užarević K, Friščić T. In situ monitoring of vapour-induced assembly of pharmaceutical cocrystals using a benchtop powder X-ray diffractometer. Chem. Commun. The Royal Society of Chemistry; 2016;52:5120–3. Available from: http://xlink.rsc.org/?DOI=C6CC01583B

40. Lu K, Meshii T. Three-dimensional T-stresses for three-point-bend specimens with large thickness variation. Eng. Fract. Mech. Pergamon; 2014;116:197–203. Available from: https://www-sciencedirect-com.umiss.idm.oclc.org/science/article/pii/S0013794413004050?_rdoc=1&_fmt=high&_origin=gateway&_docanchor=&md5=b8429449ccfc9c30159a5f9aeaa92ffb&ccp=y

41. Serajuddin ATM. Salt formation to improve drug solubility. Adv. Drug Deliv. Rev. Elsevier;

2007;59:603–16.

42. Jain KK. Drug Delivery Systems. 1st ed. Totowa: Springer; 2008.

43. Weiniger CF, Golovanevski L, Domb AJ, Ickowicz D. Extended release formulations for local anaesthetic agents. Anaesthesia. Wiley Online Library; 2012;67:906–16.

44. Santos HA, Salonen J, Bimbo LM, Lehto V-P, Peltonen L, Hirvonen J. Mesoporous materials as controlled drug delivery formulations. J. Drug Deliv. Sci. Technol. Elsevier; 2011;21:139–55.

45. Shimoni O, Postma A, Yan Y, Scott AM, Heath JK, Nice EC, et al. Macromolecule functionalization of disulfide-bonded polymer hydrogel capsules and cancer cell targeting. ACS Nano. ACS Publications; 2012;6:1463–72.

46. Ward C, Langdon SP, Mullen P, Harris AL, Harrison DJ, Supuran CT, et al. New strategies for targeting the hypoxic tumour microenvironment in breast cancer. Cancer Treat. Rev. Elsevier; 2013;39:171–9.

47. Willis L, Hayes D, Mansour HM. Therapeutic liposomal dry powder inhalation aerosols for targeted lung delivery. Lung. Springer; 2012;190:251–62.

48. Staples M, Daniel K, Cima MJ, Langer R. Application of micro-and nano-electromechanical devices to drug delivery. Pharm. Res. Springer; 2006;23:847–63.

49. Paavola A, Kilpeläinen I, Yliruusi J, Rosenberg P. Controlled release injectable liposomal gel of ibuprofen for epidural analgesia. Int. J. Pharm. Elsevier; 2000;199:85–93.

50. Santus G, Baker RW. Osmotic drug delivery: a review of the patent literature. J. Control. Release. Elsevier; 1995;35:1–21.

51. Leong KW, Langer R. Polymeric controlled drug delivery. Adv. Drug Deliv. Rev. Elsevier; 1988;1:199–233.

52. Abbadessa A, Blokzijl MM, Mouser VHM, Marica P, Malda J, Hennink WE, et al. A thermo-responsive and photo-polymerizable chondroitin sulfate-based hydrogel for 3D printing applications. Carbohydr. Polym. 2016;149:163–74. Available from: http://www.sciencedirect.com/science/article/pii/S014486171630457X

53. Sarode AL, Malekar SA, Cote C, Worthen DR. Hydroxypropyl cellulose stabilizes amorphous solid dispersions of the poorly water soluble drug felodipine. Carbohydr. Polym. 2014;112:512–9. Available from: http://www.sciencedirect.com/science/article/pii/S0144861714006158

54. Sarode AL, Obara S, Tanno FK, Sandhu H, Iyer R, Shah N. Stability assessment of hypromellose acetate succinate (HPMCAS) NF for application in hot melt extrusion (HME). Carbohydr. Polym. 2014;101:146–53. Available from: http://www.sciencedirect.com/science/article/pii/S0144861713009090

55. Zhang J, Feng X, Patil H, Tiwari R V, Repka MA. Coupling 3D Printing with Hot-Melt Extrusion to Produce Controlled-Release Tablets. Int. J. Pharm. Elsevier; 2016;

56. Kalantzi L, Reppas C, Dressman JB, Amidon GL, Junginger HE, Midha KK, et al. Biowaiver monographs for immediate release solid oral dosage forms: Acetaminophen (paracetamol). J. Pharm. Sci. Wiley Online Library; 2006;95:4–14.

57. Banks SR, Pygall SR, Bajwa GS, Doughty SW, Timmins P, Melia CD. The influence of substituted phenols on the sol:gel transition of hydroxypropyl methylcellulose (HPMC) aqueous solutions. Carbohydr. Polym. 2014;101:1198–204. Available from:

http://www.sciencedirect.com/science/article/pii/S0144861713010904

58. Colombo P. Swelling-controlled release in hydrogel matrices for oral route. Adv. Drug Deliv. Rev. Elsevier; 1993;11:37–57.

59. Siepmann J, Peppas NA. Modeling of drug release from delivery systems based on hydroxypropyl methylcellulose (HPMC). Adv. Drug Deliv. Rev. Elsevier; 2012;64:163–74.

60. Brannon-Peppas L, Peppas NA. Equilibrium swelling behavior of pH-sensitive hydrogels. Chem. Eng. Sci. Elsevier; 1991;46:715–22.

61. Pani NR, Nath LK. Development of controlled release tablet by optimizing HPMC: Consideration of theoretical release and RSM. Carbohydr. Polym. 2014;104:238–45. Available from: http://www.sciencedirect.com/science/article/pii/S0144861714000393

62. Djuris J, Nikolakakis I, Ibric S, Djuric Z, Kachrimanis K. Preparation of carbamazepine–Soluplus® solid dispersions by hot-melt extrusion, and prediction of drug–polymer miscibility by thermodynamic model fitting. Eur. J. Pharm. Biopharm. Elsevier; 2013;84:228–37.

63. Feng X, Vo A, Patil H, Tiwari R V, Alshetaili AS, Pimparade MB, et al. The effects of polymer carrier, hot melt extrusion process and downstream processing parameters on the moisture sorption properties of amorphous solid dispersions. J. Pharm. Pharmacol. Wiley Online Library; 2016;68:692–704.

64. Coats AW, Redfern JP. Thermogravimetric analysis. A review. Analyst. The Royal Society of Chemistry; 1963;88:906–24.

65. Liu X, Lu M, Guo Z, Huang L, Feng X, Wu C. Improving the chemical stability of amorphous

solid dispersion with cocrystal technique by hot melt extrusion. Pharm. Res. Springer; 2012;29:806–17.

66. Vo AQ, Feng X, Pimparade M, Ye X, Kim DW, Martin ST, et al. Dual-mechanism gastroretentive drug delivery system loaded with an amorphous solid dispersion prepared by hot-melt extrusion. Eur. J. Pharm. Sci. Elsevier; 2017;102:71–84.

67. Higuchi T. Rate of release of medicaments from ointment bases containing drugs in suspension. J. Pharm. Sci. Wiley Online Library; 1961;50:874–5.

68. Ritger PL, Peppas NA. A simple equation for description of solute release II. Fickian and anomalous release from swellable devices. J. Control. release. Elsevier; 1987;5:37–42.

69. Peppas NA, Sahlin JJ. A simple equation for the description of solute release. III. Coupling of diffusion and relaxation. Int. J. Pharm. Elsevier; 1989;57:169–72.

70. Gillespie DT, Seitaridou E. Simple Brownian diffusion: an introduction to the standard theoretical models. Oxford University Press; 2012.

71. Bunge AL. Release rates from topical formulations containing drugs in suspension. J. Control. release. Elsevier; 1998;52:141–8.

72. Peppas NA, Narasimhan B. Mathematical models in drug delivery: How modeling has shaped the way we design new drug delivery systems. J. Control. Release. Elsevier; 2014;190:75–81.

73. Higuchi T. Mechanism of sustained-action medication. Theoretical analysis of rate of release of solid drugs dispersed in solid matrices. J. Pharm. Sci. Wiley Online Library; 1963;52:1145–9.

74. Paul DR. Elaborations on the Higuchi model for drug delivery. Int. J. Pharm. Elsevier;

2011;418:13–7.

75. Siepmann J, Siepmann F. Modeling of diffusion controlled drug delivery. J. Control. Release. Elsevier; 2012;161:351–62.

76. Siepmann J, Göpferich A. Mathematical modeling of bioerodible, polymeric drug delivery systems. Adv. Drug Deliv. Rev. Elsevier; 2001;48:229–47.

77. Korsmeyer RW, Gurny R, Doelker E, Buri P, Peppas NA. Mechanisms of solute release from porous hydrophilic polymers. Int. J. Pharm. Elsevier; 1983;15:25–35.

78. Cui J, Yan Y, Wang Y, Caruso F. Templated assembly of pH-labile polymer-drug particles for intracellular drug delivery. Adv. Funct. Mater. Wiley Online Library; 2012;22:4718–23.

79. Sastry SV, Nyshadham JR, Fix JA. Recent technological advances in oral drug delivery–a review. Pharm. Sci. Technolo. Today. Elsevier; 2000;3:138–45.

80. Lee H-J, Kim J-Y, Park S-H, Rhee Y-S, Park C-W, Park E-S. Controlled-release oral dosage forms containing nimodipine solid dispersion and hydrophilic carriers. J. Drug Deliv. Sci. Technol. Elsevier; 2017;37:28–37. Available from: https://www-sciencedirect-com.umiss.idm.oclc.org/science/article/pii/S1773224716303380

81. Langer R. New methods of drug delivery. Science (80-.). JSTOR; 1990;1527–33.

82. Lepourcelet M, Chen Y-NP, France DS, Wang H, Crews P, Petersen F, et al. Small-molecule antagonists of the oncogenic Tcf/β-catenin protein complex. Cancer Cell. Elsevier; 2004;5:91–102.

83. Uhrich KE, Cannizzaro SM, Langer RS, Shakesheff KM. Polymeric systems for controlled drug release. Chem. Rev. ACS Publications; 1999;99:3181–98.

84. Crowley MM, Zhang F, Repka MA, Thumma S, Upadhye SB, Kumar Battu S, et al. Pharmaceutical applications of hot-melt extrusion: part I. Drug Dev. Ind. Pharm. Taylor & Francis; 2007;33:909–26.

85. Blagden N, De Matas M, Gavan PT, York P. Crystal engineering of active pharmaceutical ingredients to improve solubility and dissolution rates. Adv. Drug Deliv. Rev. Elsevier; 2007;59:617–30.

86. Vasconcelos T, Sarmento B, Costa P. Solid dispersions as strategy to improve oral bioavailability of poor water soluble drugs. Drug Discov. Today Elsevier Current Trends; 2007;12:1068–75. Available from: https://www.sciencedirect.com/science/article/pii/S1359644607003753

87. Sandler N, Määttänen A, Ihalainen P, Kronberg L, Meierjohann A, Viitala T, et al. Inkjet printing of drug substances and use of porous substrates-towards individualized dosing. J. Pharm. Sci. Wiley Online Library; 2011;100:3386–95.

88. Preis M, Breitkreutz J, Sandler N. Perspective: concepts of printing technologies for oral film formulations. Int. J. Pharm. Elsevier; 2015;494:578–84.

89. Zhang J, Yang W, Vo AQ, Feng X, Ye X, Kim DW, et al. Hydroxypropyl methylcellulose-based controlled release dosage by melt extrusion and 3D printing: Structure and drug release correlation. Carbohydr. Polym. 2017;177:49–57.

90. Curatolo W, Nightingale JA, Herbig SM. Utility of Hydroxypropylmethylcellulose Acetate Succinate (HPMCAS) for Initiation and Maintenance of Drug Supersaturation in the GI Milieu. Pharm. Res. 2009;26:1419–31. Available from: http://www.ncbi.nlm.nih.gov/pubmed/19277850

91. Coats AW, Redfern JP. Thermogravimetric analysis. A review. Analyst The Royal Society of Chemistry; 1963;88:906–24. Available from: http://xlink.rsc.org/?DOI=an9638800906%0Afile:///Users/rd14441/Google Drive/Papers/Papers2/Articles/1963/Coats/Analyst 1963 Coats.pdf%0Apapers2://publication/doi/10.1039/an9638800906

92. Dollimore D, Phang P. Thermal Analysis. Anal. Chem. Academic Press; 2000;72:27–36. Available from: http://pubs.acs.org/doi/abs/10.1021/a1000003j

93. Skoog DA, Holler FJ, Nieman TA. Principles of instrumental analysis. Saunders College Pub.; 1998.

94. Vo AQ, He H, Zhang J, Martin S, Chen R, Repka MA. Application of FT-NIR Analysis for In-line and Real-Time Monitoring of Pharmaceutical Hot Melt Extrusion: a Technical Note. AAPS PharmSciTech Springer International Publishing; 2018;1–5. Available from: http://link.springer.com/10.1208/s12249-018-1091-3

VITA

JIAXIANG ZHANG

Education

M.S. in **Pharmaceutical Engineering**, New Jersey Institute of Technology, USA **09/2012-05/2014**
B.E. in **Pharmaceutical Engineering**, Northwest University, China **09/2008-06/2012**

Honors and Awards

- 2018 CRS annual meeting best oral presentation award
- 2018 *AAPS Annual meeting and expo best abstract award*
- *2017 AAPS Annual meeting and expo student travel award*
- **Outstanding reviewer of** International Journal of Pharmaceutics and reviewer of several peer-reviewed journals.

Publications and Presentations:

- AAPS PharmSciTech invited review article on 3D printing special issue: **Zhang J,** Vo AQ, Feng X, Bandari S, Repka MA. Pharmaceutical Additive Manufacturing: a Novel Tool for Complex and Personalized Drug Delivery Systems. AAPS PharmSciTech [Internet]. 2018; Available from: https://doi.org/10.1208/s12249-018-1097-x
- Vo AQ, He H, **Zhang J**, Martin S, Chen R, Repka MA. Application of FT-NIR Analysis for In-line and Real-Time Monitoring of Pharmaceutical Hot Melt Extrusion: a Technical Note. AAPS PharmSciTech. 2018; Available from: https://doi.org/10.1208/s12249-018-1091-3
- **Zhang J,** Yang W, Vo AQ, Feng X, Ye X, Kim DW, et al. Hydroxypropyl methylcellulose-based controlled release dosage by melt extrusion and 3D printing: Structure and drug release correlation. Carbohydr. Polym. 2017;177:49–57.
- **Zhang J,** Feng X, Patil H, Tiwari R V., Repka MA. Coupling 3D printing with hot-melt extrusion to produce controlled-release tablets. Int. J. Pharm. 2017;519:186–97.
- Sharma PK, Panda A, Pradhan A**, Zhang J,** Thakkar R, Whang C-H, et al. Solid-State Stability Issues of Drugs in Transdermal Patch Formulations. AAPS PharmSciTech. 2017;
- 1. Vo AQ, Feng X, **Zhang J**, Zhang F, Repka MA. Dual mechanism of microenvironmental pH modulation and foam melt extrusion to enhance performance of HPMCAS based amorphous solid dispersion. Int. J. Pharm. 2018;550:216–28. Available from: http://www.ncbi.nlm.nih.gov/pubmed/30142354
- **Oral presentation**:
  - 11/2018 AAPS Rapid Fire oral presention: Development of core-shell controlled release oral dosages using 3D printing
  - 07/2018 CRS annual meeting oral presentation: Development of Controlled Release Oral Dosages with Core-shell Structure Using 3D Printing Technologies (Best oral presentation award of 2018 CRS)